Investigating the Role of Extracellular Polysaccharides in Biofilm Formation of *Klebsiella pneumoniae*

A dissertation presented for the degree of M.Sc., in the

Faculty of Health Sciences, Trinity College Dublin

by

Sinéad Moynihan

2021

Department of Clinical Microbiology,

Trinity College Dublin

Declaration

I, Sinéad Moynihan, declare that the experimentation recorded herein represents my own work, except where duly acknowledged in the text. I agree to deposit this thesis in the University's open access institutional repository or allow the library to do so on my behalf, subject to Irish Copyright Legislation and Trinity College Library conditions of use and acknowledgement.

Sinéad Moynihan

Summary

Klebsiella pneumoniae (*K. pneumoniae*) is the most significant and clinically relevant species in the *Klebsiella* genus of *Enterobacteriaceae* and is the causative agent of a variety of infections, including pneumonia, urinary tract infections and bacteraemia. The success of *K. pneumoniae* in establishing infection in a variety of sites in a host is enhanced by the production of a wide range of virulence factors. Biofilm formation is an important factor in the lifestyle of *K. pneumoniae*.

Conflicting data exist surrounding the relationship between the capsule polysaccharide (CPS) of *Klebsiella* and biofilm formation. Certain studies have found that mutations disrupting capsule synthesis result in biofilm reduction; whereas increased biofilm production has been observed as a result of capsule reduction. The composition of growth media is also considered a major determinant of biofilm formation. However, similar to the capsule, clarity is lacking surrounding the contribution of growth media to biofilm formation; nutrient-rich media has been shown to both hinder and enhance biofilm formation.

This study sought to investigate the contribution of both capsule and growth media to the biofilm formation of *K. pneumoniae* strain Kp52145. Crystal violet assays were utilised to quantify biofilm formation. A capsule mutant lacking *manC*, a gene from the CPS operon of Kp52145, was utilised to investigate the role of capsule in biofilm formation and to establish whether the contribution of growth media was strain-characteristic-dependent. Alternative *Klebsiella* isolates were subsequently incorporated into biofilm studies in an attempt to decipher whether the observed effects of growth media on biofilm formation were more widely observed in the species. Additionally, capsular genotyping of these isolates was performed to determine whether capsular type of *K. pneumoniae* influences biofilm formation.

In order to further decipher the role of capsule in biofilm formation, this study aimed to construct a Kp52145 CPS operon mutant, using λ-Red recombination technology. PCR-mediated gene replacement and a DNA assembly tool based on the Gibson Assembly technique were both utilised, however, transformation attempts were unsuccessful.

The use of a bioluminescence system was evaluated as an alternative measurement of viability in biofilm formation assays but was deemed unfeasible due to intrinsic differences in bioluminescent signal among Kp52145 strains. Minimum Inhibitory Concentration (MIC) analysis of Kp52145 strains harbouring this plasmid-based bioluminescent system revealed differential antibiotic resistance to a particular β-lactam/β-lactamase inhibitor combination antibiotic. This study proposes that the anionic charge of the capsule contributes to this observed differential phenotype.

Furthermore, this study aimed to investigate whether complementation of the Kp52145 *manC* mutant would restore the wild-type (WT) phenotype with regards to colony morphology, biofilm formation and antibiotic resistance. However, subsequent Polymerase Chain Reaction (PCR) analysis and Whole Genome Sequencing (WGS) revealed an intact *manC* gene and CPS operon. Instead, a deletion affecting a protein similar to a blue-light sensor in *Escherichia coli* (*E. coli*), YcgF, was identified. Therefore, results from this study were subsequently reinterpreted on the basis of this discovery.

Acknowledgements

Firstly, I would like to thank my supervisor Dr. Stephen Smith for granting me the opportunity to carry out this project. My time in the SPD lab has been invaluable and I have learned so much under your supervision. I am extremely grateful for all the help and advice over the years, regarding both project matters and future study plans of mine. Thank you.

Thank you to my co-supervisor Dr. Jérôme Fennell and for providing *Klebsiella* isolates from Tallaght University Hospital, that were kindly prepared by Senior Medical Scientist Niamh Fitzgerald. Thank you also to Professor José Bengochea for providing the Kp52145 strains.

I am grateful to Trinity College for the award of the E.C. Smith Scholarship in Pathology to carry out this MSc by research in the Department of Clinical Microbiology. Additionally, I am appreciative to have been given the opportunity to present my work at the Annual Microbiology Conference in Belfast which was made possible by grants provided by the Microbiology Society.

I could not have asked for better colleagues in the SPD. Naoise, it was a dream come true starting my project alongside such a good friend. Thank you for all your patience in explaining certain concepts, and then explaining again, until I finally understood! Aileen, thank you for your baked vegan treats which never failed to impress, and for sharing your WGS wisdom when required! Thanks to Rachel for always having the kettle boiled, ready for great chats over tea. Peter, thank you for all your valuable advice, chats and laughs. Most of all, thank you all for being such wonderful friends; my time in the SPD would not have been the same without each and every one of you.

Finally, to my family and David: thank you for your unconditional support and encouragement, especially over the last two years. Fionn, thanks for all the much-needed youtube comedy relief. Dad, thank you for the evening drives to get me away from my desk and your sound practical advice on everything and anything. Mam, thank you for all the “you’re nearly there”s and for (kindly) forcing me to take regular breaks during the write up in literal lockdown; your positivity, encouragement and aperitivi proved vital during the entirety of the project! David, thank you for constant

reassurance and cheering up when I most needed it, and of course for always having a bottle of prosecco at the ready to celebrate the mini landmarks throughout the write up.

Table of Contents

List of Abbreviations

Abbreviation	Full name
AMP	Antimicrobial peptide
AMR	Antimicrobial resistance
BFI	Biofilm formation index
BHI	Brain heart infusion
CAP	Community-acquired pneumonia
CFU	Colony forming units
CPS	Capsular polysaccharide
CRE	Carbapenem-resistant *Enterobacteriaceae*
CRP	cAMP receptor protein
CV	Crystal violet
DMSO	Dimethyl sulfoxide
dNTP	Deoxyribonucleotide triphosphates
ECM	Extracellular matrix
EDTA	Ethylene diamine tetra acetate
ESBL	Extended-spectrum β-lactamases
GI	Gastrointestinal
GST	Glutathione S-transferase
HAP	Hospital-acquired pneumonia
HMV	Hypermucoviscous
HV	Hypervirulent
IM	Inner membrane
IPTG	Isopropyl β-d-1-thiogalactopyranoside
KPC	*K. pneumoniae* carbapenemase
LB	Luria-Bertani
LPS	Lipopolysaccharide
MDR	Multidrug resistance
MIC	Minimum inhibitory concentration
MW	Molecular weight
OD	Optical density
OM	Outer membrane
OMP	Outer membrane protein

OMR	Outer membrane receptors
PBS	Phosphate-buffered saline
PCR	Polymerase chain reaction
PGA	Poly-beta-1,6-N-acetyl-D-glucosamine
ROS	Reactive oxygen species
RLU	Relative light units
SDS-PAGE	Sodium dodecyl sulphate-polyacrylamide gel electrophoresis
SNP	Single nucleotide polymorphism
UTI	Urinary tract infection
UV	Ultraviolet
WGS	Whole genome sequencing

List of Figures

List of Tables

Chapter 1 Introduction

1.1 *Klebsiella pneumoniae*: an introduction

Klebsiella pneumoniae (*K. pneumoniae*) was first described by Carl Friedlander in the late 19th century as an encapsulated bacillus after isolating the bacterium from the lungs of patients who had died from pneumonia (Friedlander, 1882). *K. pneumoniae* is a Gram-negative pathogen that is found ubiquitously in nature (Martin & Bachman, 2018). *K. pneumoniae* is the most significant and clinically relevant species in the *Klebsiella* genus of *Enterobacteriaceae* (Ah *et al.*, 2014).

1.1.2 Infections caused by *K. pneumoniae*

K. pneumoniae is the causative agent of a variety of infections, including pneumonia, urinary tract infections (UTIs), and bacteraemia (Paczosa & Mecsas, 2016). Classical *K. pneumoniae* does not produce excess capsule and predominantly causes infection in immunocompromised individuals (with the exception of UTIs); whereas hypervirulent (HV) strains, characterised by their hypercapsule, are capable of forming invasive infections in otherwise healthy individuals (Catalán-Nájera *et al.*, 2017, Paczosa & Mecsas, 2016). Whilst nosocomial infections are predominantly caused by classical strains, HV strains are primarily associated with community-acquired infections (Shon *et al.*, 2013, Russo *et al.*, 2011).

Pneumonia tends to arise from the aspiration of microbes that colonise the oropharyngeal tract (Scheld, 1991). *K. pneumoniae* can cause both community-acquired pneumonias (CAPs) and hospital-acquired pneumonias (HAPs) (Paczosa & Mecsas, 2016). HAPs are far more common than CAPs and are among some of the most frequent hospital-associated infections (Paczosa & Mecsas, 2016). While *K. pneumoniae* is seldom the underlying cause of CAPs in Europe, Australia and the United States, it is a leading etiological agent of CAPs in Asia and Africa (Ko *et al.*, 2002). This is thought to be due to the higher prevalence of HV strains in Asia and Africa (Ko *et al.*, 2002). Mortality rates of 50% and higher have been reported in *K. pneumoniae* pneumonia (Podschun & Ullmann, 1998).

UTIs are the most prevalent type of nosocomial infection caused by *K. pneumoniae* and are routinely treated with antibiotics (Chung, 2016, Paczosa & Mecsas, 2016). UTIs are thought to arise from the dissemination of bacteria from the gastrointestinal (GI) tract (Rodríguez-Baño *et al.*, 2008). This is of growing concern considering the increasing GI carriage of antibiotic-resistant *K. pneumoniae* (Wu *et al.*, 2014, Jacobsen *et al.*, 2008). The subsequent seeding of these strains into the bladder results in UTIs that are potentially recalcitrant to traditional antibiotic treatment and this may result in prolonged treatment and increased morbidity (Paczosa & Mecsas, 2016, Jacobsen *et al.*, 2008, Wu *et al.*, 2014).

The aforementioned nosocomial infections are frequently associated with indwelling medical devices, including ventilators and catheters. Device insertion can cause host tissue damage, expose additional adhesion sites and disrupt host immune defences (Murphy *et al.*, 2013). This is of grave concern due to the tenacity and increased antibiotic resistance associated with biofilm communities (Donlan, 2001). *Klebsiella* species are a predominant cause of ventilator-associated pneumonia (Kalanuria *et al.*, 2014) and catheter-associated UTIs account for 97% of nosocomial *K. pneumoniae* UTIs (Chung, 2016). These infections are facilitated by the innate ability of *K. pneumoniae* to form biofilms and adhere to such indwelling medical devices (Martin & Bachman, 2018).

Bacteraemia is an extremely concerning consequence of *K. pneumoniae* pneumonias and UTIs (Tsai *et al.*, 2010). Lung and bladder infections caused by Multidrug resistant (MDR) *K. pneumoniae* tend to be of a prolonged duration and this increases the chance of bacterial invasion into the bloodstream (Paczosa & Mecsas, 2016). After *E. coli*, *K. pneumoniae* is the second leading cause of bacteraemias, among Gram-negative pathogens, and is associated with mortality rates of up to 37% (Magill *et al.*, 2014, Paczosa & Mecsas, 2016).

The success of *K. pneumoniae* in establishing infection in a variety of sites in a host is enhanced by the production of a wide range of virulence factors.

1.2 Virulence factors

The four best characterised virulence factors of *K. pneumoniae* are capsule, lipopolysaccharide (LPS), fimbriae, and siderophores (Paczosa & Mecsas, 2016). Other

less characterised factors include outer membrane proteins (OMPs) and the efflux pump AcrAB-TolC (Paczosa & Mecsas, 2016). It is apparent from these virulence factors that in order to protect itself from the host immune system, *K. pneumoniae* relies on defensive strategies as opposed to offensive mechanisms (Paczosa & Mecsas, 2016). Figure 1.1 is a schematic representation of the virulence factors of *K. pneumoniae*.

1.2.1 Capsule Polysaccharide

The capsule polysaccharide (CPS) is one of the most important and most extensively studied virulence factors of *K. pneumoniae* (Martin & Bachman, 2018). The polysaccharide matrix is approximately 160 nm thick and made up of two layers of fibres, which differ in arrangement (Amako *et al.*, 1988). The inner layer comprises thick, dense bundles of fibres which stand at right angles on the outer membrane (OM) surface, while a random arrangement of fine fibre networks make up the outer layer of the capsule (Amako *et al.*, 1988).

The protective element of the capsule against the host immune system is due to a variety of mechanisms which include the generation of biofilm; the inhibition of phagocytosis; the prevention of early immune response activation; and the abrogation of lysis by complement proteins and antimicrobial peptides (Paczosa & Mecsas, 2016, Seifi *et al.*, 2016).

1.2.1.1 Serological types

Capsular polysaccharides are called K antigens and are strain-specific (Patro & Rathinavelan, 2019). The repeating capsular polymers are composed of four to six monosaccharides which can include L-fucose, D-galactose, D-glucose, D-mannose, and L-rhamnose (Patro & Rathinavelan, 2019). Uronic acids are also common components and are responsible for the negative charge of K antigens (Podschun & Ullmann, 1998). The variability in sugar composition of CPS greatly enhances the evasion of *Klebsiella* from the host immune system (Patro & Rathinavelan, 2019).

Klebsiella can be divided into 79 serological types (Pan *et al.*, 2015), and 25 serotypes are responsible for over 70% of the strains isolated from clinical samples (Cryz *et al.*, 1986). This suggests an association exists between the K antigen expressed by the infecting strain and the severity of infection (Mizuta *et al.*, 1983). K1 and K2 strains are

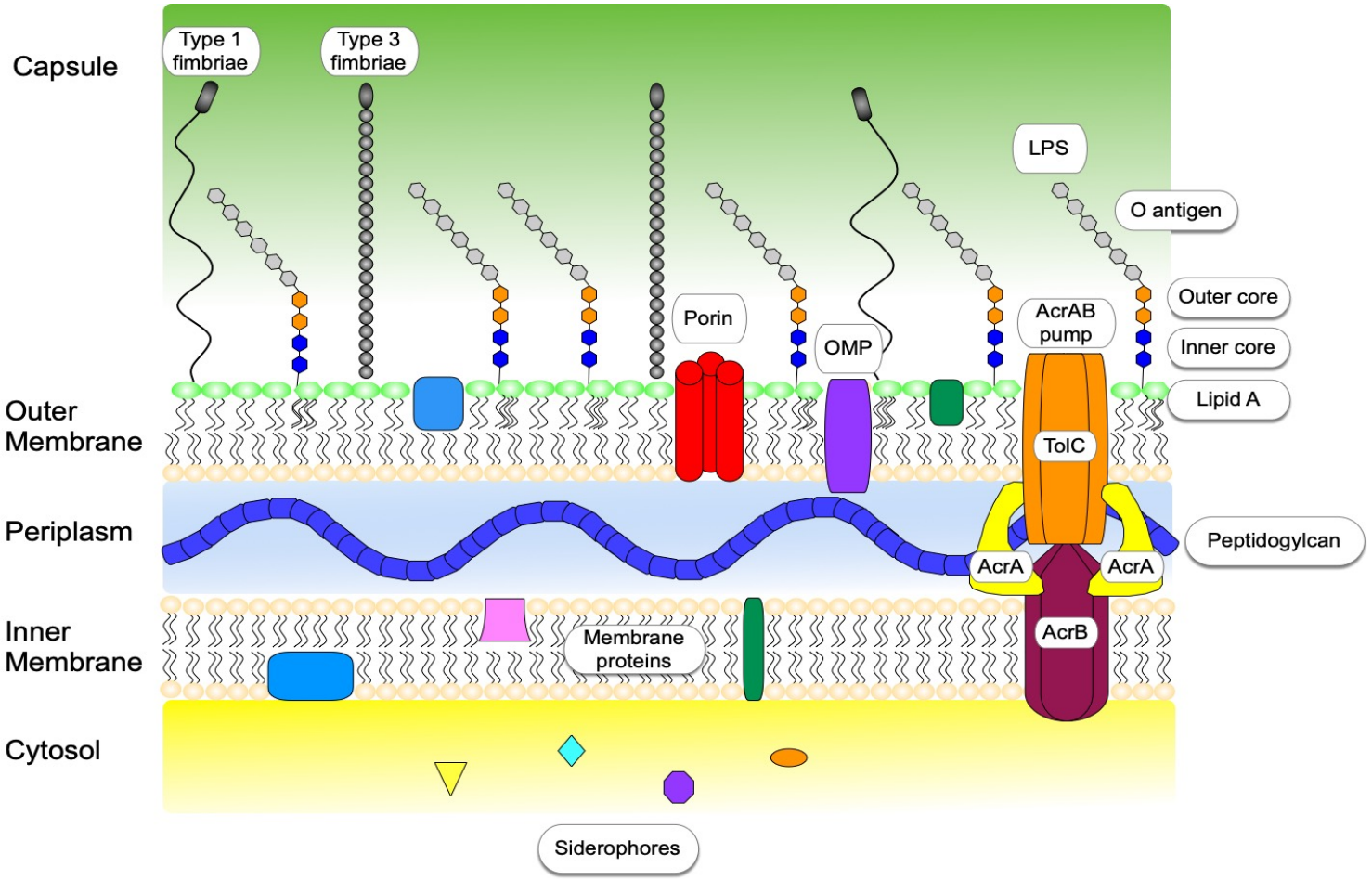

Figure 1.1: The cell envelope of *K. pneumoniae* with key virulence factors. The virulence factors of *K. pneumoniae* include capsule; fimbriae; porins; OMPs; AcrAB-TolC pump; LPS; and siderophores.

both the most prevalent and virulent (Mizuta *et al.*, 1983). Acapsular mutant strains are profoundly less virulent than encapsulated strains; the lack of CPS affects the ability of the strain to cause pneumonia and UTIs (Cortés *et al.*, 2002, Yoshida *et al.*, 2000, Lawlor *et al.*, 2005, Tomás *et al.*, 2015).

1.2.1.2 The CPS operon

The chromosomal operon, *cps*, harbours the genes required for capsule production and diversity is evident in this gene cluster both between and within strains (Paczosa & Mecsas, 2016). The *cps* gene cluster is composed of a conserved and a hyper-variable region (Lin *et al.*, 2017). Figure 1.2 is a schematic overview of the CPS operon of *Klebsiella* capsular serotype K2. The conserved region consists of six genes at the 5' end of the cluster with > 50% nucleotide sequence similarity among serotypes, namely *galF*, ORF2*, wzi*, *wza*, *wzb* and *wzc*, along with *gnd* at the 3' end (Pan *et al.*, 2008, Lin *et al.*, 2017, Shu *et al.*, 2009). In contrast, the central region of the operon is highly divergent and serotype specific, encoding proteins involved in the polymerization and assembly of CPS subunits (Shu *et al.*, 2009, Arakawa *et al.*, 1995). The genes downstream of *wzc* and upstream of *gnd* vary depending on capsule type and constitute the hypervariable region (Pan *et al.*, 2013). The *wzc* gene also has three variable regions which are flanked by conserved regions and thus a *wzc* genotyping system has been developed (Pan *et al.*, 2013). It was noted that across this variable *wzc* region, strains with the same K type exhibited ≧ 94% DNA sequence identity, while < 80% DNA sequence identity was evident among strains with distinct capsular types (Pan *et al.*, 2013). Details of the CPS cluster genes of capsular serotype K2 are listed in Table 1.1.

1.2.1.3 Phenotypic characterisation

The prominent capsule expressed by most *K. pneumoniae* isolates is responsible for the characteristic mucoid phenotype when grown on agar plates (Struve & Krogfelt, 2003). This is typical of all capsulated bacterial strains (Catalán-Nájera *et al.*, 2017). Nassif *et al.* postulated that this mucoid phenotype can be attributed to a virulence plasmid, pKP100, containing the gene *rmpA* (regulator of mucoid phenotype) (Nassif *et al.*, 1989). The *wzy* gene, located in the *cps* gene cluster, is also thought to contribute to the mucoid phenotype (Catalán-Nájera *et al.*, 2017, Pan *et al.*, 2013). A distinction exists between

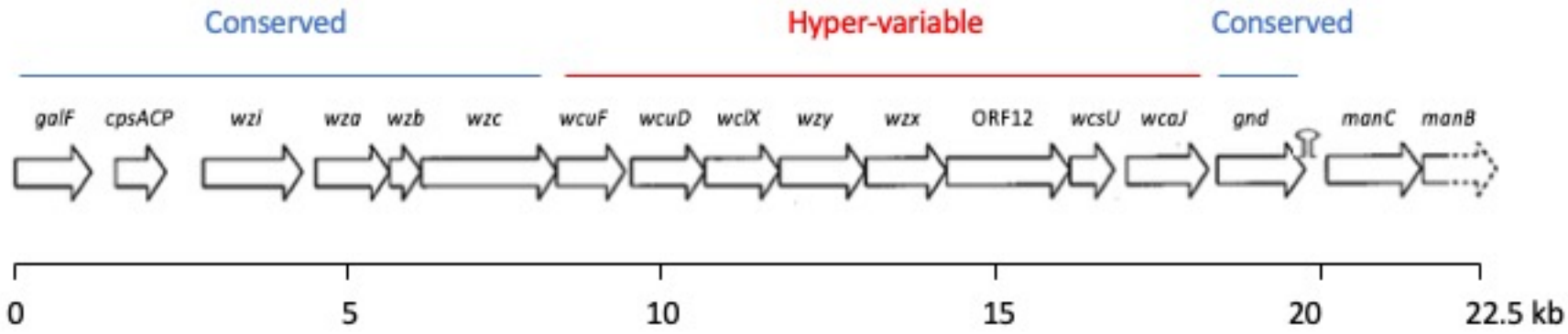

Figure 1.2: The CPS operon of *Klebsiella* capsular serotype K2. Open arrows indicate the putative positions of open reading frames (ORFs). Conserved and hyper-variable regions are indicated above the ORFs. Note: three variable regions exist in *wzc* (not shown) which are flanked by conserved regions. An approximate kb scale is located below the ORFs. Modified from (Arakawa *et al.*, 1995).

Table 1.1 Products and functions of genes in the CPS operon of *Klebsiella* capsular type K2

Gene	Product	Function	Reference
galF	UDP-glucose pyrophosphorylase	Carbohydrate metabolism	(Pan *et al.*, 2015)
cpsACP	Acid phosphatase	Carbohydrate metabolism	(Pan *et al.*, 2015)
wzi	OM lectin	Surface assembly of capsule	(Brisse *et al.*, 2013)
wza	Capsule polysaccharide export protein	Translocation channel; export polymer to bacterial surface	(Whitfield, 2006)
wzb	Protein tyrosine phosphatase	Dephosphorylate Wzc	(Whitfield, 2006)
wzc	Inner membrane (IM) periplasmic auxiliary protein	Part of trans-envelope translocation channel	(Whitfield, 2006)
wcuF	Glycosyltransferase	Catalyse the formation of the glycosidic linkage; glycoside formation	(Pan *et al.*, 2015)
wcuD	Glycosyltransferase	Catalyse the formation of the glycosidic linkage; glycoside formation	(Pan *et al.*, 2015)
wclX	Glycosyltransferase	Catalyse the formation of the glycosidic linkage; glycoside formation	(Pan *et al.*, 2015)
wzy	Polymerase	Assemble lipid-linked repeat units	(Whitfield & Roberts, 1999)
wzx	Flippase	Flip lipid-linked repeat units across the plasma membrane	(Whitfield & Roberts, 1999)
ORF12	Hypothetical protein	Unknown	(Pan *et al.*, 2015)
wcsU	Acetyltransferase	Capsule modification	(Pan *et al.*, 2015)
wcaJ	Glycosyltransferase	Catalyse the formation of the glycosidic linkage; glycoside formation	(Pan *et al.*, 2015)
gnd	Glucose-6-phosphate dehydrogenase	Carbohydrate metabolism	(Pan *et al.*, 2008)
manC	Mannose-1-phosphate guanylyltransferase	GDP-D-mannose synthesis	(Pan *et al.*, 2015)
manB	Phosphomannomutase	GDP-D-mannose synthesis	(Pan *et al.*, 2015)

the mucoid phenotype and a hypermucoviscous (HMV) phenotype; hypermucoviscosity is characterised by the formation of a viscous string ≧ 5 mm when a colony from an agar plate is stretched with a bacteriological loop (Catalán-Nájera *et al.*, 2017). The HMV phenotype has been associated with hypervirulence (Catalán-Nájera *et al.*, 2017).

1.2.2 Lipopolysaccharide

Lipopolysaccharide (LPS), a major component of the OM of Gram-negative bacteria, generally consists of a highly conserved lipid A core and highly variable repeating O antigen subunits (Ciurana & Tomás, 1987). O1 is the most common O antigen type in *Klebsiella* of the 9 identified thus far (Doorduijn *et al.*, 2016). Smooth LPS consists of long O antigen, whereas LPS is considered rough when O antigen side chains are either reduced or absent (Doorduijn *et al.*, 2016). While acting as an important virulence factor against humoral defenses, LPS can also pose as a hindrance for *K. pneumoniae* during infection. Lipid A is a potent ligand of Toll-like receptor 4 (TLR4), whose stimulation activates cellular responses which enables the prevention of spread and clearance of *K. pneumoniae* infection (Paczosa & Mecsas, 2016). Certain strains, such as those expressing K1, K10 and K16 capsule antigens have the ability to mask their LPS from detection by TLRs, while other strains, such as those with K2 antigens lack this ability (Merino *et al.*, 1992).

1.2.3 Fimbriae

With regards to pathogenesis, type 1 and 3 fimbriae are the predominant adhesin structures of *K. pneumoniae* (Paczosa & Mecsas, 2016). Type 1 fimbriae, filamentous structures that protrude from the bacterial cell surface, are the most common adhesive organelle in *Enterobacteriaceae*, being expressed in 90% of both environmental and clinical *K. pneumoniae* isolates (Stahlhut *et al.*, 2009). Type 1 fimbriae contribute to both bladder cell invasion and biofilm formation in the bladder thus playing a significant role in UTIs (Struve *et al.*, 2009). FimA is the major subunit of type 1 fimbriae, while FimH acts as the adhesin on the tip (Stahlhut *et al.*, 2009). Due to their ability to bind D-mannosylated glycoproteins, type 1 fimbriae are commonly referred to as 'mannose-sensitive' (Kline *et al.*, 2009). This is in contrast to type 3 fimbriae, helix-like structures, which are termed 'mannose-resistant' due to their affinity for extracellular matrix

proteins (i.e. type IV and V collagens) as opposed to mannose (Paczosa & Mecsas, 2016, Sebghati *et al.*, 1998). MrkA is the major subunit of type 2 fimbriae, responsible for abiotic surface binding, while MrkD on the tip binds extracellular matrix-coated surfaces (Jagnow & Clegg, 2003). Unlike their type 1 counterparts, type 3 fimbriae do not appear to contribute to UTIs, instead playing a role in ventilator-associated *pneumonia* (Ramirez *et al.*, 2012, Jagnow & Clegg, 2003). Similar to LPS, fimbriae can also hinder the success of *K. pneumoniae* infection by increasing their binding to phagocytes, prompting phagocytosis and ultimately resulting in internalisation and killing (Athamna *et al.*, 1991).

1.2.4 Siderophores

Within the bloodstream, the concentration of free iron is 10^{11} lower than that required by bacteria in order to survive (Malachowa & DeLeo, 2011). To restrict pathogen growth, iron is sequestered by the host (Bullen *et al.*, 1972); circulating iron is generally bound to storage molecules such as ferritin and hemosiderin (Malachowa & DeLeo, 2011). In order to thrive during infection, *K. pneumoniae* must employ iron acquisition strategies (Paczosa & Mecsas, 2016).

The secretion of siderophores, small ferric iron (Fe^{3+}) chelating molecules with a higher affinity for iron than host transport proteins, is the predominant strategy utilized by *K. pneumoniae* along with many other pathogens (Holden *et al.*, 2016, Wilson *et al.*, 2016). Siderophores can both scavenge iron from the environment and steal it from host iron chelators (Miethke & Marahiel, 2007). Subsequent to iron capture, ferric siderophores are imported by bacteria through siderophore-specific OM receptors (OMRs) into the periplasm, with the aid of the IM TonB-ExbB-ExbD complex (Lau *et al.*, 2016, Holden *et al.*, 2016). TonB is an IM protein that bridges the Gram-negative cell envelope (Klebba, 2016). The conformational shift of TonB, upon interacting with an OMR, is driven by IM proteins ExbB and ExbD, and by the electrochemical proton gradient across the IM (Klebba, 2016). This change in conformation promotes the uptake of ferric-siderophore complexes (Klebba, 2016). A periplasmic binding protein initiates the transport of this complex across the cytoplasmic membrane (Lau *et al.*, 2016). Upon entering the cell, Fe^{3+} is reduced to ferrous iron, allowing free intracellular iron to be incorporated into metallo-proteins to be used for various biological processes (Lau *et al.*, 2016). Various

siderophores, ranging in affinity, are expressed by *K. pneumoniae*, including enterobactin (highest affinity), yersiniabactin, salmochelin, and aerobactin (lowest affinity) (Paczosa & Mecsas, 2016). The expression and virulence contribution of each siderophore differ (Holden & Bachman, 2015). While enterobactin is almost ubiquitous among both classical and HV *K. pneumoniae* strains, the expression of yersiniabactin, salmochelin, and aerobactin is less conserved (Podschun *et al.*, 1993, Paczosa & Mecsas, 2016). Russo *et al.* found that aerobactin, but not the other three aforementioned siderophores, is required by HV *K. pneumoniae* to successfully establish infection in pneumonic mouse models (Russo *et al.*, 2015).

1.2.5 OMPs

OMPs constitute to approximately 50% of the OM of Gram-negative bacteria (Lin *et al.*, 2002). Various OMPs play important roles in *K. pneumoniae* virulence. Outer membrane protein A (OmpA) is one of the best characterised OMPs (March *et al.*, 2011) and offers protection against the innate immune response (Smith *et al.*, 2007). OmpA, an eight-stranded β-barrel, is targeted by neutrophil elastase which results in bacterial cell death, and serum amyloid A which leads to increased phagocytosis (March *et al.*, 2011, Smith *et al.*, 2007). OmpA acts as an immune evasin; an *ompA* mutant, in comparison to the WT strain, activates higher levels of inflammatory mediators and is attenuated in a pneumonia mouse model (March *et al.*, 2011). OmpA also plays a role in conferring resistance against antimicrobial peptides (AMPs) through its activation of uncharacterised systems that ameliorate cytotoxicity of AMPs (Llobet *et al.*, 2009). An *ompA* mutant, in comparison to a WT strain, displays more susceptibility to AMPs (Llobet *et al.*, 2009).

Porins are a class of OMPs that function as water filled protein channels to enable the transport of small hydrophilic molecules, such as nutrients, iron and antibiotics, across the OM (Tsai *et al.*, 2011). Porins also play a vital role in the maintenance of cell integrity, in conjunction with LPS and peptidoglycan (Albertí *et al.*, 1995). OmpK35 and OmpK36 are major porins of *K. pneumoniae* that are homologous to two extensively studied porins of *E. coli*, OmpF and OmpC respectively (Tsai *et al.*, 2011). The loss of both OmpK35 and OmpK36 results in significantly lower virulence of *K. pneumoniae* in mouse peritonitis models (Tsai *et al.*, 2011). The resulting modification of the surface structure

of *K. pneumoniae* porin mutants enables enhanced neutrophil binding and thus increases susceptibility to neutrophil phagocytosis; the exact mechanism of which is yet to be determined (Tsai *et al.*, 2011). Contrarily, the deletion of porins can prevent entry of certain antibiotics into the bacterial cell (Choi & Lee, 2019). *K. pneumoniae* strains lacking both porins have displayed higher antibiotic resistance when compared to strains expressing one or both porins (Hernández-Allés *et al.*, 2000). Tsai *et al.* postulate that OmpK35 and OmpK36 play dual roles in *K. pneumoniae* infection; porin deficiency could simultaneously increase antibiotic resistance while decreasing virulence (Tsai *et al.*, 2011).

1.2.6 AcrAB pump

The AcrAB efflux pump contributes to both *K. pneumoniae* virulence and antibiotic resistance (Padilla *et al.*, 2010). AcrB is an antiporter located in the IM responsible for the recognition of substrates and TolC is an OM protein necessary for the expulsion of harmful compounds, including particular AMPs and antibiotics, from the bacterial cell (Pos, 2009, Eswaran *et al.*, 2003). AcrA, a periplasmic protein anchored to the IM, acts as a fusion protein between AcrB and TolC (Pos, 2009). The AcrAB pump contributes to the MDR phenotype of *K. pneumoniae* and mediates resistance to lung AMPs which facilitates the onset of pneumonia (Padilla *et al.*, 2010).

1.3 Biofilm

The formation of biofilms, an accumulation of bacteria encased in an extracellular matrix (ECM) (Donlan, 2002), is one of the predominant virulence factors of *K. pneumoniae* (Seifi *et al.*, 2016). The ability of *K. pneumoniae* to form biofilms was first described in 1988 (LeChevallier *et al.*, 1988) and it is now known that they underpin the majority of device-related infections (Donlan, 2002, Vuotto *et al.*, 2014, Singh *et al.*, 2019). Figure 1.3 is a schematic diagram of the stages of biofilm formation.

1.3.1 Factors influencing biofilm development of *K. pneumoniae*

1.3.1.1 Growth conditions

Several factors influence biofilm development in *K. pneumoniae* and these include temperature, pH, the nature and concentration of the carbon source, incubation length,

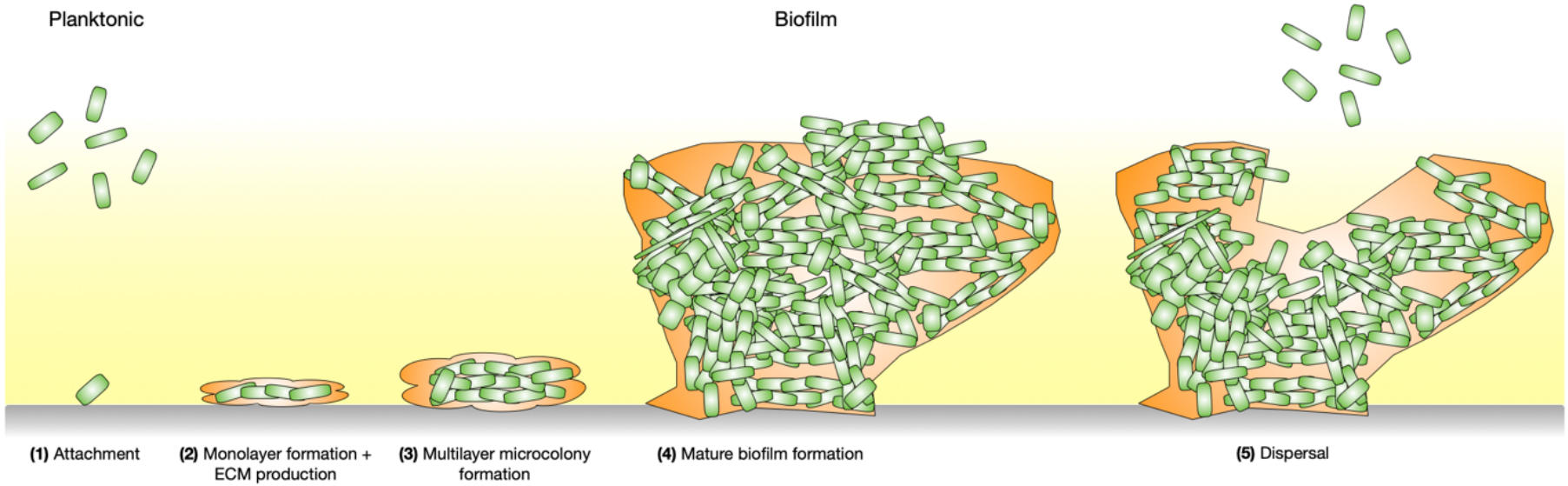

Figure 1.3: Stages of biofilm formation. (1) Reversible attachment of planktonic cells (green rods) to a surface (grey). **(2)** Formation of a monolayer and production of an ECM (orange), resulting in irreversible attachment. **(3)** Formation of a multilayer microcolony. **(4)** Maturation of the biofilm. **(5)** Detachment and reversion of some cells to planktonic growth resulting in dispersal of the biofilm. Adapted from (Vasudevan, 2014).

etc. (Singh *et al.*, 2019). A review of the literature suggests that the formation of bacterial biofilms can be markedly different and dependent on growth media composition. Differences in methodology or strain characteristics might account for these discrepancies (Naves *et al.*, 2008, Reisner *et al.*, 2006).

In general, the abundance of available nutrients in growth media influences the development and composition of the biofilm (Singh *et al.*, 2019, Bowden & Li, 1997). In comparison to many media, including Luria-Bertani (LB) broth and tryptic soy broth, various studies determined Brain Heart Infusion (BHI) broth, a nutrient-rich media, to be the most conducive media for biofilm generation in *K. pneumoniae*, *E. coli* and *Pseudomonas aeruginosa* (Wijesinghe *et al.*, 2019, Singh *et al.*, 2019, Skyberg *et al.*, 2007). BHI is rich in amino acids which are required for the formation of fimbriae and pili which mediate adherence (Singh *et al.*, 2019). BHI also contains lipids, such as choline, which enhance biofilm formation by providing resistance to desiccation (Singh *et al.*, 2017). The supplementation of media with a range of components has also been studied extensively. Biofilm formation was found to be greatly impacted by the addition of fatty acids, glucose or casamino acids to the growth media (Pratt & Kolter, 1998, Skyberg *et al.*, 2007, Lin *et al.*, 2016, Hobby *et al.*, 2019). An increase in the production of CPS and MrkA has been observed by Lin *et al*. in response to exogenous glucose (Lin *et al.*, 2016, Lin *et al.*, 2013b). Cyclic AMP (cAMP), a second messenger, plays a vital role in the global regulation of genes, *via* its interaction with the cAMP receptor protein (CRP) (Lin *et al.*, 2016). Glucose lowers the intracellular level of CRP-cAMP complex which results in catabolite repression (Ishizuka *et al.*, 1994), a hierarchal sugar utilisation system whereby bacteria preferentially catabolise glucose over other carbon sources (Aidelberg *et al.*, 2014).

On the contrary, increased biofilm formation has also been observed under nutrient-limited conditions (i.e. minimal media) (Skyberg *et al.*, 2007, Reisner *et al.*, 2006, Naves *et al.*, 2008, Dewanti & Wong, 1995). The abundance of proteins in growth media has been reported to impair attachment of bacteria to abiotic surfaces and increase dispersal of biofilms (Helke *et al.*, 1993, Fletcher, 1976, Alonso & Kabuki, 2019). Additionally, a significant increase in both ECM production and more specifically, ECM-associated proteins, has been associated with biofilms generated in low-nutrient

environments (Dewanti & Wong, 1995, Zhang *et al.*, 2015). It has been postulated that the increase in cell mass enables sedimentation to the surface, leading to a higher degree of initial attachment and subsequent ECM production further stabilises of the biofilm (Dewanti & Wong, 1995, Flemming & Wingender, 2010).

1.3.1.2 Capsule expression

The CPS of *K. pneumoniae* is widely known as a predominant virulence factor in the formation of biofilm (Seifi *et al.*, 2016, Schembri *et al.*, 2005, Boddicker *et al.*, 2006). Mutations in genes involved in CPS synthesis resulted in biofilm deficiency (Boddicker *et al.*, 2006, Wu *et al.*, 2011). On the other hand, there are a multitude of studies that provide evidence for the contrary; capsule in fact negatively impacts adhesion and biofilm formation (Huang *et al.*, 2014a, Favre-Bonte *et al.*, 1999). The biofilm formation of HMV (can be partly attributed to capsule overproduction (Walker & Miller, 2020)) and non-HMV strains of *K. pneumoniae* was compared and a significantly larger amount of biofilm was produced by the non-HMV strains (Fuursted *et al.*, 2012, Soto *et al.*, 2017). There are multiple theories as to the role capsule plays in negatively impacting the formation of biofilm.

The expression and function of adhesion factors CF29K and Antigen 43 (Ag43), respectively, are affected by the presence of capsule (Schembri *et al.*, 2004, Favre-Bonte *et al.*, 1999). These adhesins are cell-surface proteins expressed by *K. pneumoniae* strains which enhance biofilm formation (Di Martino *et al.*, 2003, Schembri *et al.*, 2004). CF29K mediates adherence to certain human intestinal cell lines and Ag43 confers bacterial cell-to-cell aggregation (Darfeuille-Michaud *et al.*, 1992, Schembri *et al.*, 2004). While the expression of CF29K could be modulated by capsule at a transcriptional level (Schembri *et al.*, 2004), capsule sterically interferes with the adhesive function of Ag43 (Favre-Bonte *et al.*, 1999). This negative influence of CPS on biofilm formation is thought to be due to the putative relationship between the capsule and fimbriae of *K. pneumoniae* (Schembri *et al.*, 2004, Schembri *et al.*, 2005, Cubero *et al.*, 2019).

1.3.1.3 Fimbriae

Fimbriae, the adhesion mediators of *K. pneumoniae*, play important roles in biofilm formation and abiotic surface (i.e. catheters) binding (Paczosa & Mecsas, 2016). Both type 1 and type 3 fimbriae have been shown to play a role in the development of biofilm.

Di Martino *et al*. theorized that type 3-dependent adherence may be the primary step in the generation of biofilm by *K. pneumoniae* (Di Martino *et al.*, 2003). Langstraat *et al.* established that MrkA, the fimbrial shaft protein, is the determining component of type 3 fimbriae for biofilm formation, as opposed to MrkD, the fimbrial adhesin (Langstraat *et al.*, 2001). The hydrophobicity of MrkA protein may facilitate bacterial interactions that enhance biofilm growth (Langstraat *et al.*, 2001).

The interaction of fimbriae type 1 and the capsule of *K. pneumoniae* has also been studied to decipher the effect this relationship has on biofilm development. Capsule has been found to physically interfere with the FimH adhesin by way of masking the adhesin with capsular material, among other mechanisms and fimbrial function can be restored upon the inhibition of CPS synthesis (Schembri *et al.*, 2005).

1.3.3 Clinical significance of biofilms

Biofilm infections, in general, are of major clinical significance due to their high frequency in infected patients and their resistance to antibiotic treatment (Römling & Balsalobre, 2012). It is proposed that the vast majority of infections, up to 80%, can be attributed to biofilm formation on either abiotic (i.e. indwelling medical devices) or biotic surfaces (de la Fuente-Núñez *et al.*, 2013, Römling & Balsalobre, 2012). The ability of *K. pneumoniae* to form biofilms is a major contributing factor to its pathogenic success (Chung, 2016). Bacterial cells enclosed in biofilms are partly shielded from the host's immune system; the ECM can provide protection to underlying bacterial cells against antibodies and AMPs as well as inhibiting phagocytosis by polymorphonuclear leukocytes (Piperaki *et al.*, 2017, Römling & Balsalobre, 2012).

In addition to immune evasion, biofilms can tolerate antibiotic concentrations up to 1000 times higher than the MIC for planktonic cells (Roberts *et al.*, 2015). There are several proposed mechanisms underlying this recalcitrance, depending on the type of biofilm-forming bacterium and the type of antibiotic treatment (Römling & Balsalobre,

2012). Firstly, long-term and recurrent antibiotic therapy is frequently required by biofilm infections which in turn exposes bacteria to prolonged antibiotic selection pressure (Fux *et al.*, 2005). Secondly, biofilm physiology plays an integral role in dictating antibiotic resistance (Fux *et al.*, 2005). The ECM can contribute to antimicrobial resistance (AMR) by facilitating the accumulation of β-lactamases as well as initiating adaptive resistance strategies (de la Fuente-Núñez *et al.*, 2013). Persister cells, dormant variants of regular cells which can be found in the 'inner core' of biofilms, can survive bactericidal antibiotics which target metabolically active cells (Piperaki *et al.*, 2017, Lewis, 2010). Complex regulatory pathways, such as stringent response, associated with nutrient limitations, may also contribute to persister cell resistance (de la Fuente-Núñez *et al.*, 2013). Finally, in addition to their contribution to the emergence of AMR, biofilms can also enable the spread of antibiotic resistance by promoting horizontal gene transfer or exhibiting adaptive mutations (Fux *et al.*, 2005).

1.4 MDR

The pangenome of *K. pneumoniae* is highly plastic and divergent, harbouring a multitude of accessory genes that enable the survival of the bacterium in hostile habitats and its resistance to environmental stresses (Moradigaravand *et al.*, 2017). One such environmental stress is antibiotic treatment. The increasing emergence of MDR *K. pneumoniae* has made the treatment of such bacterial infections increasingly challenging (Moradigaravand *et al.*, 2017). Infections caused by MDR *K. pneumoniae* are of grave concern worldwide due to their association with high mortality rates (Viale *et al.*, 2013). Figure 1.4 is a schematic representation of the antibiotic resistance mechanisms of *K. pneumoniae*.

1.4.1 β-lactams

β-lactam antibiotics interact with penicillin-binding proteins, inhibiting cell wall synthesis (Kapoor *et al.*, 2017). β-lactam resistance emerged before the widespread use of penicillin (Medeiros, 1984). β-lactamase is an enzyme that hydrolyses the β-lactam ring thus inactivating the antibiotic (Martin & Bachman, 2018). β-lactamases can be categorized into four classes on the basis of protein homology, according to the Ambler system (classes A to D); or on the basis of functional similarities, i.e. substrate and

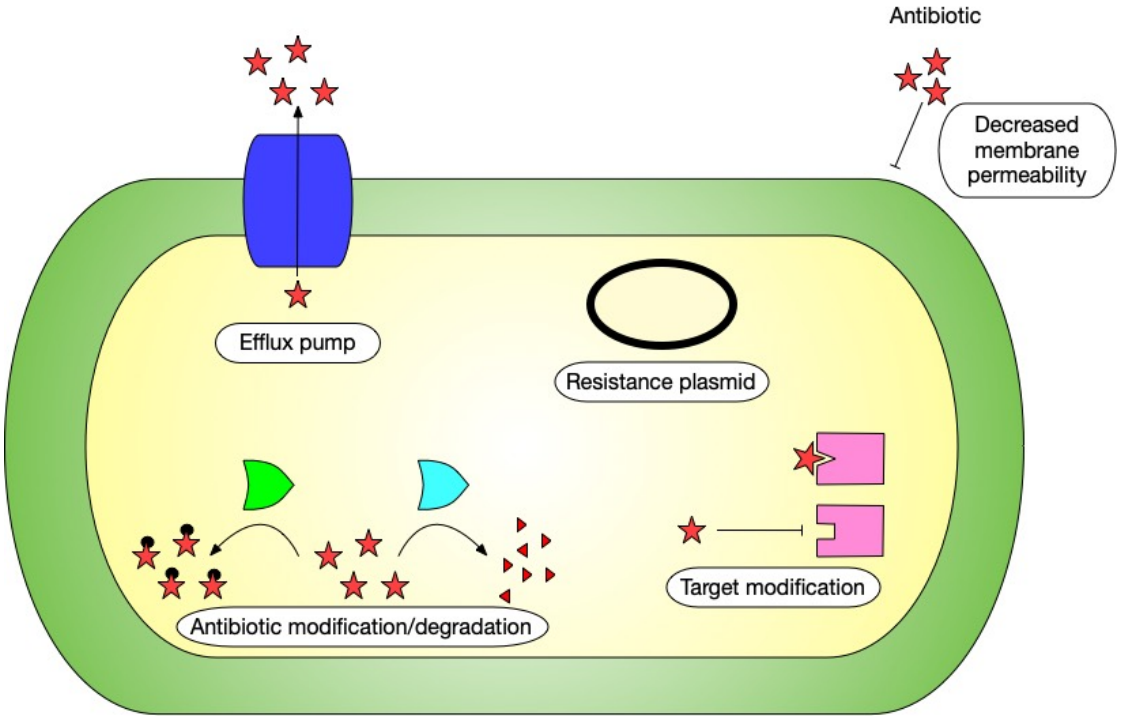

Figure 1.4: Antibiotic resistance mechanisms of *K. pneumoniae*. *K. pneumoniae* utilise a variety of antibiotic resistance mechanisms. Efflux pumps transport antibiotics out of the cell; resistance plasmids encode antibiotic resistance genes; cell membrane permeability is altered to inhibit the entry of antibiotics into the cell; antibiotics are inactivated by modification or degradation; antibiotic targets are modified to prevent/hinder antibiotic binding. The area shaded green represents the capsule. The area shaded yellow represents the cytosol. A red star represents an antibiotic molecule; the addition of a black circle represents a modified antibiotic molecule. A red triangle represents a degraded antibiotic molecule. The dark blue cylinder represents an efflux pump. The black oval represents a resistance plasmid. The green and blue semi-circle-like shapes represent enzymes. The pink square represents an antibiotic target.

inhibitor profile, according to the Bush-Jacoby-Medeiros system (classes 1 to 4, including subgroups) (Rawat & Nair, 2010). β-lactamases of *K. pneumoniae* can be encoded in the core genome, ensuring intrinsic resistance; and the accessory genome i.e. plasmid-mediated AmpC enzymes (Martin & Bachman, 2018). Extended-Spectrum β-Lactamases (ESBLs) are plasmid-mediated resistance mechanisms which form part of the accessory genome and have the ability to hydrolyse oxyiminocephalosporins (i.e. third-generation cephalosporins) (Bush *et al.*, 1995). Plasmids encoding β-lactamases often contain resistance genes to other antibiotics (Jacoby & Sutton, 1991). The combination of clavulanic acid, a β-lactamase inhibitor, with a β-lactam antibiotic such as amoxicillin (i.e. co-amoxiclav) is routinely used to treat UTIs caused by ESBL-producing bacteria (O'Kelly *et al.*, 2016). While ineffective by itself as an antibiotic, clavulanic acid inhibits ESBLs thus allowing for antibiotic resistance to be overcome in β-lactamase producing bacteria (Bush et al., 1995). Infections caused by ESBL-producing bacteria are typically treated with carbapenems (Martin & Bachman, 2018).

1.4.2 Carbapenems

Carbapenems are a class of β-lactam antibiotics that are relatively resistant to hydrolysis by most β-lactamases (Papp-Wallace *et al.*, 2011). It is postulated that carbapenem resistance emerged due to the selective pressure from prescribing carbapenems for ESBL infections (Martin & Bachman, 2018). The most common carbapenem-resistant *Enterobacteriaceae* (CRE) is *K. pneumoniae* (Martin & Bachman, 2018). In 2013, the Centre for Disease Control and Prevention (CDC) established that *Klebsiella* species were responsible for ~ 80% of 9000 infections due to CRE (CDC, 2014). The accessory genome, occasionally in combination with core genome mutations, predominantly drives carbapenem resistance (Martin & Bachman, 2018). The upregulation of efflux pumps and modification of OMPs in the core genome as well as hyperproduction of ESBL enzymes or AmpC β-lactamases in the accessory genome all contribute to carbapenem resistance in *K. pneumoniae* (Martin & Bachman, 2018).

According to the Ambler classification, three classes of carbapenemases, which are plasmid-encoded, exist in *Enterobacteriaceae*; class A, B and D (Nordmann, 2014). The most common carbapenemases found in *K. pneumoniae* are *K. pneumoniae* carbapenemase (KPC) β-lactamases, which are class A serine carbapenemases (Martin

& Bachman, 2018). β-lactamase inhibitors, particularly clavulanic acid, inhibits this first group, with the exception of KPCs (Nordmann, 2014, Papp-Wallace *et al.*, 2010). Class B, metallo-enzymes, have the ability to hydrolyse all antibiotics excluding aztreonam (Nordmann, 2014). NDM-1 is one of the best known metallo-proteins (Nordmann, 2014). The final group, class D, is that of oxacillinases, OXA-48 derivatives (Nordmann, 2014). This class hydrolyse penicillins, 1st generation cephalosporins and carbapenems; display resistance to β-lactamase inhibitors; and are weakly active against 2nd and 3rd generation cephalosporins (i.e. cefotaxime or ceftazidime) (Nordmann, 2014).

1.4.3 Fluoroquinolones

Fluoroquinolones are a bactericidal class of antibiotics that act as inhibitors of bacterial DNA gyrase (Walker & Wright, 1991). *K. pneumoniae* employs various fluoroquinolone resistance mechanisms which include mutations in DNA gyrase and topoisomerase IV, resistance plasmids, and efflux systems (i.e. AcrAB pump) (Padilla *et al.*, 2010).

1.4.4 Colistin

Colistin belongs to a class of antibiotics called the polymyxins (Martin & Bachman, 2018). Although used in the 1960s and 1970s, due to neurotoxicity and renal toxicity their use was discontinued (Jerke *et al.*, 2016). However, returning to colistin as a last resort drug has become necessary due to the recent CRE emergence (Martin & Bachman, 2018). The positive charge of colistin enables it to bind to the OM of Gram-negative bacteria, ultimately altering cell permeability and causing cell lysis and death (Ah *et al.*, 2014). In *K. pnemoniae*, mutations of the *mgrB* gene, responsible for lipid A modifications, result in the alteration of the negative charge of the OM (Ah *et al.*, 2014, Martin & Bachman, 2018). This reduces the affinity of colistin for its target and results in colistin resistance (Ah *et al.*, 2014). Colistin susceptibility was restored in *mgrB* complementation experiments involving the restoration of *mgrB* in mutants (Cannatelli *et al.*, 2014). However, even for the treatment of colistin-susceptible isolates, concern has arisen surrounding colistin monotherapy (Ah *et al.*, 2014, Poudyal *et al.*, 2008).

1.4.5 Combination antibiotic therapy

The practice of combination antibiotic therapy is generally justified by one or more of the following reasons: broadening the antibacterial spectrum; polymicrobial infections; synergy; and the prevention of AMR (Tamma *et al.*, 2012, Ahmed *et al.*, 2014). However, the combination of two antibiotics in the treatment of infections caused by MDR Gram-negative bacteria remains controversial and may in fact result in increased antibiotic resistance and adverse effects such as nephrotoxicity (Tamma *et al.*, 2012, Ahmed *et al.*, 2014). Following a review of the literature, Lee & Burgess recommended combination therapy for the treatment of KPC infections due to the significantly lower treatment failure rates compared to monotherapy (Lee & Burgess, 2012). Another retrospective study also deemed combination therapy superior for KPC infections (Qureshi *et al.*, 2012).

1.5 Scope of this study

Biofilms are germane and central to *K. pneumoniae* infection and antibiotic resistance.

This project aims to investigate biofilm formation determinants of *K. pneumoniae*. Hospital isolates are subsequently incorporated into biofilm studies in an attempt to decipher whether the observed effects of growth media on biofilm formation are more widely observed in the species of *Klebsiella*. The use of a bioluminescence system is evaluated as an alternative measurement of viability in biofilm formation assays.

Additionally, the construction of a CPS operon mutant is attempted in order to establish a role for capsule in biofilm formation. This study also sought to determine whether a relationship exists between the capsular type of *K. pneumoniae* and biofilm formation.

Finally, the genotype of the mutant *K. pneumoniae* strain used in this study is analysed with the intention of ascertaining the genotypic determinants of phenotypic characteristics, biofilm formation and antibiotic resistance observed in this study.

Chapter 2 Materials and Methods

2.1 General Methods

2.1.1 Bacterial strains and culture conditions

2.1.1.1 Bacterial strains

Details of the bacterial strains used in this study are listed in Table 2.1. Bacterial stocks were maintained in LB broth supplemented with 8.7% (v/v) dimethyl sulfoxide (DMSO) and stored at -80°C. Hospital isolates were initially received blinded, i.e. numerated, so as to be unidentifiable to the receiver. These isolates were then double-blinded, i.e. renumerated, so as to be unidentifiable to the provider; therefore ethics approval was not required.

2.1.1.2 Bacterial growth media

Bacteria were grown in LB broth (10 g/L tryptone, 5 g/L yeast extract, 5 g/L NaCl; Sigma); LB broth supplemented with 0.5% (w/v) glucose (Sigma); LB broth supplemented with 0.5% glycerol (Sigma); M9 minimal media (10x M9 salt solution (Na_2HPO_4, KH_2PO_4, NaCl, NH_4Cl), 20% (w/v) glucose, 1 M $MgSO_4$, 1 M $CaCl_2$); and Brain Heart Infusion (BHI) broth (5 g/L beef heart, 12.5 g/L calf brains, 2.5 g/L disodium hydrogen phosphate, 2 g/L D(+)-glucose, 10 g/L peptone, 5 g/L NaCl). Bacteria were also grown on LB agar (10 g/L tryptone, 5 g/L yeast extract, 10 g/L NaCl, 15 g/L agar; Sigma) and Columbia Blood Agar (0.5% peptone, 0.3% yeast extract, 1.5% agar, 0.5% NaCl, 5% horse blood; Fannin). Media were prepared using deionised H_2O and sterilised by autoclaving.

2.1.1.3 Bacterial culture conditions

Bacteria were regularly grown on LB agar plates overnight at 37°C. Liquid cultures were prepared by inoculating single colonies from agar plates into 10 ml of LB broth and grown overnight at 37°C with aerobic agitation. Exponential cultures were prepared by diluting overnight cultures 1:100 in fresh media and grown to an optical density (OD) 600_{nm} of ~ 0.6-0.8.

Table 2.1 Bacterial strains used in this study

Strain	Characteristics	Source or Reference
K. pneumoniae		
Kp52145	Clinical isolate; serotype O1:K2	(Nassif *et al*., 1989)
Kp52145 Δ*manC*	Capsule mutant	(Llobet *et al*., 2008)
44	Hospital isolate, Carbapenemase-Producing *Enterobacteriaceae* (CPE)	J. Fennell
56	Hospital isolate, CPE	J. Fennell
103	Hospital isolate, CPE	J. Fennell
202	Hospital isolate, CPE	J. Fennell
214	Hospital isolate, CPE	J. Fennell
226	Hospital isolate, CPE	J. Fennell
314	Hospital isolate, CPE	J. Fennell
344	Hospital isolate, CPE	J. Fennell
420[a]	Hospital isolate, CPE	J. Fennell
508	Hospital isolate, CPE	J. Fennell
510	Hospital isolate, CPE	J. Fennell
547	Hospital isolate, CPE	J. Fennell
576	Hospital isolate, CPE	J. Fennell
600.1[ab]	Hospital isolate, CPE	J. Fennell
600.2[b]	Hospital isolate, CPE	J. Fennell
602	Hospital isolate, CPE	J. Fennell
605	Hospital isolate, CPE	J. Fennell
611	Hospital isolate, CPE	J. Fennell
810	Hospital isolate, CPE	J. Fennell
900	Hospital isolate, CPE	J. Fennell
980	Hospital isolate, CPE	J. Fennell
E. coli		
CFT073	Urosepsis isolate; serotype O6:K2	(Mobley *et al.*, 1990)
W3110	K12; positive control for biofilm formation	C. Yanofsky
XL-1 Blue	K12; disrupted *wbbL*; negative control for O-antigen production	Stratagene (Agilent)

[a] Later identified as being *K. oxytoca*.

[b] Unknown to receiver whether numeration implies relation i.e. parallel samples from different body sites, or sequentially numbered according to hospital system.

2.1.1.4 Antibiotics and media additions

Stock antibiotics were filter sterilised through 0.2 µm Millex filters (Milipore) and stored at -20°C. Carbenicillin disodium salt (Sigma) and kanamycin sulfate (Thermo Fisher) were prepared in molecular grade H_2O as 100 mg/ml stocks and used at a working concentration of 100 µg/ml. Piperacillin sodium salt (Fluorochem) was prepared in molecular grade H_2O as 50 mg/ml stocks and used at a working concentration of 50 µg/ml. Piperacillin tazobactam (PipTazo) was prepared in a 8:1 ratio, combining piperacillin from above with Tazobactam sodium salt (Fluorochem) and used at various working concentrations dependent on the agar dilution factor required.

2.1.1.5 Automated measurement of bacterial growth

Overnight cultures were diluted 1:1000 in fresh media in sterile Eppendorf tubes. Diluted samples were further diluted 1:10 into individual wells of a clear polystyrene 96-well flat bottom plate (Greiner Bio-One) containing fresh media. Absorbance values (OD_{600nm}) of samples were measured in a microplate reader (FLUOstar OPTIMA Microplate Reader) at 37°C over a ~ 5 h period. Bacterial growth curves were constructed from the multitude of readings taken over this time period.

2.1.1.6 Measurement of bacterial growth by viable counting

Overnight cultures were diluted to an OD_{600nm} of 3.0 before carrying out 10-fold serial dilutions of samples in a 96-well plate. Using a multichannel pipette, 10 µl of dilutions 10^{-4}, 10^{-5} and 10^{-6} were plated on square LB plates and incubated overnight at 37°C. Following incubation, the number of colonies on each plate was counted. Colony Forming Units (CFU) are representative of the number of viable bacteria and CFU/ml was calculated as:

$$\text{CFU/ml} = \frac{\text{number of colonies} \times \text{dilution factor}}{\text{volume plated (ml)}}$$

2.1.2 Plasmids and oligonucleotides

2.1.2.1 Plasmids

Details of the plasmids used in this study are listed in Table 2.2.

Table 2.2 Plasmids used in this study

Plasmid	Description	Source
pACYC177	p15A replicon; Amp^r, Kan^r	(Chang & Cohen, 1978)
pBR322	pMB1 replicon; Amp^r, Tc^r	PMID: 344137
pBSKII	ColE1 replicon; Amp^r	PMID: 2555794
pilux	Encodes lux cassette enabling bioluminescence; Amp^r	(Gregor *et al.*, 2018)
pGEX (-)	Empty cloning vector of pilux; Amp^r	(Gregor *et al.*, 2018)
pKD46	Encodes lambda red recombination genes; temperature sensitive; Amp^r	(Datsenko & Wanner, 2000)
pKD4	Contains kanamycin cassette flanked by FRT sites; Kan^r	(Datsenko & Wanner, 2000)

Amp^r, ampicillin resistant; Kan^r, kanamycin resistant; Tc^r, tetracycline resistant; FRT, FLP recombination target.

2.1.2.2 Oligonucleotides

The oligonucleotides used in this study are listed in Table 2.3. Oligonucleotides were synthesised by Integrated DNA Technologies, Leuven, Belgium. Oligonucleotides were prepared in molecular biology grade H_2O as 100 µM stocks and used at a working concentration of 10 µM and stored at -20°C.

2.2 Nucleic acid methodologies

2.2.1 Transformation of *K. pneumoniae* strains

Preparation of competent cells involved repeated washes with ice-cold molecular grade H_2O and 10% (v/v) glycerol. Transformation was accomplished *via* electroporation. Transformation efficiency was calculated as:

$$\text{Transformation efficiency} = \frac{\text{number of colonies}}{\text{DNA spread on plate (µg)}}$$

The amount of DNA spread on the plate was calculated as:

$$\text{DNA spread on plate (µg)} = \frac{\text{volume spread (µl)} \times \text{DNA in transformation (µg)}}{\text{total volume of transformation}}$$

2.2.1.1 Preparation of electrocompetent encapsulated bacteria

An amended protocol developed by Fournet-Fayard *et al.* was followed to prepare electrocompetent WT cells (Fournet-Fayard *et al.*, 1995). An overnight culture of WT cells was diluted 1:100 in 100 ml of LB supplemented with 0.7 mM ethylenediaminetetraacetic acid (EDTA) and grown to an OD_{600nm} of ~ 0.2-0.4. EDTA reduces the amount of capsule produced in WT *K. pneumoniae* which may pose as a barrier to penetration of plasmid DNA, thus resulting in higher efficiencies of DNA uptake during electroporation (Fournet-Fayard *et al.*, 1995). The culture was then chilled on ice for 20 min and all subsequent procedures were carried out at 4°C. Bacteria were collected by centrifugation at 10,000 x *g* (Sigma 2-16K; Sigma Laborzentrifugen GmbH) for 10 min and the pellet was resuspended in 10 ml ice-cold distilled H_2O. Cells were harvested as before, the pellet was resuspended in 10 ml cold distilled H_2O and harvested again. The pellet was then resuspended in 1 ml ice-cold 10% glycerol and harvested for the final time at 12,000 x *g* (Mini 13-K; Hangzhou Allsheng Co. Ltd.).

Table 2.3 Oligonucleotides used in this study

Primer name	Sequence 5'-3'	Source
ManC_F	GTTACCGTTCCGCAGTTCTG	This study
ManC_R	TCATTCTGCGTTTTGTCCCG	This study
ManCa	GCATTGCTAACCTCCTGCT	(Llobet *et al.*, 2008)
ManCd	CGGGAACTGGTTCTCCTC	(Llobet *et al.*, 2008)
Wca_F	CTCCAGGCGCGTATTTCTTC	This study
Wca_R	TGTTTCGGATAAAGCTCGCG	This study
F_18148	AAATTCCACGCCTCTCCATG	This study
R_22944	GTTTAGGGTTTTGCTGTCGC	This study
F_22629	TAGCGACTTGGTCCCAACAG	This study
R_27386	CGGAATTACTTGAGTGGGCG	This study
F_27016	CCGCGATATGGATGACGTTC	This study
R_31675	CACGTATTATGCAGTGGGGC	This study
F_31151	CCGAATGAGGGAATGCCTTG	This study
R_35426	AAGAATTTGGCGGGCAGATG	This study
GalF_F[a]	GAAGAAAATGGGCTACATGCAGGCCTTCGTCA CCTACGGGATGCGTAACC**TGTGTAGGCTGGAG CTGCTTC**	This study
Gnd_R[a]	GCACCAAAGTAATCACGCTGAGCCTGAATCAG GTTAGCGGGCAGAACTGC**CATATGAATATCCT CCTTA**	This study
Ugd_F[a]	ATACCGTTCGATAAACCAACATAACCTGTACC GGAAATAGTAATTTTCAT**TGTGTAGGCTGGAG CTGCTTC**	This study
GalF_R[a]	ATGAATATGACGAATTTGAAAGCGGTTATTCC GGTCGCAGGACTAGGCAT**CATATGAATATCCT CCTTA**	This study
GalF_F_opp[a]	ATGCCTAGTCCTGCGACCGGAATAACCGCTTT CAAATTCGTCATATTCAT**TGTGTAGGCTGGAG CTGCTTC**	This study
Ugd_R_opp[a]	ATGAAAATTACTATTTCCGGTACAGGTTATGT TGGTTTATCGAACGGTAT**CATATGAATATCCT CCTTA**	This study
Char ugd_F[a]	GATTTGTGACATGTACAATTTTGCAAAACCGC GTGTTTTGCAACCAAACAGGTGAAGATG**TGTG TAGGCTGGAGCTGCTTC**	(Huang *et al.*, 2014a)
Char galF_R[a]	CGGGGAGATAAAGAAGAACACTGGCGGCAGGG AACCGCCAGTGTCAGACAGGCAGAATTA**CATA TGAATATCCTCCTTA**	(Huang *et al.*, 2014a)
GalF_R selective	AAAGCGGTTATTCCGGTCGC	This study
Ugd_F selective	CCAACATAACCTGTACCGGA	This study
A_fwd	AAGAATTTGGCGGGCAGATG	This study
B_rev[b]	TTAAAGCGGGCGATCATAG	This study

C_fwd[ab]	GCTATGATCGCCCGCTTTAA**TGTGTAGGCTGGAGCTGC**	This study
D_rev[ab]	CATACGCCACTACATCACGC**CATATGAATATCCTCCTTAGTTCCTATTCC**	This study
E_fwd[b]	GCGTGATGTAGTGGCGTATG	This study
F_rev	TGTTTCGGATAAAGCTCGC	This study
Wza CF1	TGAAAGTGTTTGTCATGGG	(Pan *et al.*, 2013)
Wza CF2	GGGTTTTTATCGGGTTGTAC	(Pan *et al.*, 2013)
Wzc CR1	TTCAGCTGGATTTGGTGG	(Pan *et al.*, 2013)
Khe_F	TTCATCTACGTGCTGGAGGG	(Weiss *et al.*, 2019)
Khe_R	TGAGCGGGTAATAAATGCGG	(Weiss *et al.*, 2019)

[a] Bold font denotes priming sequences for pKD4.

[b] Underlined font denotes overlapping sequences between NEBuilder fragments.

Ice-cold 10% glycerol (200 μl) was used to resuspend the final pellet and aliquots of 40 μl were stored at -80°C.

2.2.1.2 Preparation of electrocompetent acapsulated bacteria

A protocol from New England Biolabs was followed for the preparation of acapsulated bacteria. An overnight culture of Kp52145 Δ*manC* cells was diluted 1:100 in 100 ml of LB and grown to an OD_{600nm} of ~ 0.4-0.6. The culture was then chilled on ice for 20 min and all subsequent procedures were carried out at < 4°C. Cells were repeatedly collected as before by centrifugation at 10,000 x *g* (Sigma 2-16K) and resuspended in 25 ml ice-cold H_2O, before the third harvest step whereby cells were resuspended in 1 ml ice-cold 10% glycerol and harvested for the final time at 12,000 x *g* (Mini 13-K). Ice-cold 10% glycerol (200 μl) was used to resuspend the final pellet and aliquots of 40 μl were stored at -80°C.

2.2.1.3 Transformation by electroporation

Electrocompetent cells (40 μl) were mixed with 4 μl of DNA (concentration 2.5-500 ng/μl) and transferred into a cold electroporation cuvette (Cell Projects Ltd.; 0.2 cm width). Cells were electroporated in a Bio-Rad gene pulser at 12.5 $kVcm^{-1}$, 200 Ω and 25 μF. Bacteria were then transferred to 1 ml aliquots of pre-warmed LB and incubated for 1 h at 37°C to promote plasmid expression. Aliquots of 1 μl, 10 μl, 100 μl and ~ 900 μl of transformation mixture was then spread on selective LB agar plates and incubated overnight at 37°C. Single colony purification of transformants was carried out on fresh selective LB agar plates.

2.2.2 Purification of plasmid and chromosomal DNA

2.2.2.1 Purification of plasmid DNA

The Monarch Plasmid Miniprep Kit (New England Biolabs) was utilised for the routine purification of plasmid DNA from overnight cultures following the manufacturer's protocol. Overnight cultures were standardised to an OD_{600nm} of 3.0 and 4 ml (i.e. 12 OD_{600nm} units) was centrifuged at 6,000 x *g* (Mini 13-K) for 10 min to harvest bacteria. Bacteria were incubated for 1 min in 200 μl of an alkaline lysis buffer. The lysate was incubated for 2 min in 400 μl neutralisation buffer. Centrifugation was then performed

at 16,000 x *g* for 5 min to clear the lysate and a mini-cation exchange column was used to purify the soluble plasmid DNA. Following a desalting and washing step, purified DNA was eluted from the column in molecular grade H_2O.

2.2.2.2 Purification of chromosomal DNA

The DNeasy Blood & Tissue Kit (Qiagen) was utilised for the routine purification of genomic DNA from overnight cultures. The manufacturer's protocol was followed. Overnight cultures were standardised to an OD_{600nm} of 3.0 and 2 ml was centrifuged at 5,000 x *g* (Mini 13-K) for 10 min to harvest bacteria. Bacteria were incubated for 1 h with 20 µl proteinase K at 56°C. Ethanol (≧ 96%) precipitation was carried out and the cleared lysate was passed through a mini-cation exchange column. Following repeated washing steps, purified DNA was eluted from the column in molecular grade H_2O or Tris hydrochloride (0.1 mM).

2.2.2.3 Quantification of purified DNA

The concentration of purified DNA was determined using the Nanodrop 2000 (Thermo Fisher) at 260_{nm} and Nanodrop 2000 software (Thermo Fisher). Molecular grade H_2O or Tris hydrochloride (0.1 mM) were used to perform a 'blank' measurement. DNA (1 µl) was then loaded onto the reading pedestal. A260nm/280nm and A260nm/230nm values are indicators of DNA purity; the ideal ratio for both being ~1.8-2 (Desjardins & Conklin, 2010).

2.2.3 PCR

PCR was utilised to amplify specific DNA fragments to confirm putative mutants and for capsule genotyping purposes. The principle of PCR is based on the capacity of DNA polymerases to synthesise new DNA strands which are complementary to the provided template strand. The process involves successive cycles of thermal denaturation of a double-stranded DNA template; annealing of complementary oligonucleotides (primers); and amplification of the DNA strand by the DNA polymerase. Primers are designed to flank the target region to be amplified, complementarily binding to opposite strands of the template. Synthesis of the new DNA strand is carried out, using dNTPs, by

the DNA polymerase in the presence of Mg^{2+}. The product of each synthesis step acts as a template strand for succeeding steps, resulting in exponential amplification.

2.2.3.1 Amplification of DNA by PCR

Two different DNA polymerases were utilised in experiments detailed herein. *Taq* DNA polymerase, named after the bacterium *Thermus aquaticus* from which it was isolated, is a recombinant thermostable polymerase lacking the 3'→5' exonuclease activity required for proofreading. Therefore, its use was restricted to PCR reactions such as capsule genotyping, where the accuracy of DNA sequence after amplification was not crucial. In contrast, Q5 High-Fidelity DNA Polymerase (New England Biolabs) was suitable in reactions that required a high degree of sequence fidelity, such as the generation of DNA fragments for recombination reactions. Q5 High-Fidelity DNA Polymerase possesses the 3'→5' exonuclease activity required for proofreading, resulting in a significantly reduced misincorporation of nucleotides.

Taq 2X Master Mix (New England Biolabs) comprises Taq DNA polymerase, deoxyribonucleotide triphosphates (dNTPs), reaction buffer, and stabilisers. The master mix, added to a final concentration of 1X, was combined with 0.5 µM of forward and reverse primers, 10 ng of template DNA, and molecular grade H_2O to a final volume of 25 µl. Thermocycling conditions are detailed in Table 2.4.

Q5 High-Fidelity DNA Polymerase (1 U/µl) was combined with 10 µl of 5X Q5 Reaction Buffer, 200 µM of dNTPs (New England Biolabs), 0.5 µM of forward and reverse primers, 10 ng of template DNA, and molecular grade H_2O to a final volume of 50 µl. Thermocycling conditions are detailed in Table 2.5.

Purified genomic DNA, plasmid or cell lysates served as templates in PCR reactions. Preparation of cell lysates involved boiling a single bacterial colony in 20 µl of molecular grade H_2O at 100°C for 5 min. Crude lysate (1 µl) acted as a template in PCR reactions.

2.2.3.2 λ-Red Recombination

The λ-Red Recombination system, developed by Datsenko and Wanner, can be used to disrupt chromosomal genes, *via* insertions or deletions, ultimately generating mutants (Datsenko & Wanner, 2000). Briefly, overnight cultures were diluted 1:100 in fresh

Table 2.4 Thermocycling conditions used for Taq 2X Master Mix

Step	Temperature	Time
1 Initial denaturation	95°C	30 s
2 Denaturation	95°C	15-30 s
3 Annealing	45-68°C (corresponding to lowest melting temperature of the primer pair)	15-60 s
4 Extension	68°C	1 min per kilobase of anticipated DNA product
5 Final extension	68°C	5 min

Steps 2-4 were repeated for 34 additional cycles.

Table 2.5 Thermocycling conditions used for Q5 High-Fidelity DNA Polymerase

Step	Temperature	Time
1 Initial denaturation	98°C	30 s
2 Denaturation	98°C	5-10 s
3 Annealing	50-72°C (referred to New England Biolabs Tm Calculator)	10-30 s
4 Extension	72°C	20-30 s per kilobase of anticipated DNA product
5 Final extension	72°C	2 min

Steps 2-4 were repeated for 34 additional cycles.

media and grown to an OD_{600nm} of ~ 0.2 before the addition of L-(+)-Arabinose (Sigma) to a final concentration of 0.1% (Sigma) to the culture which was then incubated for a further 2 h. Arabinose is used for the induction of the λ-Red recombineering operon of pKD46. Incubations occurred at 30°C due to the temperature sensitivity of plasmid pKD46. Following the incubation with Arabinose, the standard protocols, as detailed in 2.2.1.1 and 2.2.1.2, were used to prepare electrocompetent cells harbouring pKD46 prior to their electroporation with the desired DNA insert. Following electroporation, all subsequent incubations were carried out at 37°C to cure the bacteria of pKD46. Transformation mixture was spread on LB agar plates supplemented with kanamycin and incubated overnight at 37°C.

2.2.3.3 NEBuilder

NEBuilder was utilised to generate an assembled linear DNA fragment that could be used to transform Kp52145, ultimately producing a mutant lacking the *cps* gene cluster. The NEBuilder Assembly tool was used to design PCR primers with overlapping sequences between the adjacent DNA fragments. The oligonucleotides used to amplify the desired fragments are listed in Table 2.3. PCR products were digested with 1 μl of Dpn1 for 1 h at 37°C in order to destroy plasmid template. The digested fragments were then added to NEBuilder HiFi DNA Assembly Master Mix. The reaction mix was assembled following the manufacturer's protocol and incubated at 50°C in a thermocycler for 15 min. Following incubation, the resulting assembled fragment was used as template DNA in a final PCR involving the primers at either end of the desired fragment. The resulting PCR products were stored at -20°C until required for transformation, which was carried out as detailed in 2.2.1.3.

2.2.4 *In vitro* manipulations of DNA

2.2.4.1 Agarose gel electrophoresis

Visualisation of DNA samples was carried out following separation on a 1% agarose gel. Briefly, 1 g of agarose was added to 100 ml of 0.5X TBE buffer (Sigma) and dissolved by heating in a microwave oven. Nucleic acid stain (4 μl; G-Biosciences) was mixed with 40 ml of the molten agarose, poured into a gel mould and allowed to set. 6X purple gel

loading dye (1 µl; New England Biolabs) was added to 5 µl of DNA sample prior to electrophoresis at 180 V for 50 min in 0.5X TBE.

2.2.4.2 Purification of DNA samples

The Monarch PCR & DNA Cleanup Kit (New England Biolabs) was utilised for the routine purification of DNA samples from PCR products following the manufacturer's protocol. In brief, 50 µl PCR products were mixed with 100 µl of supplied guanidine and isopropanol-based binding buffer. The sample was then passed through a mini-cation exchange column. Following repeated ethanol (≧ 96%) washing steps, purified DNA was eluted from the column in molecular grade H_2O or supplied elution buffer (10 mM Tris hydrochloride, 0.1 mM EDTA, pH 8.5).

The Co-Precipitant Pink Kit (Bioline) was used to improve ethanol precipitation of DNA samples. Briefly, 0.1 volumes of 3 M supplied sodium acetate buffer was added to the DNA sample. Co-Precipitant Pink (6 µl) was added, followed by 2 volumes of 96% ethanol and incubation of the mixture for 10 min at room temperature. The precipitated DNA was harvested by centrifugation for 10 min at 21,000 x *g* (Mini 13-K), the supernatant was discarded and the DNA was washed with 70% ethanol. The DNA was harvested as before and the supernatant was removed. The pellet was dried on a heat block for 10 min at 56°C. The precipitated DNA was finally dissolved in molecular grade H_2O for 10 min at 56°C.

2.3 Analysis and Manipulation of Proteins and Polysaccharides

2.3.1 SDS-PAGE

Following the Laemmli method (Laemmli, 1970), proteins and polysaccharides were separated on discontinuous denaturing polyacrylamide gels. SDS and β-mercaptoethanol are used to denature proteins, prior to their separation through a polyacrylamide gel according to their molecular weight. SDS masks proteins' intrinsic charge, coating each protein with a uniform negative charge, ultimately resulting in similar mass:charge ratios amongst proteins, thus allowing separation on the basis of molecular weight, rather than charge. The formation of the discontinuous gel system is created using buffers of varying composition and pH. Firstly, the stacking gel ensures

the formation of narrow well-defined bands. This is followed by the resolving gel, which finally separates the proteins bases on their size.

2.3.1.2 Preparation of total cellular extract for SDS-PAGE analysis

Overnight cultures were diluted to an OD_{600nm} of 3.0 (stationary phase) before centrifugation of 1 ml at 10,000 x *g* (Mini 13-K) for 2 min. The supernatant was discarded and the pellet was resuspended in 290 µl of 1X Laemmli buffer (4% SDS, 20% glycerol, 10% β-mercaptoethanol, 0.004% bromophenol blue, 0.125 M Tris HCl, pH 6.8; Sigma). The sample was boiled at 100 °C for 10 min before cooling for 5 min. Proteinase K (10 µl; 20 µg/ml; Qiagen) was added to samples prior to incubation at 56°C for 1 h. Samples were stored at -20°C and boiled at 100°C for 5 min prior to use.

Extraction of LPS from exponential phase cultures was carried out in the same manner; instead of immediate extraction, overnight cultures were diluted 1:100 in fresh media and grown until achieving an OD_{600nm} of 0.6. After the initial centrifugation step, the pellet was resuspended in 50 µl of 1X Laemmli buffer. Succeeding steps, as outlined above, remained the same.

2.3.1.1 Sarkosyl enrichment of OM proteins

OM fractions were prepared as previously described (Deighan *et al.*, 2000). This method involves the use of N-laurylsarcosine (Sarkosyl) to isolate the desired OMPs from the cytoplasmic membrane components.

Overnight cultures were standardised to an OD_{600nm} of 3.0 and 4 ml (i.e. 12 OD_{600nm} units) was centrifuged at 6,000 x *g* (Mini 13-K) for 10 min to harvest bacteria. The supernatant was discarded and the pellet was resuspended in 600 µl of sonication buffer (10% sucrose, 50 mM TrisCl, 100 mM NaCl, 1 mM EDTA), after which the bacteria were lysed by sonication. Centrifugation at 9,300 x *g* for 5 min was carried out to remove intact bacteria. Supernatants were incubated with 0.5% Sarkosyl for 30 min with agitation to ensure solubilisation of IM. The OMs, contained within the Sarkosyl-insoluble fraction, were collected by centrifugation at 21,000 x *g* for 30 min. The supernatant was discarded and the pellet was dried at 56°C for 5 min prior to resuspension in 100 µl of 1X Laemmli buffer.

2.3.1.3 Electrophoresis of samples

Boiled sample (10 μl) was loaded into wells of a TruPAGE Precast Gel (4-20%; Sigma). Laemmli buffer (1X) acted as a blank in empty lanes. Electrophoresis was carried out in 1X TruPAGE SDS Buffer (Sigma) at 180 V for 45 min. Following electrophoresis, OMP gels were stained for 90 min using Coomassie brilliant blue R-250 (0.25% Coomassie brilliant blue R-250, 45% (v/v) methanol, 10% (v/v) acetic acid) and destained for 3 h using destain solution (45% (v/v) methanol, 10% (v/v) acetic acid).

LPS gels were stained using the Pro-Q Emerald 300 LPS Gel Stain Kit (Thermo Fisher). Polysaccharides were visualised using a blue light LED epi-illuminator (B-BOX; SMOBIO).

2.3.2 Mucoviscosity

2.3.2.1 String test

The tested strains were grown on blood agar plates overnight at 37°C. Mucoviscous strings were stretched from colonies using bacteriological loops. A positive string test (i.e. HMV) was defined as the formation of viscous strings > 5 mm in length (Fang *et al.*, 2004).

2.4 Phenotypic assays

2.4.1 Biofilm analysis

2.4.1.1 Biofilm formation assays

Protocols developed by Naves *et al.* and O'Toole were modified and followed to examine biofilm formation by *K. pneumoniae* strains in microtitre plates (Naves *et al.*, 2008, O'Toole, 2011). Briefly, 1.3 μl of overnight culture was inoculated into 130 μl of broth in individual wells of a tissue culture treated clear polystyrene 96-well flat bottom plate (Greiner Bio-One). LB broth was used as a negative control and *E. coli* W3110, a strong biofilm former (Serra *et al.*, 2013), was routinely used as a positive control. To prevent dehydration of the wells, plates were covered with sealing film, before static incubation at 37°C for 24 h. Biofilm formation was quantified using the Crystal Violet (CV) assay (CVA).

2.4.1.2 Crystal violet assays

Following incubation, excess broth was discarded from each well. Wells were washed with 150 μl of phosphate-buffered saline (PBS) to remove planktonic bacteria, before drying the plate at 60°C for 1 h. CV (130 μl; 0.1%; Sigma) in H_2O was used to stain each well for 15 min. CV was then discarded from each well and 180 μl of H_2O was used to rinse excess dye from wells. Four washing steps were carried out, before drying the plate at 60°C for 10 min. 130 μl of 33% acetic acid (Sigma) was added to each well to resuspend biofilm-bound CV dye. The plate was agitated on an orbital shaker for 5 min, after which the OD_{595nm} of the stained bacteria was measured using the FLUOstar OPTIMA Plate Reader. Biofilm formation (BF) was calculated as BF = AB – CW, where AB is the OD_{595nm} of the CV stained attached bacteria, and CW is the OD_{595nm} of the stained negative control wells (Naves *et al.*, 2008). Naves *et al.* used this formula to classify a result of ≥ 0.300 as strong; 0.200-0.299 as moderate; 0.100-0.199 as weak; and < 0.100 as negative biofilm formation (Naves *et al.*, 2008). The biofilm formation index (BFI) for each well was calculated as BFI = (B − C)/G, where B is the OD_{595nm} of the stained test wells, C is the OD_{595nm} of the stained control wells and G is the OD_{595nm} of the bacteria grown in broth pre staining (Kumar *et al.*, 2015).

2.4.2 Bioluminescence quantification

The bioluminescence of Kp52145 harbouring the pilux plasmid was measured both qualitatively and quantitatively. Transformed bacteria were grown overnight on carbenicillin LB agar plates. Bioluminescence of the plated colonies was measured using a CCD camera (LAS 4000, Fujifilm) and an analysis software application (Image Gauge Software, Fujifilm) was used to visualise the signal intensity. Cultures of colonies from these plates were incubated overnight at 37°C. For endpoint assays, overnight cultures were diluted to an OD_{600nm} of 3.0; for incremental reading assays, overnight cultures were diluted 1:100 in fresh media. Aliquots (130 μl) of each sample were transferred to a white polystyrene 96-well white flat bottom plate (Greiner Bio-One). Bioluminescence of each well was quantified in a microplate reader (as in 2.1.1.5) at luminometric output.

2.4.3 Minimum inhibitory concentration assays

The agar dilution method involved the addition of varying concentrations of antibiotics to non-selective nutrient agar medium, prior to solidification. The prepared MIC plates were then inoculated, using bacteriological swabs, with standardised bacterial concentrations of overnight culture of strains to be tested.

2.4.4 VITEK

The VITEK system is utilised for both bacterial identification and antibiotic susceptibility testing (Shetty *et al.*, 1998). In brief, tested strains were grown on blood agar plates for 24 h at 37°C. Bacterial colonies were suspended in 0.45% saline and the cell density was adjusted to 0.5 McFarland. VITEK cards containing dilutions of antibiotics were inoculated with the suspension vials and loaded into the VITEK automated reader incubator.

2.5 Statistical analysis

GraphPad Prism 8 software was used to perform statistical analyses. Four biological replicates (n=4) were performed in experiments unless otherwise stated. Two-way analysis of variance (ANOVA) with either Tukey's or Sidak's multiple comparisons test were used as appropriate. In all data, a p value of ≤ 0.05 is denoted *; a p value of ≤ 0.01 is denoted **; a p value of ≤ 0.001 is denoted ***; and a p value of ≤ 0.0001 is denoted ****.

Chapter 3 The influence of growth media and capsule status on biofilm formation of *K. pneumoniae*

3.1 Introduction

When cultured *in vitro*, growth media is thought to play an important role in the biofilm formation of bacteria (discussed in 1.3.1.1). However, clarity regarding the particular contribution of media components is lacking, as enhanced biofilm development has been observed in both nutrient-rich and nutrient-limited conditions in numerous bacteria, including *Klebsiella* (Lin *et al.*, 2016, Singh *et al.*, 2019, Skyberg *et al.*, 2007). The differing contribution of nutrients to biofilm formation may be strain-dependent (Naves *et al.*, 2008, Reisner *et al.*, 2006).

Conflicting data exist surrounding the relationship between the capsule and biofilm formation of *K. pneumoniae*. Certain studies have found that mutations disrupting capsule synthesis result in biofilm reduction or deficiency (Wu *et al.*, 2011, Boddicker *et al.*, 2006). On the contrary, increased biofilm production has been observed as a result of reduction or absence of capsule (Huang *et al.*, 2014a). These observations may be strain-dependent or determined by the nature of the allele manipulated. Additionally, type 1 and type 3 fimbriae are thought to contribute to the complex relationship between capsule and biofilm (Schembri *et al.*, 2005, Langstraat *et al.*, 2001). Some studies suggest that capsule hinders fimbria-mediated biofilm and in turn capsule loss enhances fimbrial function. However, Huang *et al.* noted that their capsule mutant, which displayed increased biofilm, was not fimbriated (Huang *et al.*, 2014a). Evidently, this area of research requires additional clarity with regards to the additional variables affecting the role capsule plays in the biofilm formation of *K. pneumoniae.*

To date, 79 chemically distinct capsular types have been identified in *K. pneumoniae* (discussed in 1.2.1.1). Although numerous studies have investigated the contribution of capsule to the formation of biofilm, a review of the literature indicates that the role of capsular type in biofilm formation has not undergone substantial analysis. The range of biofilm formation amongst the hospital isolates (detailed in Table 2.1) irrespective of growth media, indicated that another factor was contributing to this phenotype. Using

a *wzc* genotyping system for *K. pneumoniae*, the capsular types of the isolates were investigated (as explained in 1.2.1.2).

To further elucidate the role of capsule in biofilm formation, the generation of a Kp52145 CPS operon mutant was attempted, using the λ-Red recombination system. The λ-Red system, derived from the λ-Red bacteriophage, is a recombination technique that facilitates the precise generation of insertions and deletions at *loci* specified by flanking homology regions (Datsenko & Wanner, 2000). The essential components of this recombineering system are the proteins Exo, Gam and Beta (Murphy, 2016). Exo, a 5' → 3' dsDNA-dependent exonuclease, degrades linear dsDNA to generate a partially dsDNA duplex with single-stranded 3' overhangs. Gam prevents the digestion of linear DNA by the endogenous nucleases, RecBCD and SbcCD. Beta is involved in the protection of the ssDNA created by Exo and the promotion of its annealing to a complementary ssDNA target in the cell. The λ-Red genes are under control of the arabinose-inducible pBAD promoter and the replicon is temperature-sensitive which enables for its easy elimination (Datsenko & Wanner, 2000).

The plasmid pKD46 (detailed in Table 2.2) expresses the aforementioned λ-Red proteins and thus bacteria harbouring this plasmid can be transformed with substrate DNA that has homologous flanking regions to the desired knockout region. A kanamycin resistance cassette with external overlaps with the target knockout gene(s) in the CPS operon acted as the original DNA substrate for transformation attempts. Using this recombination system, Huang *et al*. have successfully generated a capsule mutant in *K. pneumoniae* strain MGH 78578.

NEBuilder was also utilised to generate an alternative DNA recombination substrate; an assembled DNA fragment spanning the entirety of the CPS operon. NEBuilder HiFi DNA Assembly Cloning Kit is a DNA assembly tool based on the Gibson Assembly technique. The components of the reaction include an exonuclease that creates single-stranded overhangs that facilitate the annealing of fragments that share complementarity; a polymerase that fills gaps within each annealed fragment; and a ligase that seals nicks in the assembled DNA fragment.

A range of bacterial species, including *K. pneumoniae* and *E. coli*, have successfully been transformed with NEBuilder-assembled plasmids (Lee *et al.,* 2018, McGarry,

unpublished). However, a review of the literature suggests that the transformation of *Klebsiella* with an assembled linear fragment of double-stranded (ds) DNA has not been carried out, and thus it is uncertain as to whether this is a viable mutagenesis method. It was proposed that using NEBuilder, DNA fragments could be assembled to accomplish the desired mutation in the CPS operon. This linear dsDNA fragment with single-strand overhangs, composed of the kanamycin cassette insert flanked by genes upstream and downstream of the CPS operon, could then be transformed into electrocompetent Kp52145 harbouring pKD46, to replace the intact innate CPS operon by homologous recombination. However, despite the successful assembly of the desired fragment, subsequent transformations using this fragment were unsuccessful.

This study sought to investigate the influence of growth media and capsule status on biofilm formation of *K. pneumoniae*. A brief outline of this chapter is listed below.

- The colony morphology of Kp52145 strains was examined and strains were assessed for mucoviscosity using the string test.
- Initially, WT and mutant Kp52145 were grown in different media and the biofilm formation capacity of each of the media was compared.
- This was followed by comparison of the biofilm formation of WT and mutant, to establish a role for capsule in biofilm formation.
- The λ-Red recombination system and NEBuilder were utilised in attempts at constructing a CPS operon mutant.
- Hospital isolates were incorporated into biofilm studies in order to establish whether capsular type played a role in the biofilm formation of *K. pneumoniae*.

3.2 Results

3.2.1 The colony morphology and string test results differ between Kp52145 WT and mutant

When cultured on blood agar plates, both Kp52145 WT and mutant produced non-haemolytic grey-white colonies. WT Kp52145 appeared as mucoid colonies and the mutant produced non-mucoid colonies.

A positive string test is defined as the formation of viscous strings > 5 mm in length (Fang *et al.*, 2004). String tests were carried out as described in 2.3.2.1. WT tested positive in this regard, forming strings > 5 mm in length. This was in contrast to the mutant, which tested negative, failing to form viscous strings of any length (Figure A.1).

3.2.2 Biofilm formation of Kp52145 is influenced by growth media

As outlined above, growth media has been shown to impact the formation of biofilms. Biofilm formation assays were carried out as described in 2.4.1.1, in various media, including LB broth, LB broth supplemented with glucose or glycerol, M9 minimal media, and BHI broth, the components of which are detailed in 2.1.1.2. Following incubation, and prior to carrying out the CVA, the OD_{595nm} of the bacteria in each well was measured. The absorbance values of the bacteria were measured again following the CVA.

3.2.2.1 Biofilm formation quantification

As seen in Figure 3.1 (A), biofilm formation varied greatly depending on the media in which Kp52145 was grown. The biofilm formation of WT was significantly higher when grown in M9 and BHI in comparison to LB, LB + glucose and LB + glycerol. There was no significant difference between the biofilm produced by WT when grown in M9 or BHI. When the mutant was grown in BHI, a significantly higher amount of biofilm was produced than when grown in any other media. The biofilm formation of the mutant was significantly higher when grown in LB + glucose in comparison to LB, LB + glycerol and M9.

These data indicate that the optimum growth media to support biofilm formation may be capsule-dependent. However a consistency when comparing WT and mutant is the mutual significant increase in biofilm formation when grown in BHI. BHI was thus determined the most conducive growth medium for studying the biofilm formation of both strains.

3.2.2.2 Biofilm formation index

The biofilm formation index (BFI) was calculated as described in 2.4.1.2. Two absorption measurements were required for the calculation; the OD_{595nm} of the bacteria grown in broth pre-staining and the OD_{595nm} of the CV-stained bacteria. This measurement

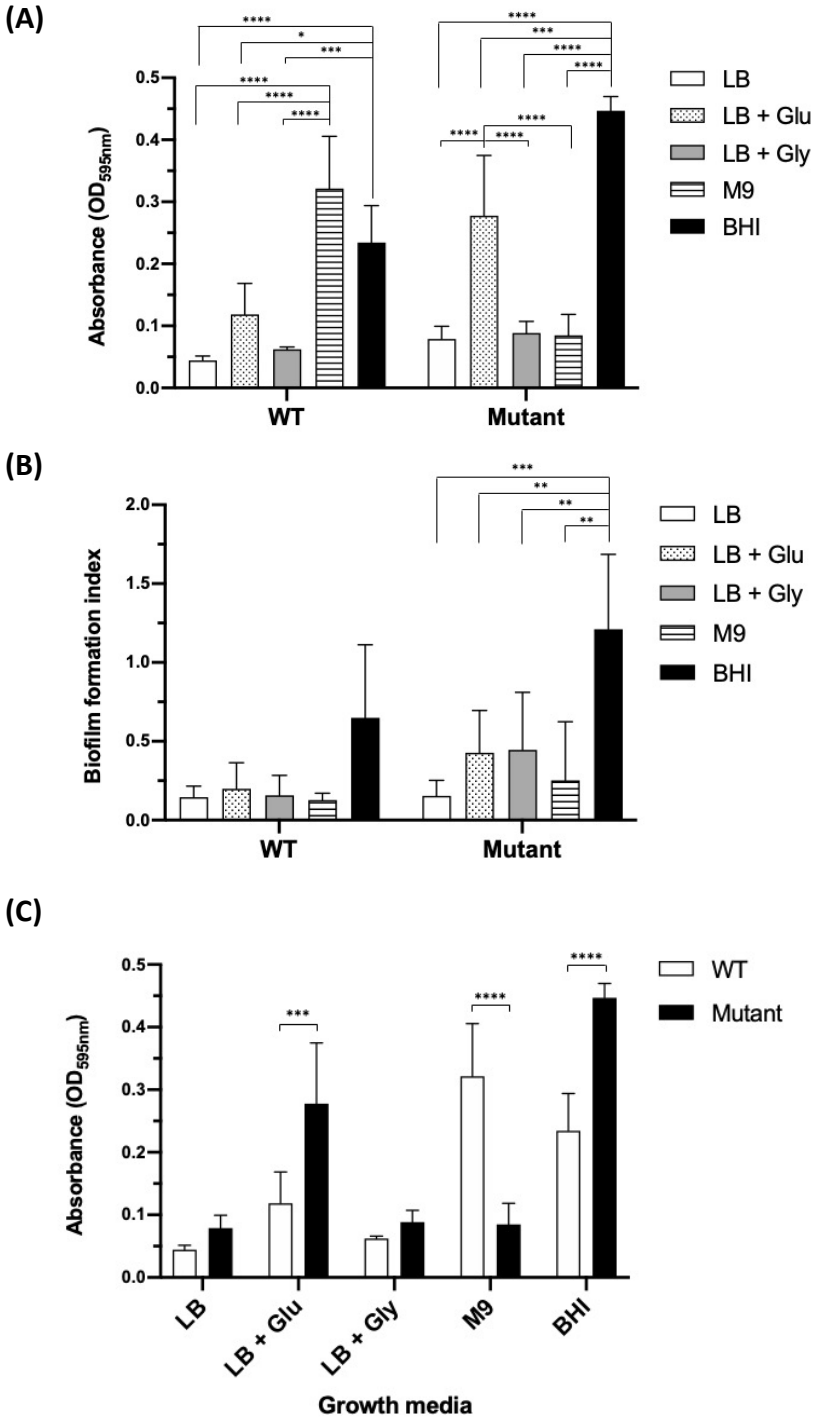

Figure 3.1: Biofilm formation of WT and mutant Kp52145. Bacteria were grown in a range of growth media for 24 h in 96 well plates. CVAs were carried out and the resulting OD_{595nm} of the CV-stained bacteria was measured. Assays were carried out as described in 2.4.1.1 and 2.4.1.2. LB broth was used as a negative control and *E. coli* W3100 acted as a positive control (not shown on graph). Statistical significances were calculated by two-way ANOVA with (A)(B) Tukey's multiple comparisons test; and (C) Sidak's multiple comparisons test and are indicated on the graph; * = $p \leq 0.05$; ** = $p \leq 0.01$; *** = $p \leq 0.001$; **** = $p \leq 0.0001$. n=4. **(A)** Comparison of growth media for biofilm formation. **(B)** BFI of WT and mutant. **(C)** Comparison of biofilm formation of WT and mutant.

removes discrepancies regarding the growth rate of strains which may influence biofilm formation and thus aims to normalise the values mentioned above. These data are displayed in Figure 3.1 (B). No significant differences in the BFI of WT existed between any of the growth media. The BFI of the mutant was significantly higher when grown in BHI when compared to all other media. There was no significant difference noted between the BFI of WT and mutant in any of the growth media.

3.2.3 The biofilm formation of Kp52145 is influenced by capsule

As alluded to above, different amounts of biofilm are produced by WT and mutant in various media. The biofilm formation of the strains are compared in Figure 3.1 (C). In LB and LB + glycerol, the biofilm formation of both WT and mutant was negative (OD_{595nm} < 0.100), according to the Naves classification system (discussed in 2.4.1.2). In LB + glucose, WT formed weak biofilm and the mutant formed moderate biofilm. Strong biofilm was produced by WT when grown in M9 while biofilm formation of the mutant was negative. In BHI, WT produced moderate biofilm and the mutant produced strong biofilm. A significant difference in biofilm formation is evident between the strains when grown in LB + glucose, M9 and BHI. The mutant produces a significantly higher amount of biofilm than WT when grown in LB + glucose and BHI. The biofilm formation of WT is significantly higher than that of the mutant when grown in M9. These data further confirm that the growth media most favourable for biofilm formation may be capsule-dependent.

3.2.4 Attempted constructions of CPS mutants

The generation of a confirmed capsule mutant was considered, in order to investigate the potential effect this could have on biofilm formation. The insertion of an antibiotic resistance cassette with flanking Flippase recombinase target sites enables the generation of a clean deletion mutant, which is desirable to prevent upstream or downstream effects. WT and mutant Kp52145 were successfully transformed with pKD46 by electroporation, as described in 2.2.3.2.

3.2.4.1 PCR-mediated gene replacement

3.2.4.1.1 Designing primers for the target knockout region

Primers for the template, detailed in Table 2.3, were designed with an internal overlap (~ 20 nucleotides) of the kanamycin resistance cassette of pKD4 and an external overlap (~ 50 nucleotides) with the target knockout gene(s) located in the CPS operon (Figure 3.2). GalF_F and Gnd_R included an external overlap of *galF* and *gnd*, respectively. The genes located between and including *galF* and *gnd*, discussed in 1.2.1.2, are the target knockout genes and thus would be expected to be replaced by the kanamycin resistance cassette during the recombination process.

Using these primers and pKD4 DNA as the template, a kanamycin resistance cassette, with flanking regions homologous to the target knockout region, was amplified. A ~ 1.5 kb DNA fragment corresponding to this cassette can be seen in Figure 3.3 (A). This PCR product was subsequently purified and electroporated into *K. pneumoniae*, as described in 2.2.2.1 and 2.2.1.3, respectively. However, following antibiotic selection of putative transformed mutants, it was evident that the transformation attempts of both WT and the capsule mutant harbouring pKD46, using this amplified kanamycin resistance cassette, had been unsuccessful.

3.2.4.1.2 Extension of the target knockout region

Primers were then redesigned to extend the target region to include all of the genes within the CPS operon, detailed in Figure 3.2 (B). The forward primer, Ugd_F, included an external overlap of *ugd*, and the reverse primer, GalF_R, included an external overlap of *galF*. This extended the target knockout region to include *manB* and *manC*. Using these primers and pKD4 DNA as the reaction template, a kanamycin resistance cassette, with flanking regions homologous to the extended target knockout region, was amplified. A ~ 1.5 kb DNA fragment corresponding to this cassette can be seen in Figure 3.3 (B). However, after repeating the steps outlined above, transformation attempts of both WT and the capsule mutant harbouring pKD46 were unsuccessful.

As discussed in 3.1, Huang *et al.* have successfully transformed *K. pneumoniae* (Huang *et al.*, 2014a). The primers designed by Huang *et al*. were amended to account for the

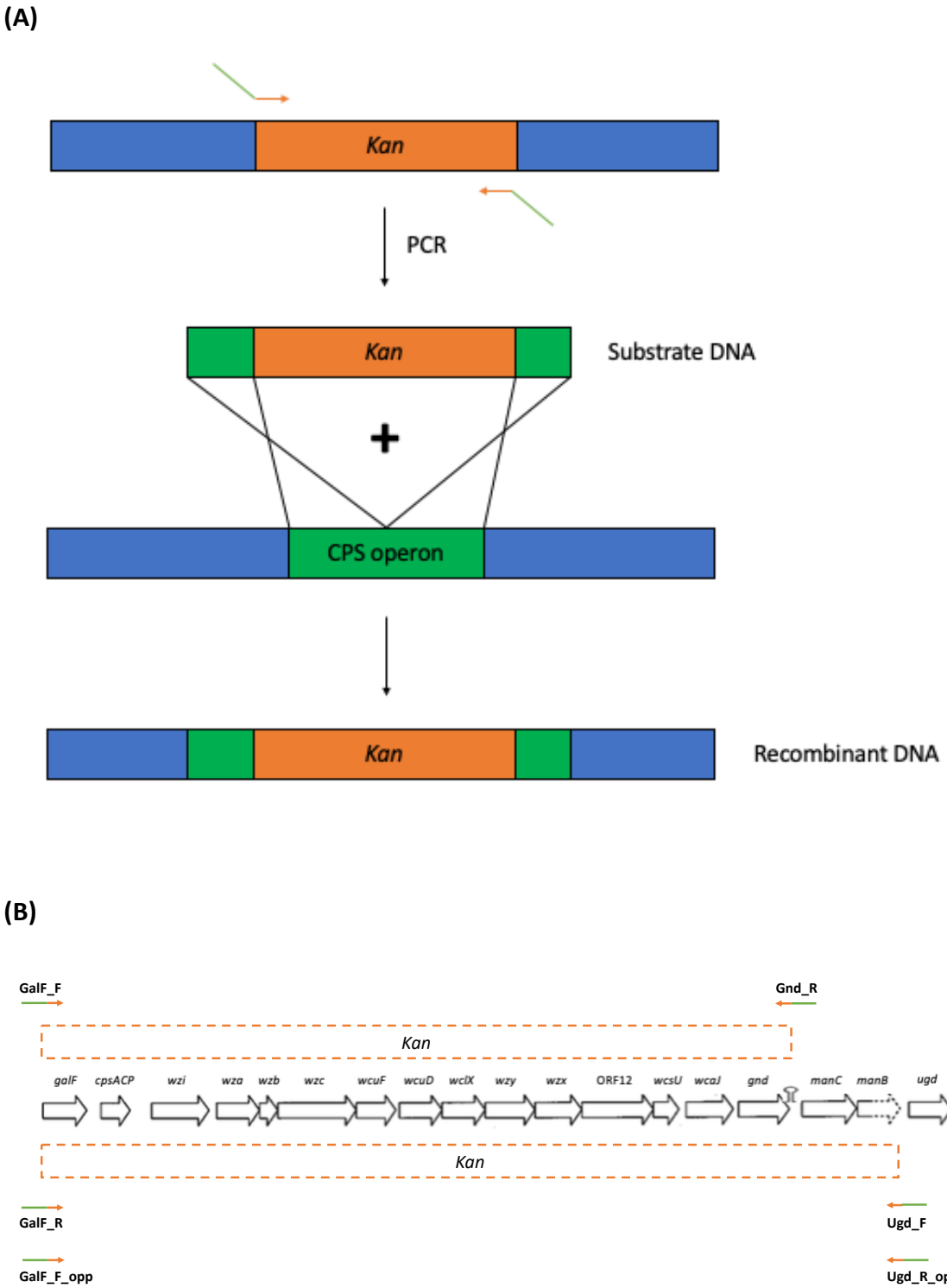

Figure 3.2: Overview of the λ-Red recombination system. (A) Schematic diagram of the λ-Red recombination system to replace the CPS operon with a kanamycin resistance cassette. (B) Schematic overview of the location in the CPS operon of primers designed with an internal overlap (~ 20 nucleotides) of the kanamycin resistance cassette of pKD4 and an external overlap (~ 50 nucleotides) with the target knockout gene(s) located in the CPS operon. The orange arrow heads represent the priming sequences of pKD4 while the green arrow tails represent the external overlap sequences with the target knockout gene(s). The area shaded blue represents DNA upstream and downstream of the CPS operon.

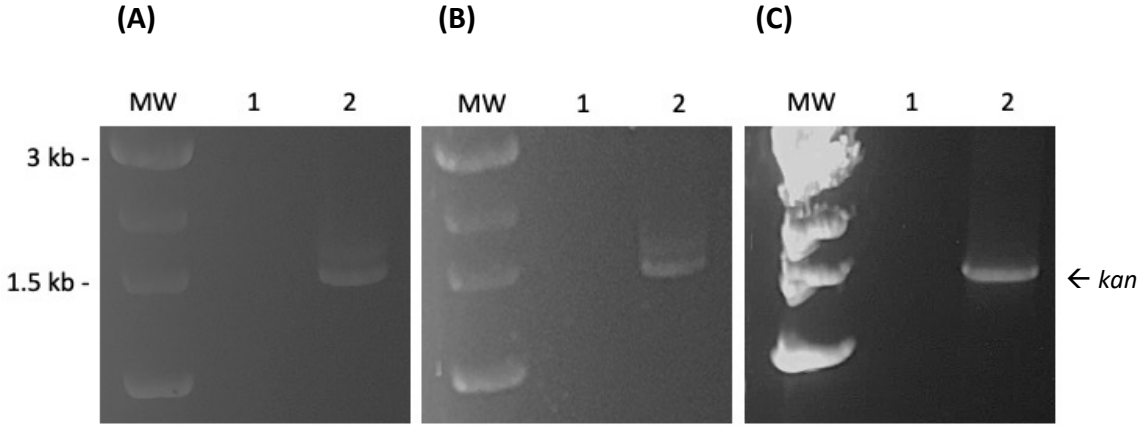

Figure 3.3: Amplification of an antibiotic cassette with flanking homology to the CPS operon. Agarose gel electrophoresis of the kanamycin resistance cassette (*kan*) amplified by PCR using primers **(A)** GalF_F and Gnd_R; **(B)** Ugd_F and GalF_R; and **(C)** GalF_F_opp and Ugd_R_opp. Bands corresponding to the kanamycin resistance cassette are marked with arrows and DNA size standards are indicated with molecular weight (MW) markers.

strain and kanamycin resistance cassette source variation. However, PCRs using primers Char ugd_F and Char galF_R failed to amplify the kanamycin resistance cassette.

3.2.4.1.3 Selection and transformation method amendments

Due to the numerous unsuccessful transformation attempts, the concentration of the kanamycin agar plates was adjusted. Transformants were selected for on agar plates supplemented with as low as 12.5 µg/ml kanamycin; Kp52145 is sensitive to this concentration. Additionally, a type 1 restriction inhibitor (2.5 µg/ml) was used in subsequent electroporations with the aim of increasing transformation efficiencies.

3.2.4.1.4 Adjusting the orientation of the kanamycin resistance cassette

As a final attempt, new primers were designed to orientate the kanamycin resistance cassette in the opposite direction in the substrate. GalF_F_opp and Ugd_R_opp successfully amplified the kanamycin resistance cassette (Figure 3.3 (C)). The type 1 restriction inhibitor was incorporated into electroporations of WT using the PCR products from 3.2.4.1.1 and from the aforementioned newest primer set. Selection was carried out on LB agar plates supplemented with the lower concentration of kanamycin.

The transformation using the product amplified using GalF_F_opp and Ugd_R_opp was unsuccessful. A low transformation frequency of 3.48×10^2 CFU/µg was achieved by WT using the PCR product from 3.2.4.1.1. However these transformants failed to survive following selection onto fresh kanamycin agar plates. This indicated that the original 'transformants' may have been kanamycin tolerant and the CPS operon of Kp52145 had not been successfully replaced by the kanamycin resistance cassette as anticipated.

3.2.4.1.5 Extending homologous regions using NEBuilder

The use of ~ 50 nucleotide homologous regions proved unsuccessful in promoting recombination; thus NEBuilder was considered as a potential mutagenesis option. As outlined in 2.2.3.3, the objective was to generate an assembled linear DNA fragment, from three individual fragments, that could be used to transform Kp52145, ultimately producing a mutant lacking the *cps* gene cluster.

Primers, detailed in Table 2.3, were designed with overlapping sequences between the adjacent DNA fragments, and can be seen in Figure 3.4 (A). A_fwd and B_rev flank the

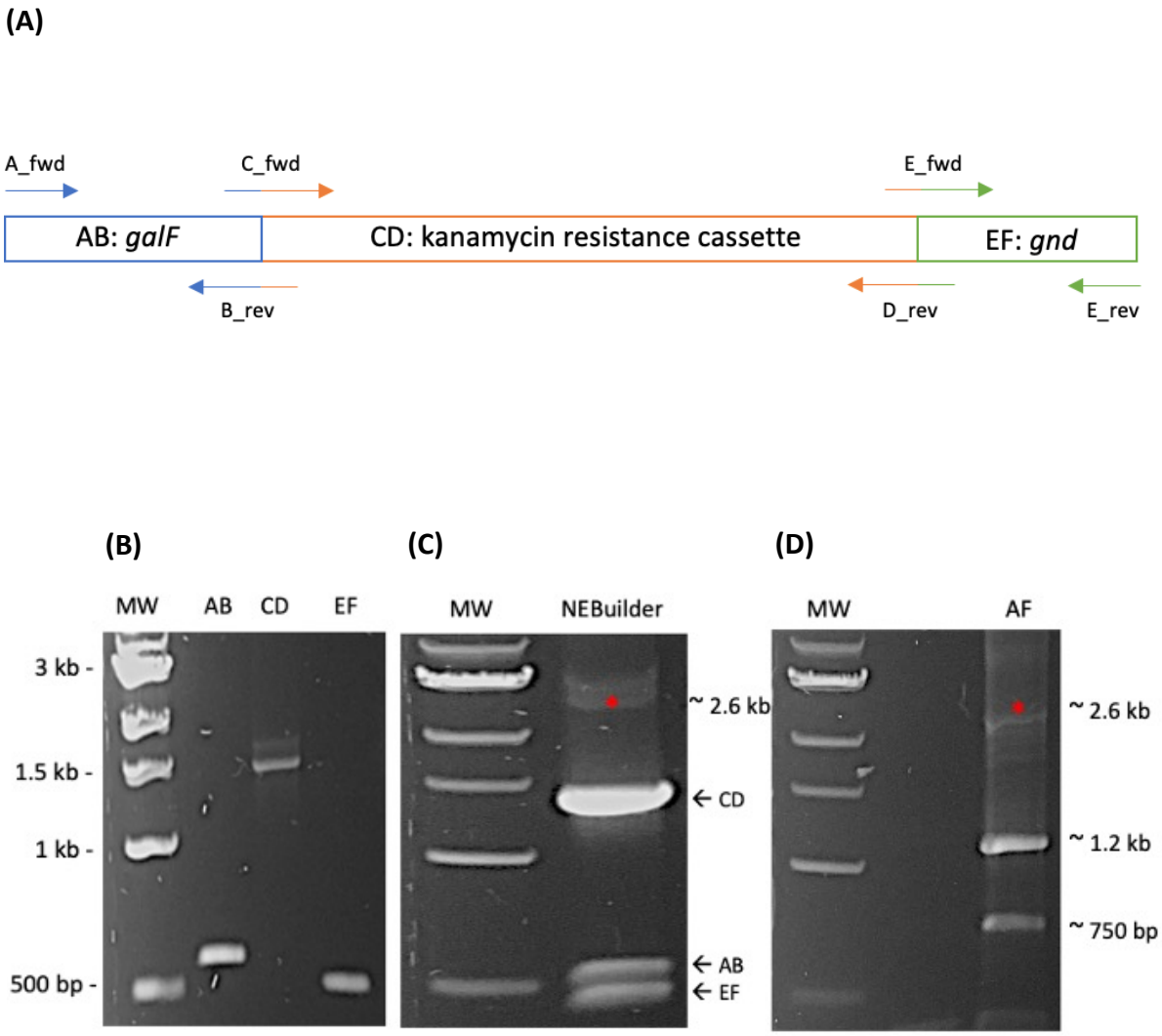

Figure 3.4: Amplification of an antibiotic cassette with extensive homology to the CPS operon. (A) Primers with overlapping sequences between the adjacent DNA fragments to generate an assembled linear DNA fragment. Agarose gel electrophoresis of **(B)** the three fragments prior to assembly; **(C)** the putative assembled fragment following incubation of the three individual fragments with NEBuilder HiFi DNA Assembly Master Mix; and **(D)** the putative assembled fragment amplified using primers A_fwd and F_rev. AB corresponds to the PCR product amplified using A_fwd and B_rev; CD corresponds to the PCR product amplified using C_fwd and D_rev; and EF corresponds to the PCR product amplified using E_fwd and F_rev. Bands corresponding to the three individual fragments are marked with arrows and the putative assembled fragment is marked with a red asterisk. DNA size standards are indicated with MW markers.

galF region of the CPS operon, while E_fwd and F_rev flank the *gnd* region. The product length of these primer sets are ~ 600 bp ('AB') and ~ 500 bp ('EF'), respectively. C_fwd and D_rev flank the kanamycin resistance cassette of pKD4 which is ~ 1.5 kb ('CD').

The amplification of the three fragments, following incubation with Dpn1, can be seen in Figure 3.4 (B). The fragments were combined and incubated with the NEBuilder HiFi DNA Assembly Master Mix and the putative assembled fragment was visualised on an agarose gel. The expected size of the assembled fragment was ~ 2.6 kb ('AF'). A fragment correlating to this size was evident which indicated that assembly of the three linear fragments had occurred (Figure 3.4 (C)). Additional shorter fragments corresponding to the individual PCR products, as visualised in Figure 3.4 (B) were also present. Using primers A_fwd and F_rev, and the NEBuilder product as template, there was weak amplification of the ~ 2.6 kb putative assembled fragment and shorter fragments differing in size to the those mentioned above were evident (Figure 3.4 (D)). Successive transformations of Kp52145/pKD46 using these final PCR products were unsuccessful.

3.2.5 Growth media influences the biofilm formation of hospital isolates

Further investigation surrounding the observed effects of growth media on biofilm formation was warranted in order to establish whether this was more widely observed in the species *Klebsiella*. *Klebsiella* isolates, blinded with no patient identifiers nor clinical data, from Tallaght University Hospital were provided by Dr. Jérôme Fennell (Table 2.1). The isolates were transferred from agar slants onto fresh blood agar plates and grown overnight in LB broth. Bacterial stocks of each isolate were added to the frozen collection of the laboratory, as described in 2.1.1.1, for further use. These isolates were subsequently incorporated into biofilm studies.

Biofilm formation varied among isolates, as can be seen in Figure 3.5 (2D graphs with error bars displayed in Figure A.3). Consistent with data discussed in 3.2.2, biofilm formation appeared to be influenced by growth media. Biofilm formation was classified in accordance with Naves *et al*. (2008). The large majority of isolates formed strong biofilms ($OD_{595nm} \geq 0.300$) in all media. With the exception of 344, 600.1, 900, and 980, the strongest biofilm formation was observed in all isolates grown in BHI compared to other growth media. This data is in accordance with data detailed in 3.2.2. The biofilm

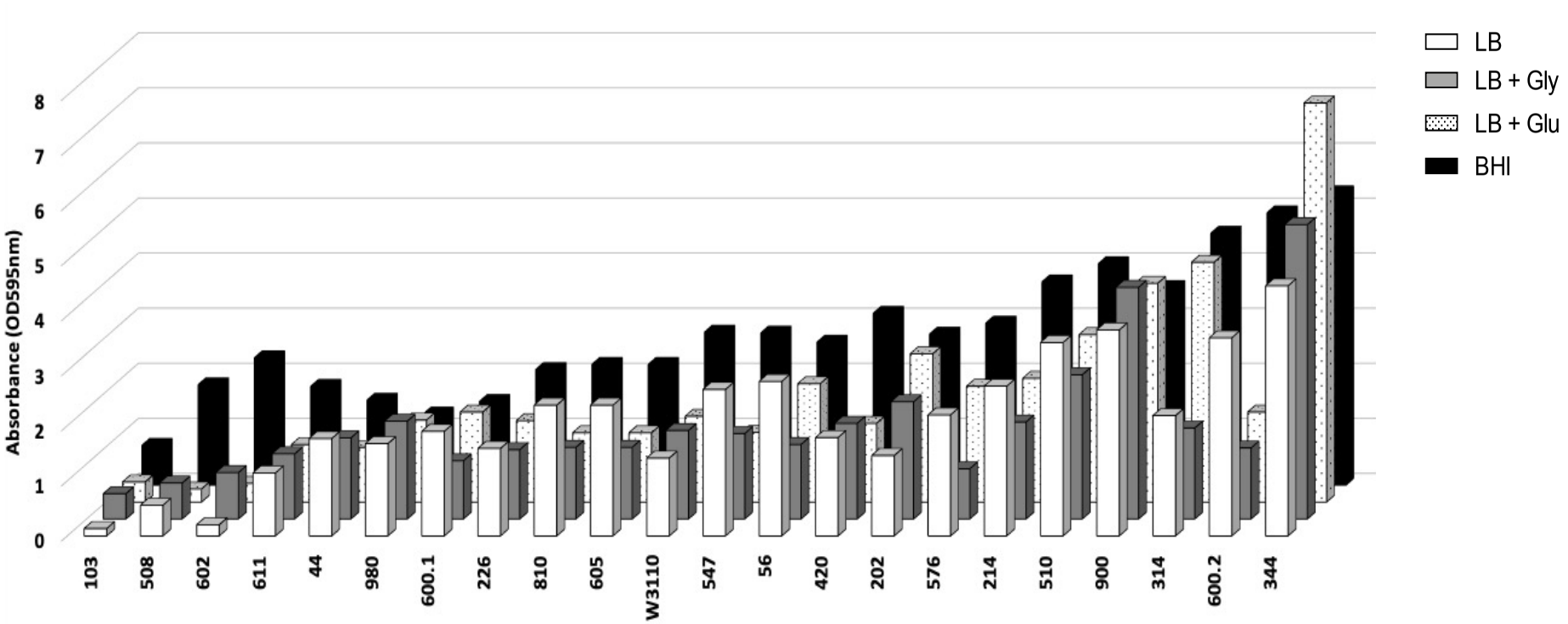

Figure 3.5: Biofilm formation of hospital isolates. Collation of the biofilm formation of hospital isolates. Isolates are plotted on the X axis; absorbance is plotted on the Y axis; and growth media are plotted on the Z axis. Isolates and growth media ordered in manner to maximise visualisation of data. Error bars unable to be generated on XYZ graph.

formation of isolates grown in either LB or LB supplemented with glucose or glycerol varied among isolates, with no notable pattern evident to be able to determine a ranking of these media in terms of their enhancement of biofilm formation among the hospital isolates. Another interesting observation from the data is the biofilm formation of 344. This isolate proved to be the strongest biofilm former, irrespective of growth media, amongst all other isolates. In contrast, 103, 508 and 602 were consistently the weakest three biofilm formers in every growth media tested (with the exception of 602 that ranks as a stronger biofilm former when grown in BHI). Apart from these observations, biofilm formation of the hospital isolates varied greatly depending on the growth media. Patient history, i.e. previous infections and antibiotic treatment, and the source of infection from which these isolates were collected are also factors that could be taken into consideration, however, due to data blinding these data were not available to analyse. This led to the consideration as to whether another factor, such as capsule, was playing a role in biofilm formation.

3.2.6 Capsular types of hospital isolates were identified using a *wzc* genotyping system

Due to the large variation in biofilm formation among isolates, it was postulated that the capsular type of isolates could be influencing this variation. A *wzc* genotyping system for *K. pneumoniae* developed by Pan *et al.* was utilised for capsule typing of the isolates (Pan *et al.*, 2013). Primer pair combinations are used to amplify *wzc*. Using primer pair 1 (Wza CF1 and Wzc CR1) and primer pair 2 (Wza CF2 and Wzc CR1) the expected size of PCR amplicons is ~ 2.7 kb and ~ 3.4 kb, respectively. The combination of these primer pairs yields products from 97% of the 78 documented capsule types (Pan *et al.*, 2013).

Genomic DNA was extracted from isolates and samples were visualised on an agarose gel prior to PCR to confirm successful extraction. Amplification of *wzc* using either or both primer pairs occurred in 5 out of the 21 hospital isolates. Using primer pair 1, a ~ 2.7 kb DNA fragment corresponding to *wzc* was amplified in 314, 420, and 547 (Figure 3.6 (A)). Using primer pair 2, a ~ 3.4 kb DNA fragment corresponding to *wzc* was amplified in 314, 344, 547, and 576 (Figure 3.6 (B)). The remaining 16 isolates tested negative for *wzc*, using the aforementioned primer pairs.

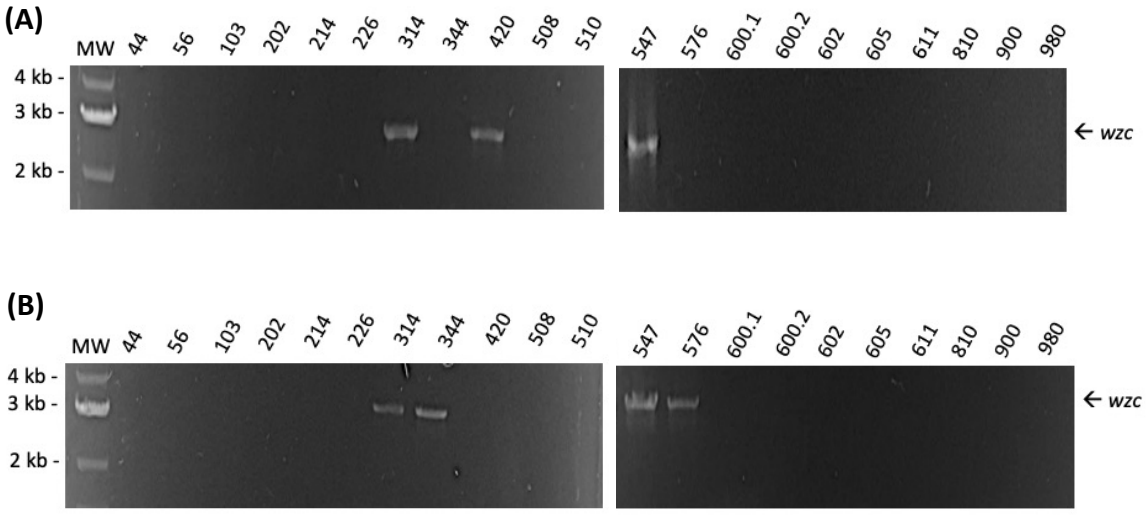

Figure 3.6: *wzc* genotyping PCR. Genomic DNA extracted from hospital isolates was used as template in PCRs **(A)** using primer pair 1 and **(B)** primer pair 2 to amplify *wzc*. Bands corresponding to the *wzc* gene are marked with arrows and DNA size standards are indicated with MW markers.

The *wzc* sequence amplified by the combination of primer pair 1 and 2 is highly similar among strains of the same capsular types (Pan *et al.*, 2013). Apart from some exceptions, low levels of similarity are noted among strains with different capsular types (Pan *et al.*, 2013). The genomic data of the amplified sequences were obtained from Source BioScience and compared to reference sequences, provided by Pan *et al*., on GenBank. The percentage identity is utilised to describe how similar a query sequence (i.e. hospital isolate) is to a target sequence (i.e. capsular type reference). The higher the percentage identity, the more similar the sequences are. The results are displayed in Table 3.1.

The *wzc* sequences of 314 and 547 were highly similar, i.e. 100% percentage identity, to the reference sequence for capsular type K14. A high similarity, i.e. 100% percentage identity, was detected between the *wzc* sequence of 420 and the reference sequence for K52. The percentage identity of the *wzc* sequences of 344 and 576 was lower than 100% when matched with any of the reference sequences. Therefore, the best match, i.e. the highest percentage identity, was chosen for both. Percentage identities of > 99% were detected between 344 and 576, and the reference sequences for K52 and K2, respectively.

3.2.7 *khe* acts as an internal control to screen for *K. pneumoniae* isolates

According to the *wzc* genotyping system, the majority of hospital isolates were lacking this gene. In order to establish whether the lack of amplification of *wzc* in these isolates was due to absence of the gene as opposed to insufficient genomic DNA for PCR, an internal control was selected. *khe*, the *Klebsiella* haemolysin gene, is present in all *K. pneumoniae* and thus is a reliable species-specific gene for species identification of the isolates (Weiss *et al.*, 2019). This provided a convenient alternative to 16S sequencing since sequencing is not required. While *khe* is highly conserved in the most tested *K. pneumoniae* isolates (Weiss *et al.*, 2019), three single nucleotide polymorphisms (SNPs) exist in the *khe* of Kp52145 and primers designed by Weiss *et al*. were amended to avoid these (Table 2.3).

khe was amplified by PCR using the aforementioned primers. A ~ 126 bp DNA fragment corresponding to *khe* was visible in both WT and capsule mutant Kp52145, and 19 out

Table 3.1 Capsular types of hospital isolates

Strain	Putative capsular type	Percentage identity
314	K14	100%
344	K52	99.8%[a]
420	K52	100%
547	K14	100%
576	K2	99.19%[a]

[a] Closest percentage identity match.

of the 21 hospital isolates (Figure 3.7). 605 initially tested falsely negative but upon second attempt tested positive for *khe* (Figure 3.7 (B)). 420 and 600.1 tested negative for *khe*, suggesting that they were not *K. pneumoniae* isolates. VITEK analysis identified 420 and 600.1 as *K. oxytoca* isolates. The amplification of *khe* in isolates that tested negative for *wzc* implied that the genomic DNA of the samples was sufficient. This indicated that these isolates are either of the two capsular types, K15 or K50, that do not yield a product using the combination of primer pairs (Pan *et al.*, 2013), or are *wzc* mutants.

3.3 Discussion

The characteristic mucoid phenotype when most *K. pneumoniae* isolates are grown on agar plates is as a result of its prominent capsule (Struve & Krogfelt, 2003). Therefore, without capsule, the Kp52145 mutant produces non-mucoid colonies. The string test is qualitative and thus serves to purely assess the phenotype of a strain (Walker *et al.*, 2019). Not all mucoid colonies of *K. pneumoniae* test positive in the string test (Catalán-Nájera *et al.*, 2017). As discussed in 1.2.1.3, a positive string test is what differentiates a HMV phenotype from a mucoid phenotype (Catalán-Nájera *et al.*, 2017). Thereby, WT Kp52145 displays a HMV phenotype, whereas the phenotype of the acapsular mutant is non-mucoid and non-HMV.

The results from the phenotypic characterisation of the Kp52145 strains are in accordance with their putative genotypes. The HMV phenotype is associated with hypervirulence (hv) and Kp52145 is widely considered a hvKP isolate (Moura *et al.*, 2017, Wang *et al.*, 2018a, Struve *et al.*, 2015). Additionally, Walker *et al.* have observed a significant reduction in mucoviscosity as a result of a *manC* deletion in *K. pneumoniae* (Walker *et al.*, 2019). Mucoviscosity can be assessed quantitatively by measuring the OD_{600nm} of supernatants following low-speed centrifugation of cultures grown overnight (Paczosa *et al.*, 2020). HMV strains fail to sediment efficiently during centrifugation and as a result, the supernatant remains turbid. Therefore, measurement of turbidity after centrifugation serves as a quantitative indicator of HMV (Walker *et al.*, 2019).

Biofilm formation can be quantified directly and indirectly. CVAs are routinely used in the study of biofilms due to their simplicity, rapid analysis and high-throughput nature.

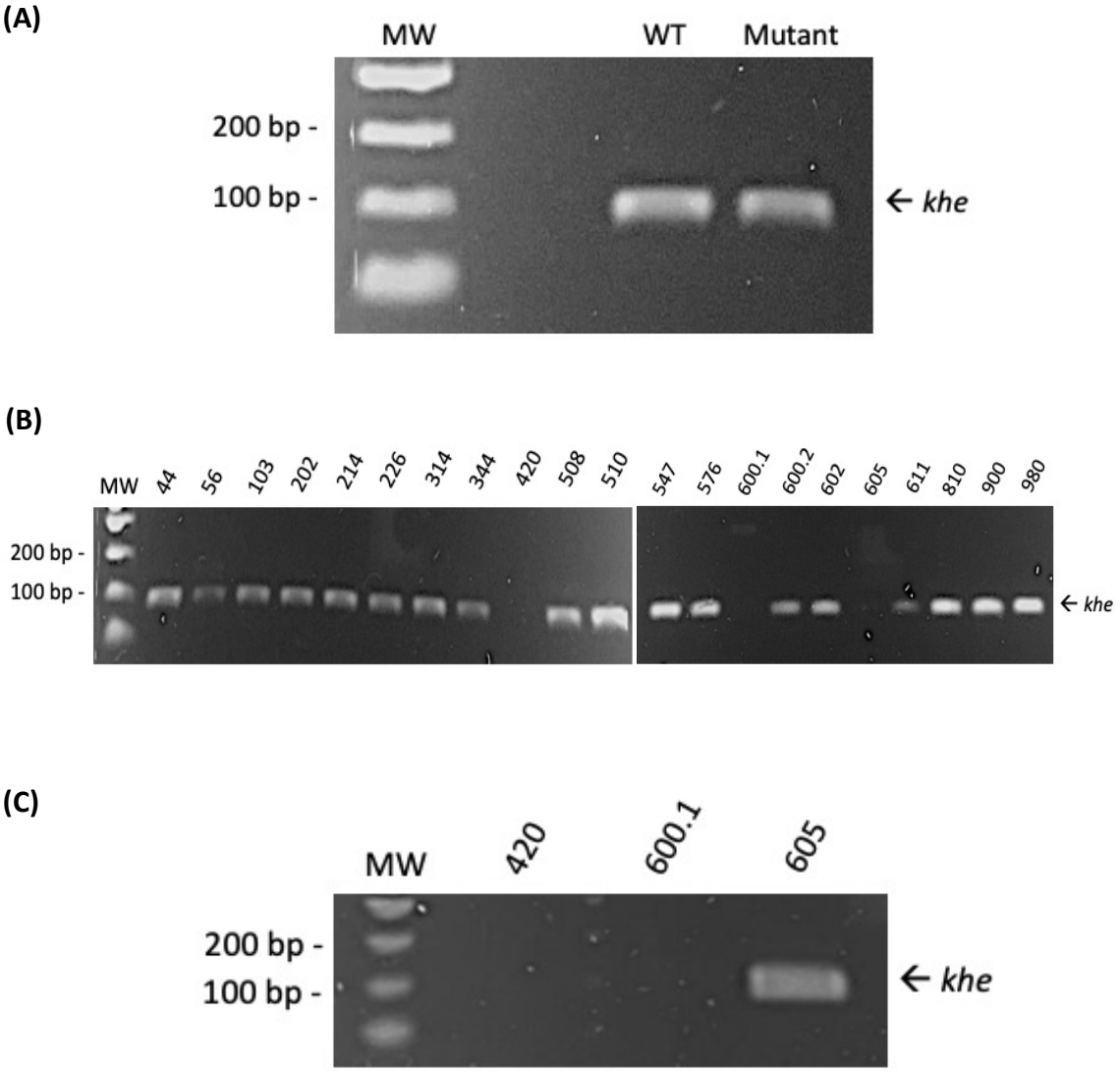

Figure 3.7: Speciation of *Klebsiella* by *khe* genotyping. Genomic DNA extracted from **(A)** WT and mutant Kp52145; and **(B)** and **(C)** hospital isolates was used as template in PCRs to amplify *khe*. Bands corresponding to the *khe* gene are marked with arrows and DNA size standards are indicated with MW markers.

The use of CV is an indirect quantification method; stained biomass acts as a proxy marker to infer biofilm quantity (Wilson *et al.*, 2017). Therefore the non-specific nature of CV means that the assay cannot differentiate between viable biofilm-forming cells and other biomass components such as ECM or dead cells (Roberts *et al.*, 2015). Direct quantification methods enable the enumeration of biofilm forming cells thus providing the specificity that CVAs lack. Such methods include, viable counting of biofilm suspensions (following a similar protocol as described in 2.1.1.6); fluorescent markers; and various microscopy techniques (Wilson *et al.*, 2017). The incorporation of microscopic analysis into biofilm studies enables biofilm to be visually distinguished from additional biomass components, ultimately providing confirmatory evidence of biofilm formation. Additionally, the use of bioluminometry (discussed in Chapter 4), would enable real-time monitoring of biofilm formation, as carried out by Pearson, 2019.

The composition of growth media is a contributing factor to biofilm formation (Naves *et al.*, 2008). The optimum growth media for biofilm formation of WT and mutant Kp52145 differed. This observation supports the hypothesis that the contribution of certain nutrients to biofilm formation may be capsule-dependent. WT forms biofilms optimally in M9 and BHI, the mutant in LB + glucose and BHI (Figure 3.1 (A)). These three media provide an exogenous source of glucose to the bacteria. The concentration of glucose (w/v) in LB + glucose, M9 and BHI is 0.5%, 20% and 5%, respectively. This variance in glucose abundance could be a contributing factor to the observed differences in biofilm formation in these media. As discussed in 1.3.1.1, exogenous glucose levels can induce type 3 fimbriae expression and increase CPS production (Lin *et al.*, 2013b, Lin *et al.*, 2016), indicating that these structures may contribute to biofilm formation in Kp52145. Both the WT and mutant produced significantly less biofilm in LB and LB + glycerol compared to glucose supplemented media. This observation provides additional evidence that glucose is an important external factor of biofilm formation. Further research is warranted to decipher the differences in biofilm formation between the glucose supplemented media. Additionally, the complex media M9 and BHI could be analysed to establish the growth-determining components of these media and whether

these affect the expression of the different biofilm-mediating structures of *K. pneumoniae.*

These data regarding the modulation of virulence factors by glucose are of clinical relevance considering the heightened susceptibility of diabetic patients to *K. pneumoniae* infections (Lin *et al.*, 2013c, Lee *et al.*, 2017). As discussed in 1.3.1.1, cAMP and carbon catabolite repression proteins such as CRP, regulate the stimulation of CPS biosynthesis by glucose (Lin *et al.*, 2013a). An increase in CPS production, confers both a mucoid phenotype, the degree of which positively correlates with successful establishment of infection, and resistance to phagocytosis and serum killing (Sahly *et al.*, 2000, Nassif & Sansonetti, 1986); and thus intensifies the pathogenicity of *K. pneumoniae* (Lee *et al.*, 2016). Therefore, it has been suggested that diabetes provides a specialised environment that enables the dissemination of *K. pneumoniae* from the lungs or intestines into the blood (Lin *et al.*, 2011).

Figure 3.1 (B) displays the differences in the biofilm formation of WT and mutant Kp52145. The mutant produced significantly higher levels of biofilm compared to WT when grown in LB + glucose and BHI. However, the biofilm formation of WT is significantly higher than that of the mutant when grown in M9. This suggests that the capsule may be both hindering and enhancing biofilm formation when grown in particular media. As discussed in 3.1, the capsule plays a complex role in biofilm formation. Several studies have reported that the reduction or absence of capsule results in biofilm deficiencies, therefore establishing the capsule of *K. pneumoniae* as a key factor in biofilm formation (Wu *et al.*, 2011, Zheng *et al.*, 2018, Boddicker *et al.*, 2006). On the contrary, increased biofilm formation has also been associated with *K. pneumoniae* capsule mutants, with numerous explanations proposed for this observation. Huang *et al.* reported that capsule loss results in a strong up-regulation of the *pga* operon, which synthesises poly-beta-1,6-N-acetyl-D-glucosamine (PGA), a secreted extracellular component of the biofilm matrix (Huang *et al.*, 2014a). The capsule's interference with adhesive fimbrial structures has also been investigated (Schembri *et al.*, 2004). Evidently, the biofilm formation of *K. pneumoniae* is multifactorial. The conflicting data regarding the role capsule plays in biofilm formation may be due to strain and/or mutation differences. Additionally, the contribution and

roles of different biofilm-mediating factors is thought to vary at different stages of biofilm formation (Schembri *et al.*, 2005, Balestrino *et al.*, 2008).

As discussed above, a range of biofilm formation was evident amongst the hospital isolates. Due to the large number that tested negative for the *wzc* gene, the capsular types of just five isolates could be determined (Table 3.1). The biofilm formation of these isolates is summarised in Table 3.2. As mentioned in 3.1, the loss of *wzc* can result in either prevention or reduction in CPS synthesis. Additionally, it is important to note that capsular types K15 and K50 do not yield a product using the primer sets employed by the genotyping system. This is due to the replacement of both the *wzb* and *wzc* genes with genes encoding transposases in K15 and K50 (Pan *et al.*, 2013). Furthermore, Alcian blue staining has revealed the absence of capsule in reference strains of capsular types K15 and K50 (Pan *et al.*, 2013).

Therefore, it can be inferred from these particulars that the isolates are either acapsular; encapsulated in a reduced CPS; or of capsular type K15 and K52 and hence acapsular. Sequencing the CPS operon of the isolates that tested negative for this gene would be essential in providing clarity on this matter. Additionally, type-specific primers, as designed by Pan *et al.*, could elucidate whether the *wzc*-negative isolates are either of these two capsular types (Pan *et al.*, 2013). As mentioned in 3.1, a knowledge gap appears to exist in this area, and evidently requires further study which could address unanswered questions. For instance, do isolates of the same capsular type produce similar levels of biofilm and do particular capsular types enhance or hinder biofilm formation?

Although the λ-Red recombination technology has been optimised for use in *E. coli*, it has not been as widely employed in *Klebsiella*. However, various *K. pneumoniae* strains, including Kp52145, have been genetically manipulated using the λ-Red recombineering tool (Kidd *et al.*, 2017, Huang *et al.*, 2014a, Wei *et al.*, 2012), indicating that the mutagenesis failure is not strain-dependent. Recombination frequency is markedly affected by the plasmid expressing the λ-Red proteins (Murphy & Campellone, 2003, Egan *et al.*, 2016). Alternative λ-Red systems to pKD46 have been employed in *K. pneumoniae*, including pKOBEG, pKD6, and pACBSR-Hyg (Wang *et al.*, 2018b, Wei *et al.*, 2012, Huang *et al.*, 2014a); the latter of which was considered prior to discovering that

Table 3.2 Capsular serotypes in relation to biofilm formation of *wzc* positive isolates

			Biofilm formation			
Strain	**Putative capsular type**	***khe***	**LB**	**LB + Glu**	**LB + Gly**	**BHI**
314	K14	Positive	+++	+++	+++	+++
344	K52	Positive	+++	+++	+++	+++
420	K52	Positive	+++	+++	+++	+++
547	K14	Positive	+++	+++	+++	+++
576	K2	Positive	+++	+++	+++	+++

Biofilm formation classified according to Naves *et al*. -, negative; +, weak; ++, moderate; +++, strong.

the Kp52145 strains were hygromycin-resistant. An alternative resistance marker could also be used to investigate whether higher concentrations of the desired insertion fragment could be achieved. Additionally, expression levels of the resistance marker can be affected by its orientation and/or position within the chromosome (Murphy & Campellone, 2003), the former of which was investigated (3.2.4.1.4) without success.

The consideration of alternative λ-Red systems, resistance markers and knockout regions has the potential to alter future transformation results. Furthermore, recombination may be hindered by endogenous nucleases of *Klebsiella*, such as KpnI (Tomassini *et al.*, 1978), which can degrade exogenous DNA acting as the recombination substrate. Hence, the removal of such nucleases would be required to improve recombineering properties. Chen *et al*. discovered that Gam has a weak inhibitory effect on the RecBCD exonuclease of *K. pneumoniae* and the mutation of *recB* enhances λ-Red recombination in *K. pneumoniae* (Chen *et al.*, 2016). Moreover, it was suggested that this was contributing to the lower efficiency of gene replacement in *K. pneumoniae* than in *E. coli* (Chen *et al.*, 2016). I have also previously had success using the pKD46 system for the mutagenesis of *E. coli* CFT073 (Moynihan, 2018), indicating that mutagenesis success may be dependent on the species type. Therefore, an alignment of the *recB* genes of both *K. pneumoniae* and *E. coli* would be informative as to whether this gene is hindering the mutagenesis success of Kp52145.

The lack of success generating a CPS operon mutant could also be methodology-dependent. Several adjustments could be made to the current protocol used in this study that may enable the successful transformation of Kp52145. Murphy & Campellone found that the addition of a heat-shock step, following induction of the λ-Red genes (as described in 2.3.2.2) and prior to the harvesting of electrocompetent cells, induced higher frequency of gene replacement (Murphy & Campellone, 2003). However this could only be considered alongside a non-temperature sensitive plasmid donor, unlike pKD46. Additionally, the arabinose induction of λ-Red proteins could be evaluated by Western blot using Red antibodies (Subramaniam *et al.*, 2016). Gel extraction of the desired PCR product prior to purification could increase the concentration of the DNA substrate for electroporation and eliminate the presence of shorter fragments, as seen in Figure 3.4.

An alternative gene replacement method, developed by Link *et al.*, has also been carried out in Kp52145 (Llobet *et al.*, 2008, Regué *et al.*, 2005). In-frame deletion constructs are generated *in vitro* and carried in the gene replacement vector, pKO3, which is subsequently electroporated into the bacteria (Link *et al.*, 1997). This system was utilised by Llobet *et al*. to construct the Kp52145 mutant used in this study and therefore represents a viable alternative mutagenesis option for future work involving Kp52145.

Chapter 4 Phenotypic and genotypic analysis of Kp52145 strains

4.1 Introduction

Bacterial viability assays are widely employed in a variety of research areas, which include the evaluation of antimicrobial properties, investigation of bacterial growth determinants and environmental monitoring (Conway *et al.*, 2020). Due to its high-throughput and user-friendly nature (Riss *et al.*, 2011, Paley & Prescher, 2014), this study considered the utilisation of bioluminescence to monitor bacterial viability.

Bioluminescence refers to the process by which chemical energy is converted to light by living organisms (Wilson & Hastings, 1998). Adenosine triphosphate (ATP) acts as the primary energy source in all organisms and thus is considered a prime marker for cell viability (Wilson & Hastings, 1998, Wilson *et al.*, 2017). Bioluminescence has been widely applied to analytical methods to study areas such as pathogenicity and antimicrobials (Sánchez *et al.*, 2013, Huang *et al.*, 2014b, Gonzalez *et al.*, 2012, Kadurugamuwa *et al.*, 2003b), as well as biofilm formation (Sharp *et al.*, 2005, Kadurugamuwa *et al.*, 2003a, Garcez *et al.*, 2013).

ATP is required by luciferase, a light-producing enzyme, to generate a light signal (Wilson & Hastings, 1998). The production of ATP occurs only in catabolically active cells; hence the main indicator of cell viability is intracellular ATP content (Wilson *et al.*, 2017). Yellow-green light, produced by hydrolysis of ATP by luciferase, can be detected using a luminometer and reported as relative light units (RLUs) (Sun *et al.*, 2002). A proportional relationship exists between the light intensity from the reaction and the amount of ATP in the sample; hence the number of bacteria, from which ATP is released, is considered to be proportional to the amount of light emitted during the reaction (Sun *et al.*, 2002). Figure 4.1 is a schematic diagram of the bacterial bioluminescence reaction.

The bacterial luciferase gene cassette (*lux*) is a stable luminescent reporter which enables real-time monitoring of bacteria (Close *et al.*, 2012). The *lux* operon contains genes (*luxCDABE*), which are conserved across all *lux* systems and required for the bacterial bioluminescence reaction (Meighen, 1994). The reaction is catalysed by luciferase, which requires a luciferin as a substrate (Gregor *et al.*, 2018). Bacterial

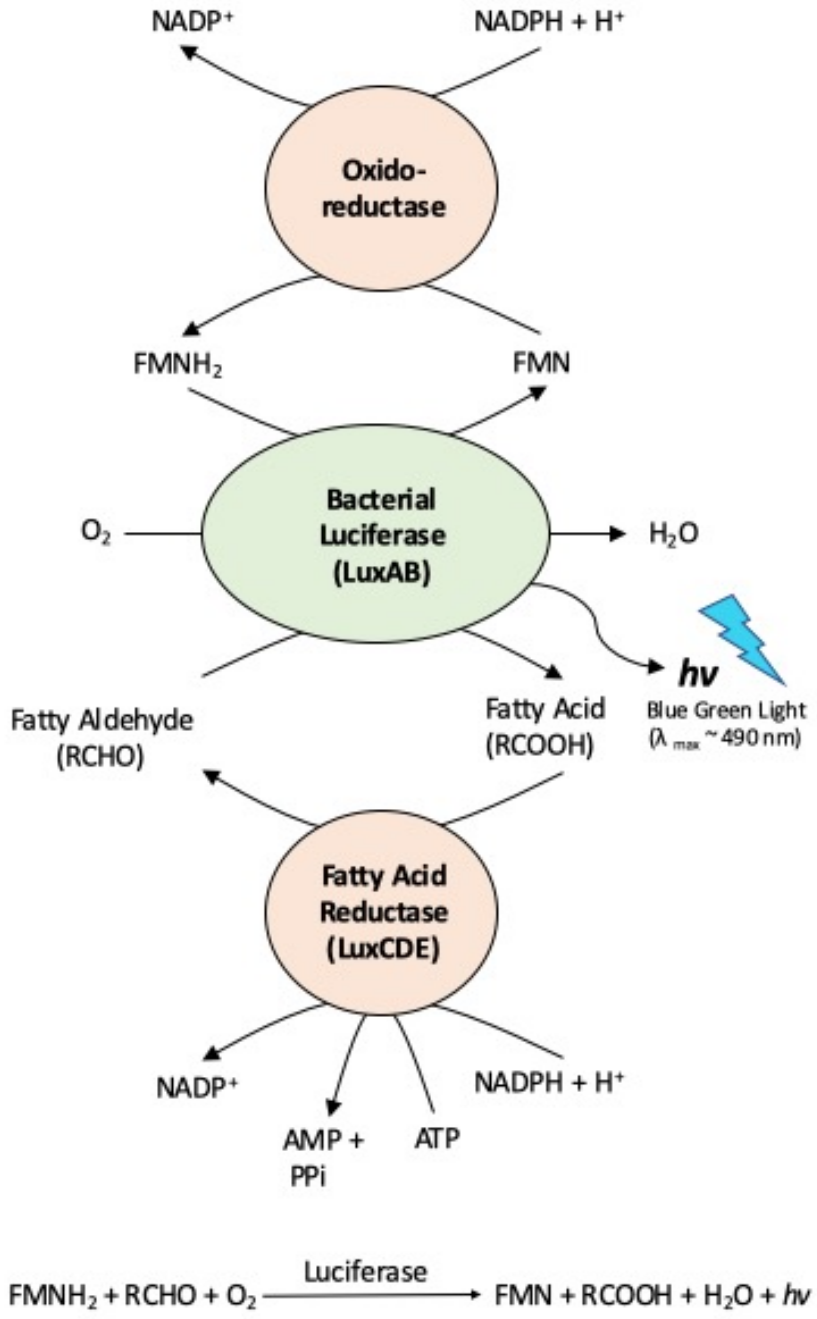

Figure 4.1: Bacterial bioluminescence reaction. Flavin mononucleotide (FMN) is reduced to $FMNH_2$ by oxidoreductase. A fatty acid reductase complex, encoded by *luxCDE*, produces fatty aldehydes from fatty acids. The regeneration of $FMNH_2$ and fatty aldehyde requires a continuous supply of ATP and NADPH. Bacterial luciferase, encoded by *luxAB*, catalyses the oxidation of $FMNH_2$ and fatty aldehyde with molecular oxygen to produce FMN, fatty acid and water, resulting in the emission of light. Adapted from (Widder & Falls, 2014).

luciferase does not require exogenous substrate and thus can function independently (Close *et al.*, 2012). In contrast, *Renilla* luciferase, isolated from the sea pansy *Renilla reniformis*, requires an exogenous supply of the luciferin coelenterazine (Bhaumik & Gambhir, 2002).

The *luxA* and *luxB* genes encode the a and b subunits of luciferase, respectively; while *luxC*, *luxD*, and *luxE* genes encode a fatty acid reductase, transferase and synthase, respectively, that constitute the fatty acid reductase complex for aldehyde synthesis (Meighen, 1994, Close *et al.*, 2012). The LuxAB complex catalyses the light-emitting reaction, which involves the oxidation of the bacterial luciferin $FMNH_2$ to FMN (flavin mononucleotide) and the conversion of a long chain fatty aldehyde to its cognate acid. LuxC, D and E are involved in various reactions responsible for recycling the fatty acid back to aldehyde (Meighen, 1994).

An optimised bacterial bioluminescent system, with a seven-fold increase in brightness, has been developed by Gregor *et al.* (Gregor *et al.*, 2018). The *lux* operon from the bioluminescent bacterium, *Photorhabdus luminescens*, was enhanced by mutagenesis of the *luxCDABE* genes and the introduction of an additional FMN reductase to increase the amount of $FMNH_2$ being generated (Gregor *et al.*, 2018). The resulting improved operon was termed *ilux* (Gregor *et al.*, 2018). *ilux* was subsequently cloned into pGEX(-), a Glutathione S-transferase (GST)-deleted version of vector pGEX-6P-1 (Figure 4.2), which is *tac* promoter driven and carries an ampicillin resistance cassette (Gregor *et al.*, 2018). The resulting plasmid has been designated the term pilux by this study. A full sequence map is displayed in Figure 4.3. Bacterial strains harbouring the plasmid can produce light, without the requirement of the addition of an exogenous substrate.

The bioluminescent system developed by Gregor *et al.* was originally expressed in *E. coli* cells (Gregor *et al.*, 2018). A review of the literature indicates that the use of *lux* systems in *K. pneumoniae* is an area that has not been extensively explored. Nevertheless, bioluminescent *K. pneumoniae* have been generated by several studies. The thick capsule of *K. pneumoniae* may pose as a barrier to penetration of plasmid DNA by electroporation. Huang *et al.* constructed a conjugative plasmid carrying the *lux* genes, in order to overcome the difficulty of transformation for *K. pneumoniae* (Huang *et al.*, 2014b).

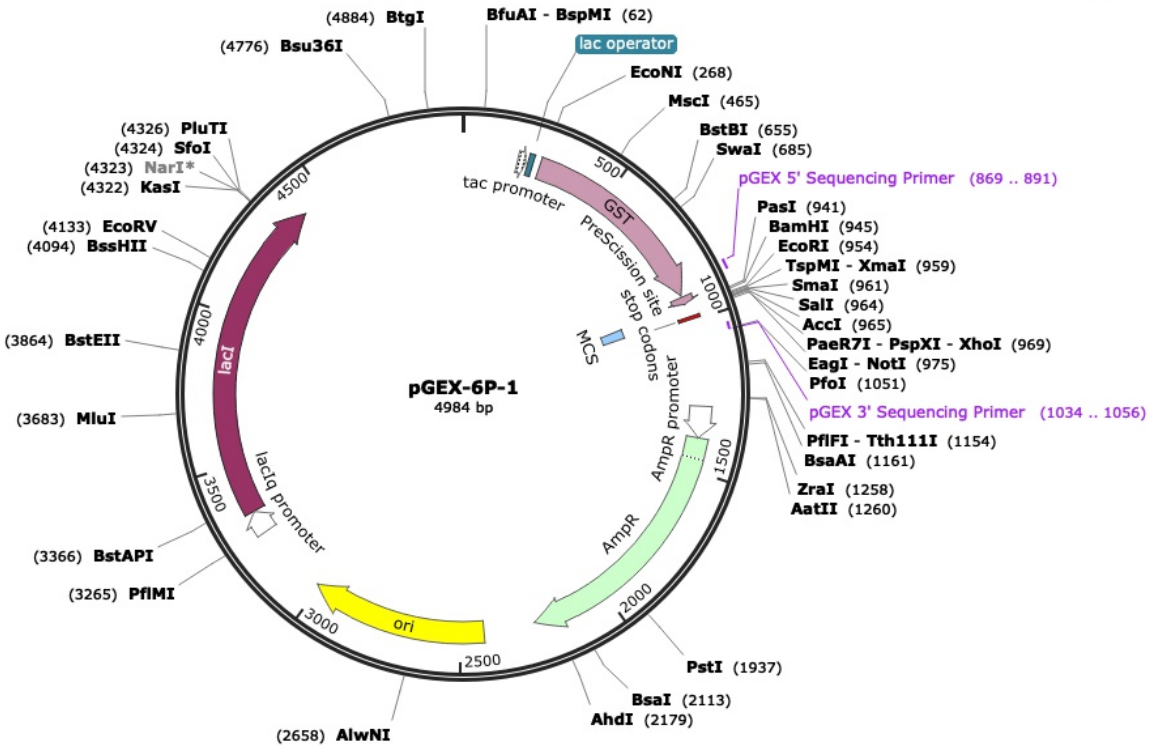

Figure 4.2: Sequence map for pGEX-6P-1 plasmid. The GST region of this plasmid was deleted; resulting in a vector termed pGEX(-). The origin of replication is ColE1. The *lac1* gene, which encodes the repressor of the *lac* operon, is under the control of the Isopropyl β-d-1-thiogalactopyranoside (IPTG) inducible *lac1q* promoter. An ampicillin resistance gene is contained in the plasmid and is controlled by the AmpR promoter. The positions of primers and restriction sites are also indicated. Diagram from SnapGene.

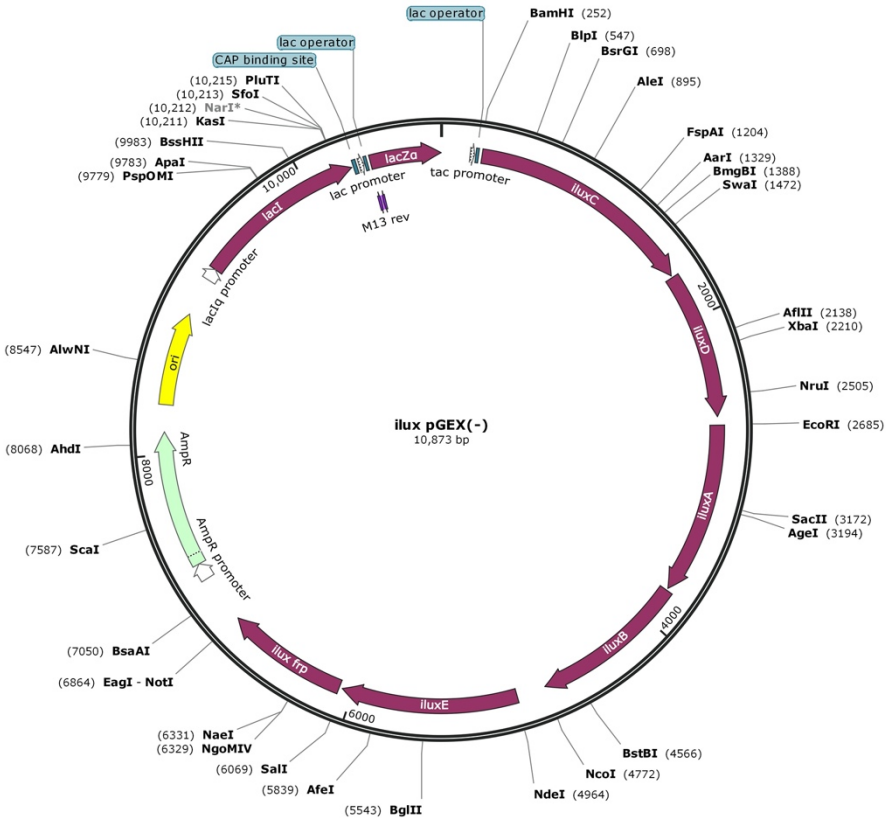

Figure 4.3: Sequence map for pilux plasmid. The *luxCDABE* operon of *P. luminescens* was cloned into the vector pGEX-6P-1 (Figure 4.2) (Gregor *et al.*, 2018). Plasmid description is as outlined in Figure 4.2 with the addition of the *lux* operon and *frp* gene, under control of the *tac* promoter, from position ~ 113 → 6900. The *frp* gene, from *Vibrio campbellii*, encodes the additional FMN reductase (discussed in 4.1) which is coexpressed with the *lux* genes. Diagram from SnapGene.

Piperacillin is an extended spectrum β-lactam antibiotic that inhibits bacterial cell wall synthesis by binding to penicillin binding proteins located in the cytoplasmic membrane of bacteria (Doi & Chambers, 2015). β-lactams penetrate the bacterial OM *via* porins, which are OMPs that serve as transmembrane diffusion channels for antibiotic entry (Nikaido, 2003).

Tazobactam is a penicillanic acid β-lactamase inhibitor that shares structural similarities with penicillin, and thus is recognised as a substrate for β-lactamases (Drawz & Bonomo, 2010). Tazobactam thereby broadens the spectrum of piperacillin by preventing its degradation by β-lactamases (Doi & Chambers, 2015).

A brief outline of this chapter is listed below.

- In order to investigate the use of bioluminescence as a means of real-time cell viability monitoring, bioluminescent Kp52145 strains, harbouring pilux, were constructed.
- The bioluminescent signal of these strains was measured both qualitatively, using a CCD camera and image analysis software, and quantitatively, using a microplate reader.
- MIC analysis of Kp52145 strains was carried out.
- Finally, the genotype of the mutant was investigated. PCRs were carried out to amplify regions throughout the CPS operon in order to identify the location of the mutation.
- WGS revealed that the CPS was intact, and mutations were present elsewhere in the genome of the mutant.

4.2 Results

4.2.1 Adaption of bioluminescence for viability measurement of *K. pneumoniae*

WT and mutant Kp52145 were transformed with pilux (Table 2.2) by electroporation. As described in 2.2.1.1, growth media was supplemented with EDTA during the preparation of electrocompetent cells which resulted in a reduction in capsule production by Kp52145. This enabled successful transformation of WT Kp52145. Transformed isolates were initially screened for bioluminescence using a CCD camera and image analysis

software. Bioluminescent signal was detected from isolates harbouring pilux (Figure A.2). Kp52145 isolates without pilux acted as negative controls due to their innate inability to emit light.

4.2.2 Quantification of bioluminescence in *K. pneumoniae*

The bioluminescence of Kp52145 strains harbouring pilux was measured quantitatively by luminometry. Overnight cultures were diluted 1:100 (as described in 2.1.1.3) and grown to OD_{600nm} measurements of 0.2, 0.4, 0.6 and 0.8. Upon reaching these absorbance values, aliquots of the culture were transferred to a white 96 well plate and bioluminescence was measured in a microplate reader. Bioluminescent signal was measured, in RLU, by a microplate reader (FLUOstar Optima; BMG Labtech). Kp52145 isolates without pilux acted as negative controls. The results are displayed in Figure 4.4 (A). IPTG induction was not required for bioluminescent emission, which indicated that leaky expression of the *lac* operon was occurring. At all absorbance points, the WT emitted a significantly higher bioluminescent signal in comparison to the mutant.

Additionally, the absorbance and bioluminescence of the Kp52145 strains harbouring pilux was measured incrementally over a 3 h period, as outlined in 2.4.2. These data are displayed in Figure 4.4. In general, both the absorbance and bioluminescence of the Kp52145 strains increased over time. However a clear relationship between absorbance and bioluminescent is not apparent, as displayed in Figure 4.4 (B) and (C). The data points appear somewhat inverse from the time point 140 min onwards, which is also when both strains reach an OD_{600nm} of 0.4. While the absorbance of WT is lower than the mutant at 160 min and 180 min, the opposite is true when examining the bioluminescent data. WT emits a higher bioluminescent signal at both these time points in comparison to the mutant. Up until 140 min, the strains appear to grow at a similar rate and equally, emit similar levels of bioluminescence. Evidently, it would be of interest to carry out this assay over a longer period in order to observe if and how this pattern progresses.

Bioluminescence was also utilised as a measure of viability of Kp52145 strains in serum killing assays (data not shown). However, due to the intrinsic differences in light emission by these strains, this method was deemed inappropriate for further use.

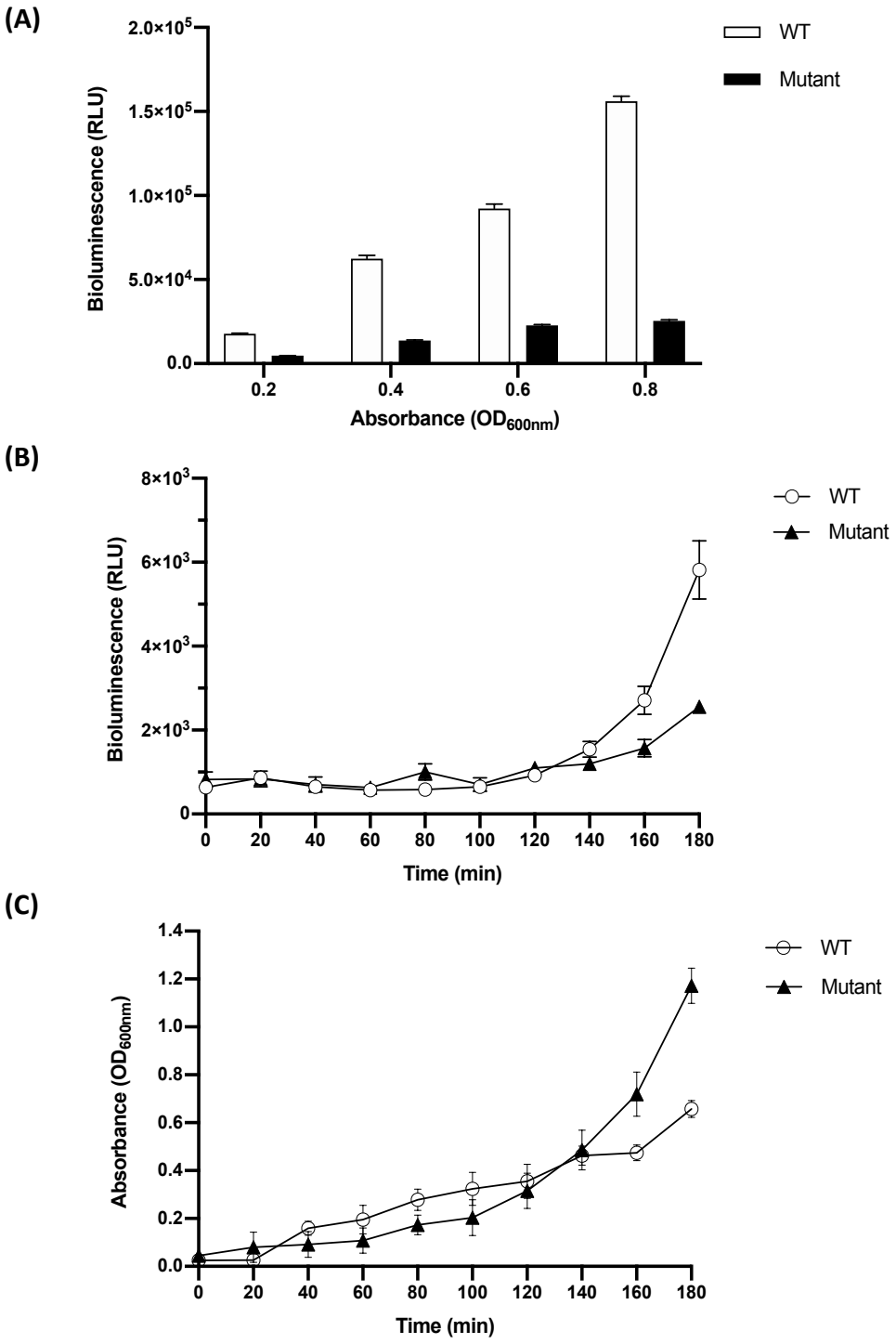

Figure 4.4: Quantification of bioluminescence in Kp52145 strains harbouring pilux. (A) Overnight cultures of the Kp52145 strains harbouring pilux were diluted 1:100 and grown to different OD_{600nm} values. Upon reaching the desired absorbance value, aliquots of cultures were transferred to 96 well plates and the bioluminescent signal was measured. Statistical significances were calculated by two-way ANOVA with Sidak's multiple comparisons test and are indicated on the graph; **** = $p \leq 0.0001$. n=4. **(B)** The absorbance and **(C)** bioluminescence of the Kp52145 strains harbouring pilux was measured incrementally over a 3 h period. Kp52145 strains without pilux acted as a negative control and did not emit bioluminescent signal (not shown on graph). n=4.

4.2.3 Differential PipTazo resistance is observed in strains when harbouring pilux

During routine plating of WT and mutant Kp52145, with and without pilux, on LB agar plates supplemented with carbenicillin, discrepancies arose regarding the level of susceptibility of these strains to carbenicillin. The MIC of carbenicillin for the Kp52145 strains was investigated by agar dilutions (as described in 2.4.3) and revealed a differing level of selectivity of carbenicillin for WT and mutant Kp52145 harbouring pilux. Therefore, in order to establish the optimal concentration of carbenicillin to select for pilux in Kp52145, the MIC results for the Kp52145 strains were obtained by VITEK and are displayed in Table 4.1. The MIC of piperacillin was carried subsequently out by agar dilution.

The introduction of pilux, which contains an ampicillin resistance cassette, confers resistance to penicillin antibiotics. As expected, without pilux, Kp52145 is sensitive to all tested antibiotics which include penicillins, cephalosporins, carbapenems, aminoglycosides and glycylcyclines (MIC ≦ 4 μg/ml). Both Kp52145 strains harbouring pilux were determined resistant to ampicillin (MIC ≧ 32 μg/ml) piperacillin (MIC ≧ 512 μg/ml). However, the data revealed differential PipTazo resistance in WT and mutant Kp52145 when harbouring pilux. When compared to Kp52145 strains without pilux, the MIC of PipTazo for WT/pilux increased 32-fold (≧ 128 μg/ml), while there was an 8-fold increase for the mutant/pilux (32 μg/ml). Therefore, a 4-fold difference exists between the MIC of PipTazo for WT and mutant Kp52145 harbouring pilux. This observation is specific to PipTazo; the MIC of amoxicillin/clavulanic acid, another β-lactam/β-lactamase inhibitor combination antibiotic, was identical for both Kp52145 strains harbouring pilux (MIC ≧ 32 μg/ml).

4.2.4 Differential PipTazo resistance is not observed with common cloning plasmids

In order to determine whether this property observed in the strains harbouring pilux was specific to this plasmid, the WT and mutant were transformed with various plasmids, carrying ampicillin resistance cassettes, by electroporation. The MIC of PipTazo for Kp52145 harbouring plasmids pACYC177, pBSKII and pBR322 (described in Table 2.2) was determined by agar dilution assays and confirmed by VITEK. The results are displayed in Table 4.2. The MIC of PipTazo was identical for WT and mutant Kp52145

Table 4.1 Antimicrobial susceptibility testing of Kp52145

	MIC (μg/ml)			
Antimicrobial	**WT**	**Mutant**	**WT/pilux**	**Mutant/pilux**
Ampicillin	≦ 2	≦ 2	≧ 32	≧ 32
Amoxicillin/Clavulanic Acid	≦ 2	≦ 2	≧ 32	≧ 32
Piperacillin/Tazobactam	≦ 4	≦ 4	≧ 128[a]	32[a]
Cefuroxime	4	4	4	4
Cefuroxime Axetil	4	4	4	4
Cefoxitin	≦ 4	≦ 4	≦ 4	≦ 4
Cefotaxime	≦ 0.25	≦ 0.25	≦ 0.25	≦ 0.25
Ceftazidime	0.25	0.25	0.25	0.25
Cefepime	≦ 0.12	≦ 0.12	≦ 0.12	≦ 0.12
Aztreonam	≦ 1	≦ 1	≦ 1	≦ 1
Ertapenem	≦ 0.12	≦ 0.12	≦ 0.12	≦ 0.12
Meropenem	≦ 0.25	≦ 0.25	≦ 0.25	≦ 0.25
Amikacin	≦ 2	≦ 2	≦ 2	≦ 2
Gentamicin	≦ 1	≦ 1	≦ 1	≦ 1
Tobramycin	≦ 1	≦ 1	≦ 1	≦ 1
Ciprofloxacin	≦ 0.25	≦ 0.25	≦ 0.25	≦ 0.25
Tigecycline	≦ 0.5	≦ 0.5	≦ 0.5	≦ 0.5
Trimethoprim/Sulfamethoxazole	≦ 20	≦ 20	≦ 20	≦ 20

[a] Denotes differential MIC values.

harbouring the aforementioned plasmids. This indicated that the differential PipTazo resistance phenotype is confined to Kp52145/pilux. However, plasmids appeared to confer varying degrees of resistance to PipTazo. The MIC of PipTazo for strains harbouring pBSKII and pBR322 is ≧ 128 μg/ml while strains harbouring pACYC177 are as sensitive to PipTazo as strains without a plasmid (MIC ≦ 4 μg/ml).

4.2.5 Resistance to PipTazo is not affected by the Lux system

It was unknown as to whether the observed resistance to piperacillin was affected by the Lux system or whether it was a property of the cloning vector, pGEX(-). Both WT and mutant Kp52145 were transformed with pGEX(-) plasmid DNA by electroporation.

Agar dilution assays were carried out to determine the MIC of PipTazo for the strains harbouring pGEX(-). The results are displayed in Table 4.2. The MIC values of PipTazo for WT and mutant Kp52145 harbouring pGEX(-) when compared to isolates harbouring pilux were identical. These results correlated with subsequent results obtained from MIC tests generated by VITEK. This observation indicated that differential PipTazo resistance is a property of the cloning vector pGEX(-) and thus is not associated with *lux* gene expression.

4.2.6 OM profiles differ in WT and mutant Kp52145 harbouring pilux

As discussed in 4.1, OMPs act as permeability channels for antibiotics and their deficiency has been associated with both antibiotic resistance and susceptibility (Liu *et al.*, 2012, Tsai *et al.*, 2011, Smani *et al.*, 2014). In an effort to establish whether the observed differential resistance phenotype was as a result of a loss or gain of OMPs in Kp52145, OM profiles of strains were studied.

SDS-PAGE analysis of sarkosyl-extracted protein samples revealed highly similar profiles when comparing the strains harbouring pilux to the strains without the plasmid (Figure 4.5). As discussed in 1.2.5, the two major porins of *K. pneumoniae* are OmpK35 and OmpK36. These porins are 40 kDa and 37 kDa, respectively, and thus likely correlate to the closely spaced double bands above the 35 kDa marker (Sugawara *et al.*, 2016, Ye *et al.*, 2018). OmpA is 35 kDa protein but visualisation of such could be hindered by the close proximity of OmpK36.

Table 4.2 MIC (μg/ml) of piperacillin and PipTazo for Kp52145

	PipTazo		Piperacillin	
Plasmid	**WT**	**Mutant**	**WT**	**Mutant**
No plasmid	≦ 4	≦ 4	≦ 4	≦ 4
pilux	≧ 128	32	≧ 512	≧ 512
pACYC177	≦ 4	≦ 4	≧ 512	≧ 512
pBR322	≧ 128	≧ 128	≧ 512	≧ 512
pBSKII	≧ 128	≧ 128	≧ 512	≧ 512
pGEX (-)	≧ 128	32	≧ 512	≧ 512

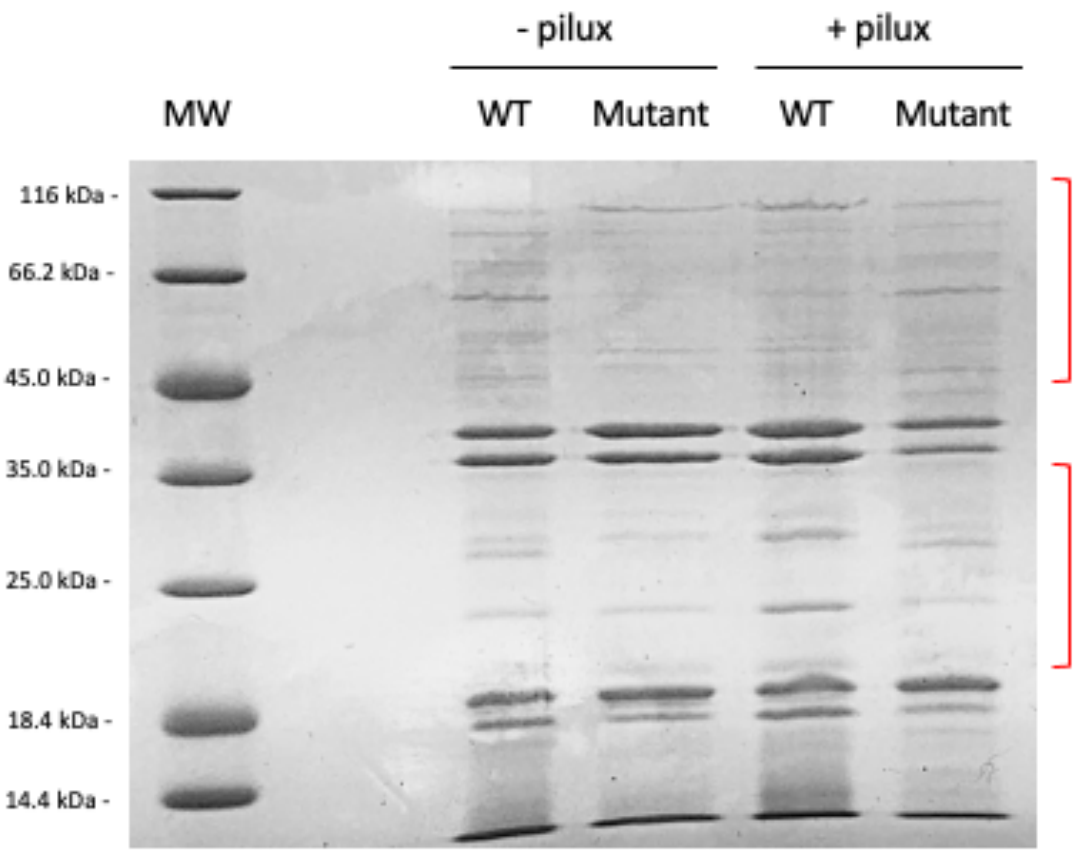

Figure 4.5: Outer membrane profiles of Kp52145 strains harbouring pilux. SDS-PAGE analysis of OMPs of Kp52145 strains with and without pilux. Regions with varying levels of protein prominence between the four profiles are marked with a red bracket. Protein size standards are indicated with MW markers.

Additionally, bands between ~ 18.4 kDa and ~ 35 kDa, and between ~ 45 kDa and ~ 116 kDa, differing in size and prominence, are apparent in the profiles of both strains with and without pilux. The putative identities of these proteins will be discussed in 4.3. It should be noted that comparable levels of expression of proteins are evident across all four profiles at ~ 18.4 kDa and ~ 35 kDa indicating that the aforementioned observed differences are not due to method variables such as varying loading volumes.

4.2.7 O antigen profiles are similar in WT and mutant Kp52145 harbouring pilux

LPS is another structural element of the OM that contributes to antibiotic resistance. LPS fortifies the membrane against antibiotics; bridging interactions are formed between neighbouring LPS molecules which results in an extremely hydrophobic sealed membrane (May & Grabowicz, 2018). SDS-PAGE analysis of LPS was carried out on the Kp52145 strains harbouring pilux in order to determine whether the presence of pilux was resulting in an alteration of LPS, in either strain, which was contributing to the observed resistance phenotype. *E. coli* CFT073 expresses smooth LPS and thus was used as a positive control to which the LPS of Kp52145 could be compared to. On the contrary, the cluster responsible for O antigen biosynthesis is disrupted in *E. coli* XL-1 Blue and thus this strain was used as a negative control. The growth-phase-dependent regulation of LPS production has been previously observed (Moynihan, 2018) and thus LPS from strains grown to both midlogarithmic and stationary phase were visualised.

Results are displayed in Figure 4.6. Overall, the mutant produced more O antigen than the WT. Very short chain O antigen, which is absent from the WT profiles at both growth phases, was more prominent in the mutant grown to stationary phase compared to midlogarithmic phase. In comparison to the mutant, WT Kp52145 produced more long chain O antigen; WT grown to midlogarithmic phase appeared to produce slightly more than that of WT grown to stationary phase. Additionally, it became apparent that the capsule of Kp52145 cannot be visualised using the Pro-Q Emerald 300 LPS Gel Stain Kit. A band of high molecular weight correlating to the capsule of *E. coli* CFT073 was present, however a band of similar size was not evident in the profiles of Kp52145. An assumption could be made that the molecular weight of the *E. coli* capsule would be similar to that of *K. pneumonia* capsule (Rahn *et al.*, 1999).

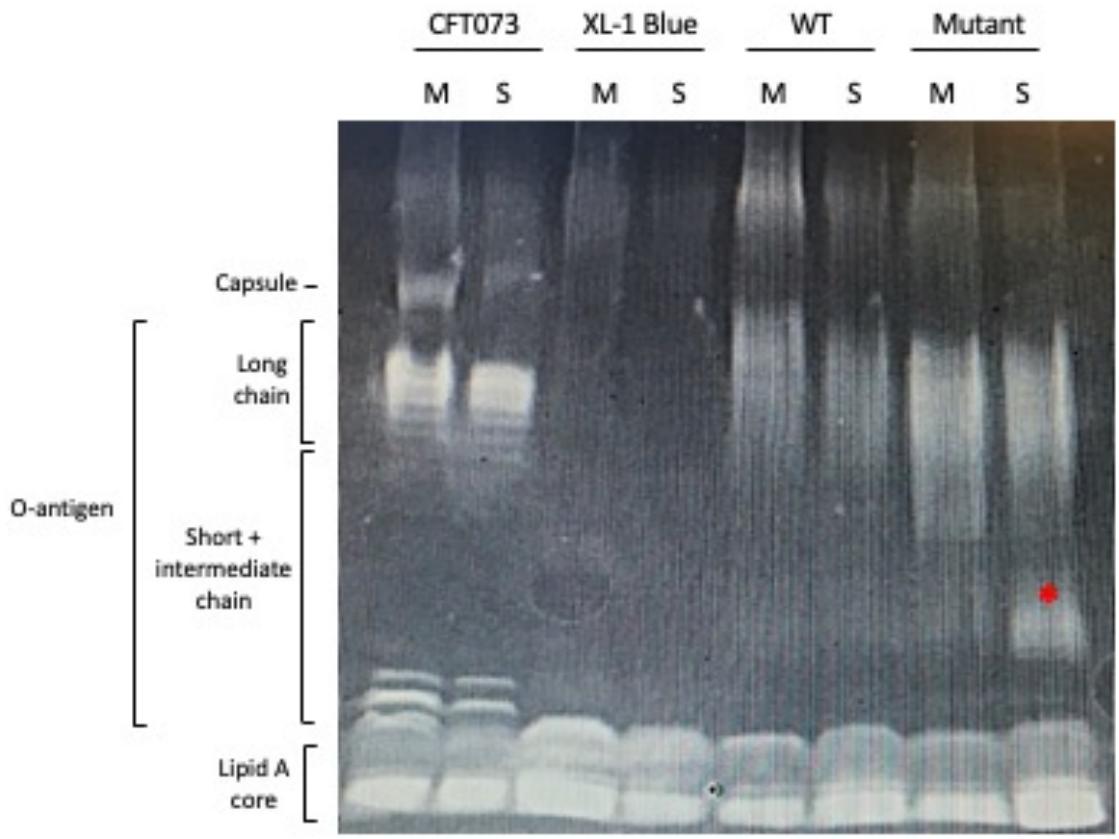

Figure 4.6: LPS profiles of *E. coli* and Kp52145 strains. SDS-PAGE analysis of LPS fractions was carried out as described in 2.3.1.3**.** LPS from strains grown to both midlogarithmic (M) and stationary (S) phase were visualised. *E. coli* CFT073 was used as a positive control; *E. coli* XL-1 Blue was used as a negative control. The prominent short chain O antigen of the mutant is marked with a red asterisk. LPS components are indicated with brackets. 'Capsule' refers to that of K2 *E. coli*.

Additionally, unidentified polysaccharides, of higher molecular weight than that of the capsule, were also present in all profiles, including that of *E. coli* XL-1 Blue, a K12 strain. It could be postulated that this band correlates to colanic acid, an exopolysaccharide common to many *Enterobacteriaceae* strains, including *E. coli* and *Klebsiella* (Rahn *et al.*, 1999, Grant *et al.*, 1969, Rättö *et al.*, 2006).

4.2.8 The mutation in the capsule mutant does not appear to be in CPS cluster

The Kp52145 strains, listed in Table 2.1, were provided by Professor Jose Bengochea. The paper published by Llobet *et al.*, described the construction of a wca_{K2} mutant (Llobet *et al.*, 2008). Using the mutagenesis strategy developed by Link *et al.,* an in-frame deletion of 1132 bp was generated to construct this Kp52145 mutant. However, using the primers provided by Llobet *et al.*, listed in Table 2.3, the mutation was mapped specifically to the *manC* region of the CPS operon. Thereby, it was postulated that complementation of this mutant with *manC* would correct the previously observed differential PipTazo sensitivity.

Therefore, it became necessary to genotypically confirm the CPS cluster mutation of the capsule mutant. Primers, detailed in Table 2.3, were designed to amplify various regions of the CPS cluster in order to identify the location of the mutation. WT Kp52145 acted as a positive control for the amplification of such CPS genes.

4.2.8.1 Both WT and mutant Kp52145 harbour an intact *manC*

Primers ManC_F and ManC_R, were designed to amplify the *manC* region of the CPS operon. A ~ 2 kb DNA fragment corresponding to this gene was amplified in the mutant as well as the WT (Figure 4.7 (B)). Although, this observation was expected for the WT, amplification of this gene in the mutant was unanticipated. Therefore, primers designed by Llobet *et al*., ManCa and ManCd, were subsequently used to amplify this region (Llobet *et al.*, 2008). Similar to our previous attempt, a ~ 2 kb DNA fragment corresponding to *manC* was amplified in both the WT and mutant (Figure 4.7 (C)). It was inferred from these results that the mutation is not in the *manC* gene. Therefore, the genomic data of the amplified *manC* region of both WT and mutant Kp52145 were obtained from Source BioScience. An alignment of these sequences revealed a similarity

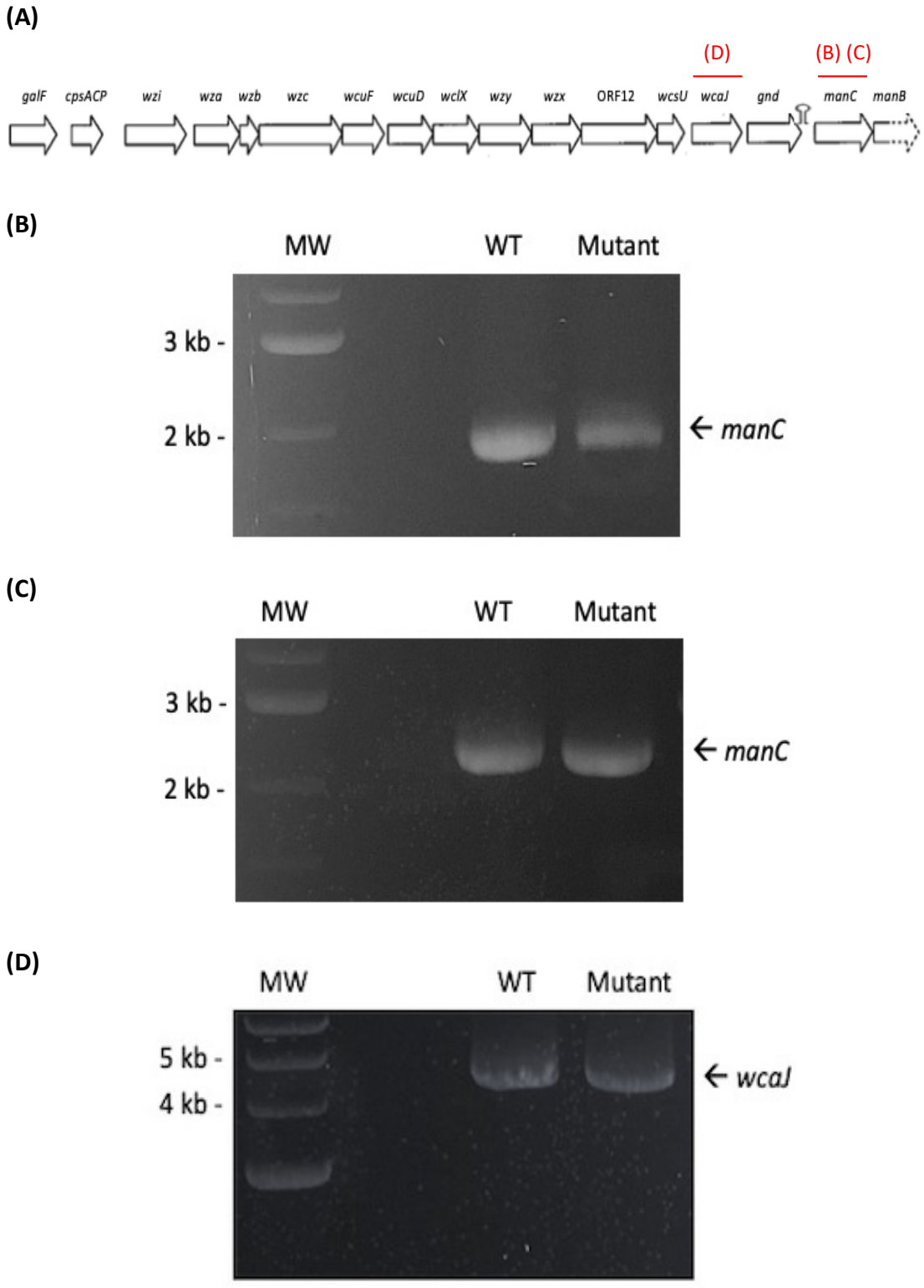

Figure 4.7: PCR amplification of *manC* and *wcaJ*. (A) Schematic overview of the location in the CPS operon of PCR products amplified by primer pairs. Red labels correspond to subsequent agarose gel image labels. Genomic DNA extracted from WT and mutant Kp52145 was used as template in PCRs. *manC* was amplified by PCR using primers **(B)** ManC_F and ManC_R; and **(C)** ManCa and ManCd. **(D)** *wcaJ* was amplified by PCR using primers Wca_F and Wca_R. Bands corresponding to the genes are marked with arrows and DNA size standards are indicated with MW markers.

of > 99% (Figure A.4) which provided further evidence that both WT and mutant Kp52145 harbour an intact *manC* gene.

4.2.8.2 The mutation does not appear to affect *wcaJ*

It was postulated that the mutation may be in an alternative gene in the CPS operon. *wcaJ* is just upstream from *manC*, as can be seen in Figure 4.7 (A), and hence it was possible that the mutation had instead affected this gene. Additionally, the mutant strain is called Kp52145 wca_{K2} in a paper published by Llobet *et al.* (Llobet *et al.*, 2008).

Primers Wca_F and Wca_R, were designed to amplify the *wcaJ* gene. However, a ~ 4.5 kb DNA fragment corresponding to this gene was amplified in the mutant as well as the WT (Figure 4.7 (D)). This result indicated that the mutation is not in the *wcaJ* gene.

4.2.8.3 The mutation does not appear to be in any gene in the K2 cluster

Due to our lack of success identifying the gene affected by the mutation, primers were designed to span the entirety of the CPS operon (Figure 4.8 (A)). Primers F_18148 and R_22944 flank the region between and including *wzx* → *wcsU*; F_22629 and R_27386 flank the region between and including *wcuF* → *wzy*; F_27016 and R_31675 flank the region between and including *wza* → *wzc*; F_31151 and R_35426 flank the region between and including *galF* → *wzi*. The product size of the aforementioned primers ranged between ~ 4 kb and ~ 5 kb. DNA fragments corresponding to the various regions of the CPS operon were amplified by both WT and mutant Kp52145 (Figure 4.8). These data implied that the mutation was in fact not affecting any part of the CPS operon.

4.2.9 Sequencing data confirmed that the CPS cluster is intact in the capsule mutant

In order to successfully establish the genotype of the Kp52145 mutant, WGS was carried out on this strain. A DNA preparation of mutant Kp52145 was sent to Novogene who performed sequencing at 100X depth. Tables listing the mutations of mutant Kp52145, compared to the WT, were formulated on a Linux operating system. Aileen Hartnett, Trinity College Dublin, converted these Linux files to Excel format and these mutations were mapped onto the chromosome by Stephen Smith, Trinity College Dublin. Analysis of these sequencing data led to several discoveries. Firstly, the CPS cluster of this mutant Kp52145 is intact. Secondly, a 500 bp deletion was identified. This deletion affects a

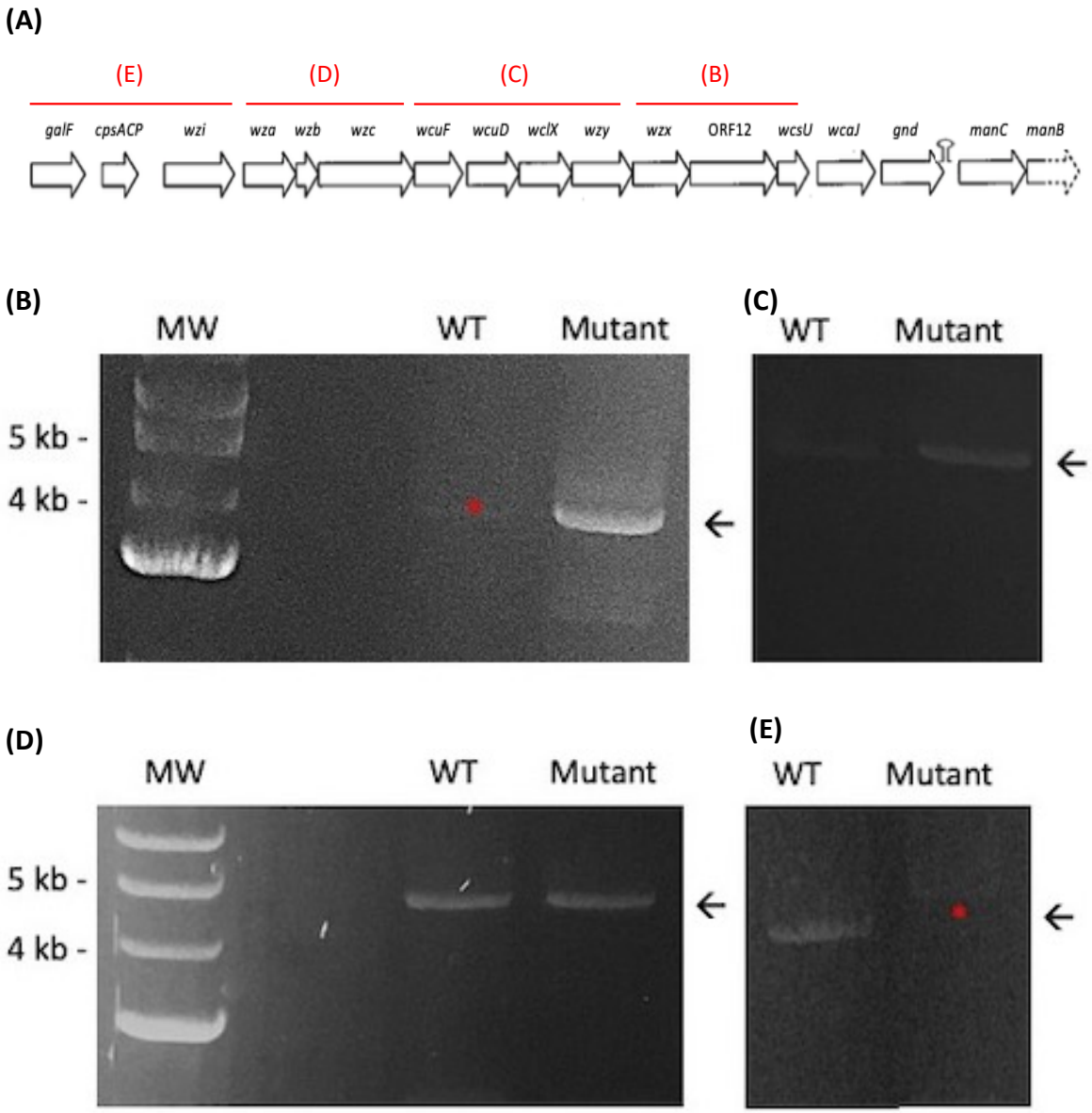

Figure 4.8: Amplification of genes in the CPS operon. (A) Schematic overview of the location in the CPS operon of PCR products amplified by primer pairs. Red labels correspond to subsequent agarose gel image labels. Genomic DNA extracted from WT and mutant Kp52145 was used as template in PCRs. Regions in the CPS operon were amplified by PCR using primers **(B)** F_18148 and R_22944; **(C)** F_22629 and R_27386; **(D)** F_27016 and R_31675; and **(E)** F_31151 and R_35426. Bands corresponding to the anticipated product are marked with arrows and faint amplification bands (repeated three times to ensure product not accidental), that are difficult to visualise, are marked with a red asterisk. DNA size standards are indicated with MW markers.

protein similar to a blue-light sensor in *E. coli*, YcgF. The importance of this discovery will be discussed in Chapter 5.

4.3 Discussion

As seen in Figure 4.4 (A), in comparison to the mutant, the WT emitted a significantly higher bioluminescent signal at all absorbance points. This raises the possibility that WT could be more energetically charged than the mutant and thus produces more ATP to be hydrolysed by luciferase, resulting in an increased production of light. Therefore, due to the noted differences in light emission among Kp52145 strains harbouring pilux, it is not feasible to use this bioluminescent system as a measure of viability in biofilm formation or serum killing assays.

The leading cause of β-lactam resistance in Gram-negative bacteria is the production of β-lactamase enzymes (Martin & Bachman, 2018, Bonnet, 2004). The classification systems used for β-lactamases is discussed in 1.4.1. Studies have revealed that porin loss contributes to the β-lactam resistant phenotype of *K. pneumoniae* that produce ESBLs or AmpC-type β-lactamases; however OM alterations alone are not determinants of antibiotic resistance (Hernández-Allés *et al.*, 2000, Tsai *et al.*, 2011).

ESBL-producing infections are predominantly treated with carbapenems despite often demonstrating *in vitro* activity to other β-lactams (Tamma & Rodriguez-Bano, 2017). This has led to the emergence of carbapenem-resistant *Enterobacteriaceae* and the consideration of carbapenem-sparing regimens, i.e. β-lactam/β-lactamase inhibitor combination antibiotics, for the treatment of infections caused by *Enterobacteriaceae* such as *Klebsiella* spp (Harris *et al.*, 2018). Class A enzymes, which include ESBLs, are generally susceptible to β-lactamase inhibitors, with the exception of KPC-producing *Klebsiella* (Papp-Wallace *et al.*, 2010). PipTazo remains active against a considerable proportion of ESBL-producing bacteria (Schuetz *et al.*, 2018). PipTazo is used to treat a variety of bacterial infections, including UTIs, pneumonias and intra-abdominal infections (Perry & Markham, 1999). On the contrary, classes B, C and D generally exhibit resistance to β-lactamase inhibitors (Drawz & Bonomo, 2010) and hence alternative β-lactams, such as cephalosporins and carbapenems, would be the optimal treatment of such infections caused by bacteria harbouring these β-lactamase enzymes.

Transformation of Kp52145 with various plasmids containing ampicillin resistance cassettes conferred resistance to piperacillin, without tazobactam (Table 4.2). This indicates that the ampicillin resistance cassettes encode a β-lactamase. Hence, without any plasmid, Kp52145 is susceptible to piperacillin. Tazobactam appears to inhibit the β-lactamase encoded by pACYC177, i.e. Kp52145/pACYC177 is susceptible to PipTazo (MIC ≦ 4 μg/ml). This suggests that this plasmid encodes a β-lactamase of class A. However, despite a reduction in MIC, Kp52145 harbouring pilux, pBR322 and pBSKII remains resistant to PipTazo. This implies an inability of tazobactam to inhibit the β-lactamases encoded by these plasmids, indicating they are of classes B, C or D. Evidently, genomic analysis of the β-lactamases encoded by each plasmid would be warranted in order to establish if differences in class or sequence contribute to the variation in PipTazo susceptibility.

Additionally, comparison of these common cloning vectors reveals differences in copy number and origin of replication. ColE1 is the origin of replication in pGEX, which is a medium copy number plasmid. pMB1 is the origin of replication in pBR322, which is also a medium copy number plasmid. pBSKII is a high copy number plasmid and has a ColE1 origin of replication. Lastly, p15A is the origin of replication in pACYC177, which is a low copy number plasmid. The variations in copy number may be a contributing factor to the differences in PipTazo susceptibility. Hence, the high susceptibility of pACYC177 to PipTazo could be due to the low copy number nature of the plasmid.

The differential PipTazo resistance among Kp52145 strains harbouring pilux was an unanticipated result from the VITEK MIC analysis (Table 4.1). This phenotype was attributed to the cloning vector pGEX(-), indicating that *lux* gene expression does not affect PipTazo resistance. As mentioned above, this observation was confined to the plasmid and the antibiotic. It was initially postulated that pilux could be altering the OM, i.e. OMPs or LPS, of *Klebsiella* and thus affecting the susceptibility of such strains to PipTazo.

The OM profile of Kp52145 strains without pilux appeared similar to those harbouring the plasmid (Figure 4.5). However, as mentioned in 4.2.6, differences regarding prominent proteins of varying sizes between 18.4 kDa and 35 kDa, and 45 kDa and 116 kDa, were apparent between the profiles of strains with and without pilux. According to

Brinkworth *et al.*, some OMPs of *K. pneumoniae* approximately correlating size to this range include Tsx, MipA and OmpW (Brinkworth *et al.*, 2015). It is possible that one or more of these proteins, or an unidentified protein from the OMP profile, is a determining factor of the differential PipTazo phenotype, however further study would be required to elucidate their putative roles in antibiotic resistance. Evidently, sequence analysis would be required to confirm the putative identities of proteins in the OMP profile. Additionally, the use of densitometry software, such as Quantity One, would provide quantitative data with regards to the intensity of the protein bands and thus be more indicative of differential production of OMPs among Kp52145 strains harbouring pilux in comparison to Kp52145 strains without this plasmid.

Differences were also apparent between the O antigen profiles of WT and mutant Kp52145 harbouring pilux. WT produced larger amounts of long chain O antigen, while the mutant produced more O antigen overall. Thereby, the increased resistance of WT to PipTazo, raises the possibility that the longer chain O antigen is the determining factor. Additionally, growth phase appeared to contribute to differences in LPS. It is important to note that MIC tests, generated by agar dilution or VITEK, would generally analyse strains grown to stationary phase. Hence, a possibility arises that the large amount of short chain O-antigen exclusively produced by the mutant grown to stationary phase, could be contributing to its increased susceptibility to PipTazo. However, a review of the literature indicates a knowledge gap exists regarding a role for LPS in β-lactam resistance.

It would be of interest to study the OMP and O antigen profiles of Kp52145 harbouring the alternative cloning plasmids mentioned in 4.2.4 and compare these to the profiles of Kp52145 without a plasmid. This could decipher whether the OMPs or LPS of Kp52145 is altered by the presence of any of these plasmids and the effect these modifications may have on the strain's susceptibility to PipTazo.

Several alternative resistance mechanisms were also proposed to explain this observed phenotype. As discussed in 1.2.1, the capsule of *K. pneumoniae*, a pronounced polysaccharide matrix that coats the cell, is a prominent virulence factor of *K. pneumoniae* that acts as a physical barrier to host immune defences (Paczosa & Mecsas, 2016). The extent of protection the capsule confers to *Klebsiella* is determined by the

thickness of the capsular layer, as opposed to its chemical composition (de Astorza *et al.*, 2004). While it was initially postulated that the thick K2 capsule of Kp52145 could be inhibiting entry of PipTazo to the cell, this hypothesis was subsequently eliminated. Piperacillin is ~ 518 Da and Tazobactam is ~ 299 Da (Rodriguez *et al.*, 2016) and hence, depending on the presence of OMPs, this manner of size exclusion would result in the inhibition of numerous nutrients from the cell (Sugawara *et al.*, 2016).

Furthermore, capsule polysaccharides are anionic whereas tazobactam is cationic. This raises the possibility that the capsule binds to tazobactam, reducing the amount of antibiotic reaching the bacterial surface, and ultimately neutralises the bactericidal activity of PipTazo. Yu *et al.* observed a similar interaction between the capsule of *K. pneumoniae* and polymyxin B (Yu *et al.*, 2015). It would be of interest to establish whether complementation of the mutant would restore the level of resistance to PipTazo displayed by WT Kp52145.

However, it is unclear as to why this phenotype is not observed in response to amoxicillin/clavulanic acid, an alternative β-lactam/β-lactamase inhibitor combination antibiotic. The structural differences between the two antibiotics may account for this. While piperacillin and amoxicillin are both penicillin derivatives, their side chains differ. Piperacillin has a ureido group attached to the core penicillin backbone, whereas the side chain of amoxicillin is an amino group. Ureidopenicillins have an increased affinity for penicillin binding proteins which results in an increased spectrum of activity (Gin *et al.*, 2007), in comparison to aminopenicillins. Additionally, tazobactam and clavulanic acid differ in structure (Padayatti *et al.*, 2005). In order to establish the determining component of the differential PipTazo resistance, the combination of the aforementioned β-lactams and β-lactamase inhibitors could be alternated, e.g. piperacillin paired with clavulanic acid, etc.

Chapter 5 General Discussion

In this thesis, an association between capsular status, biofilm formation and antibiotic resistance was defined, in that a Kp52145 capsule mutant generally produced more biofilm and displayed decreased resistance to PipTazo when harbouring the pilux plasmid (Figure 3.1 and Table 4.1, respectively).

WGS revealed that the CPS operon of the Kp52145 mutant is in fact intact and that the mutation is affecting another region; a protein similar to the YcgF protein of *E. coli*. This discovery supports the *manC* sequencing results and CPS operon PCR data from Chapter 4. YcgF, the blue light using FAD (BLUF)-EAL protein, is a blue-light sensor of *E. coli* (Tschowri *et al.*, 2009). It is present in a variety of bacterial species, including *K. pneumoniae* which has two YcgF homologues (Tschowri *et al.*, 2012). In response to blue light irradiation, YcgF directly antagonises YcgE, the MerR-like repressor, resulting in the induction of a distinct regulon of small proteins (Tschowri *et al.*, 2009). These regulatory proteins, *via* the Rcs system, modulate biofilm functions; colanic acid, a component of the ECM, is upregulated, while curli fimbriae are downregulated (Tschowri *et al.*, 2009). Evidently, this signaling pathway is pleiotropic in that it appears to effect multiple phenotypic characteristics. In addition to blue light signals, the YcgF/YcgE/small protein signalling pathway is also affected by low nutrient and low temperature stress signals (Tschowri *et al.*, 2009).

Hence, it could be deduced that the deletion of YcgF would result in inhibition of the induction of the aforementioned small regulatory proteins involved in biofilm modulation. Tschowri *et al*. found that YmgA and YmgB, two of the eight proteins under YcgF/YcgE control, increase the production of capsule material such as colanic acid, causing a mucoid phenotype (Tschowri *et al.*, 2009). These data indicate that the non-mucoid appearance and negative string test of the mutant is a result of the YcgF deletion. Similarly, the intact YcgF protein of WT Kp52145 could explain its mucoid colony phenotype and positive string test. Complementation of the mutant would be required to confirm that the YcgF protein is responsible for these observed phenotypic differences.

However, according to the role the YcgF/YcgE/small protein signalling pathway plays in biofilm formation, as outlined by Tschowri *et al.*, the mutant would be anticipated to form reduced amounts of biofilm in comparison to WT Kp52145. This was not the case, as discussed in 3.2.3; the mutant produces a significantly higher amount of biofilm than WT when grown in LB + glucose and BHI. Nevertheless, this phenomenon may be explained by an observation made by Lee *et al.*; the YmgB protein represses biofilm formation of *E. coli* grown in rich media containing glucose (Lee *et al.*, 2007). Therefore, this may account for the differences observed in the biofilm formation of WT and mutant Kp52145 in growth media LB + glucose and BHI, both of which contain glucose. However, the contrary is observed in M9, an additional growth medium containing glucose, whereby the biofilm formation of WT is significantly higher than that of the mutant.

Despite this discovery, the initial interpretation of the biofilm data, discussed in 3.3, remains valid, due to the putative resulting capsule phenotype of the YcgF mutant. Furthermore, it supports the proposal that capsule contributes to the observed differential PipTazo resistance, as discussed in 4.3; the neutralisation of PipTazo activity is lessened as a result of the reduced anionic charge that occurs due to capsule reduction. Additionally, it was postulated that these regulatory proteins may affect the expression of OMPs or LPS and thus may explain observations made in Chapter 4. Complementation of the mutant with each individual protein involved in the YcgF/YcgE/small protein signalling pathway could provide further clarity with regards to the role each protein plays in capsule production, biofilm formation and OMP or LPS expression.

Alternative methods of capsule visualisation should also be explored, considering the inability of SDS-PAGE analysis of *K. pneumoniae* LPS to do so (Figure 4.6). While the Pro-Q Emerald 300 LPS Gel Stain Kit has been used by other studies to visualise *K. pneumoniae* LPS (March *et al.*, 2013), literature surrounding the success of this method to visualise capsule is lacking.

Nigrosin staining of the capsule could be employed and examined by light microscopy (Struve & Krogfelt, 2003). Alternatively, a capsule swelling test could be performed by mixing K2 capsule specific antisera with bacterial solutions and examining by phase-

contrast microscopy (Ørskov & Ørskov, 1984). Additionally, glucuronic acid is routinely used as an indicator of capsule content because it is a key component of the *Klebsiella* capsule (Walker *et al.*, 2019). Similarly, measurements of L-fucose, a constituent of colanic acid, are utilised to quantify colanic acid (Zhang *et al.*, 2008). Quantification of these polysaccharides would be valuable in further elucidating the structural consequences of the discovered mutation.

A review of the literature indicates that a role for the YcgF/YcgE/small protein signalling pathway in antibiotic resistance has not been identified. However, the relationship between biofilm and antibiotic resistance has been extensively studied. As discussed in 1.3.3, in comparison to planktonic cells, cells within a biofilm can display up to a 100-fold increase in antibiotic resistance (Ceri *et al.*, 1999).

'Biofilm tolerance' is the term given to the additional resistance provided by biofilms, that occurs as a result of biofilm-specific resistance mechanisms (Olsen, 2015). Biofilms are slow growing and the bactericidal action of β-lactam antibiotics, such as piperacillin, is contingent on rapid bacterial growth (Tuomanen *et al.*, 1986). Furthermore, it is widely acknowledged that faster-growing bacteria are more susceptible to β-lactam killing (Lee *et al.*, 2018). Retardation of antibiotic diffusion into biofilm, as a result of the shielding effect of the ECM, has also been reported to provide protection against β-lactam antibiotics (Stewart, 1996, Shigeta *et al.*, 1997). Additionally, a neutralization interaction similar to that discussed above, could occur between the anionic ECM and cationic antimicrobials. In order to decipher whether biofilm tolerance is observed in WT Kp52145 and similarly, whether the YcgF mutant displays increased antibiotic susceptibility in comparison; MIC analysis on biofilm cells produced by these Kp52145 strains is warranted. The anticipated effects of the YcgF mutation are summarized in Figure 5.1. It is important to note that these do not necessarily correspond with observations made in this study.

Moreover, it would be of interest to carry out the following procedures in the dark, i.e. without blue-light irradiation; overnight culturing on agar plates and biofilm formation assays. This could establish whether the phenotype and biofilm formation of WT Kp52145 would resemble that of the mutant as a result of preventing the blue-light-induction of the aforementioned regulon of small regulatory proteins. Additionally, MIC

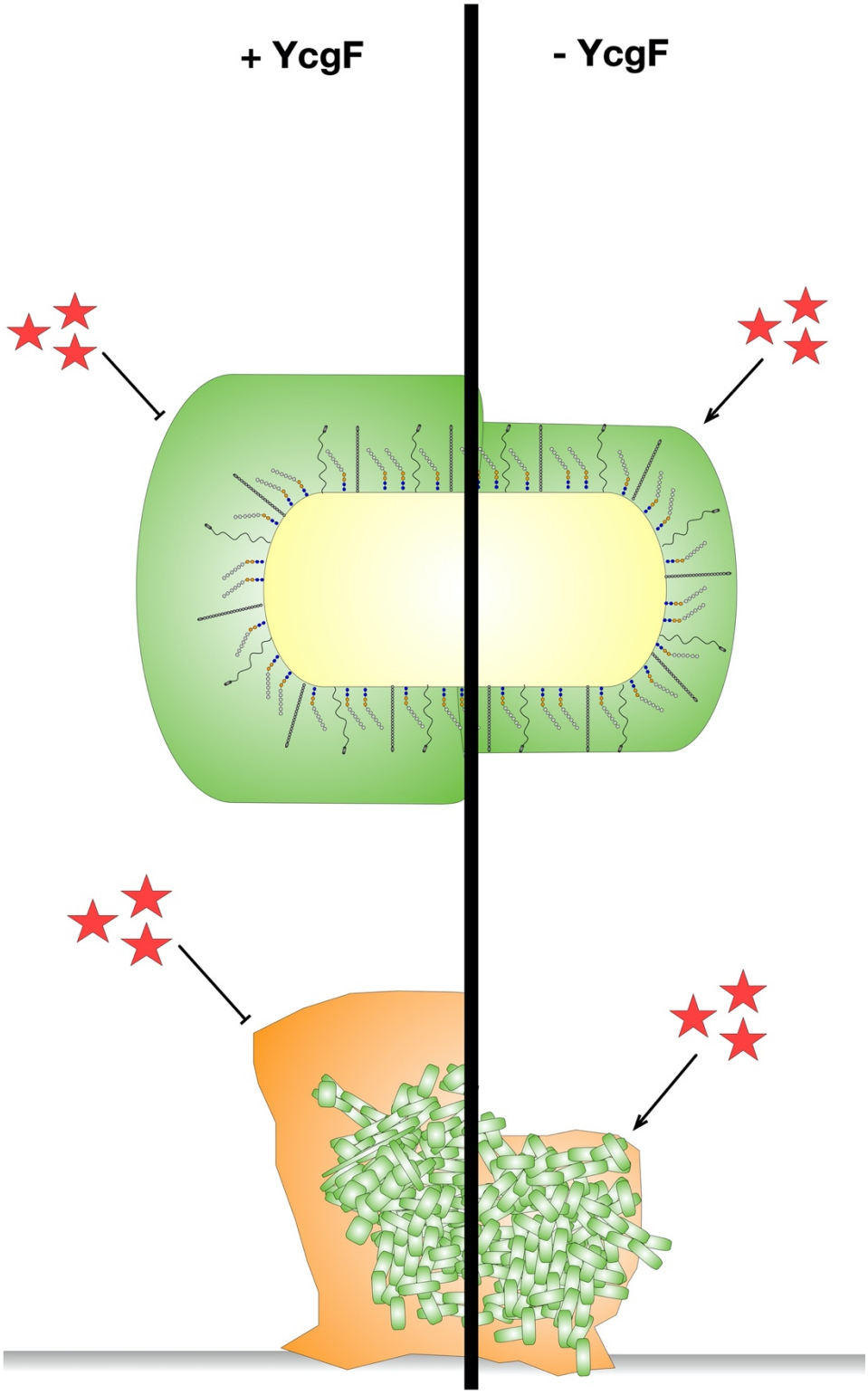

Figure 5.1: Summary of the anticipated effects of a YcgF mutation. Deletion of YcgF results in reduced capsule (green shaded area) and reduced biofilm (area shaded orange represents the ECM; a green rod represents a *K. pneumoniae* cell). This study postulates that as a result, antibiotic (red star) resistance decreases.

analysis on Kp52145 strains grown in the same manner, i.e. in the dark, could elucidate whether the observed differential PipTazo resistance is as a direct result of the YcgF mutation. Furthermore, the hospital isolates could be sequenced in order to establish whether this regulatory system is present and whether this regulation is serotype-specific.

The rapidly increasing emergence of AMR has led to an increase in research focussing on alternatives to conventional antimicrobial agents (Halstead *et al.*, 2016). Blue-light therapy is an innovative non-antibiotic approach with numerous advantages over both alternative conventional and light-based antimicrobial therapies. While the exact mechanism of antimicrobial action is not yet fully understood, a widely accepted explanation is that blue light (400-470 nm) activates endogenous photosensitizers of pathogens, leading to the formation of cytotoxic reactive oxygen species (ROS), ultimately resulting in cell death (Dai *et al.*, 2012). Due to the multi-target nature of blue light, the development of blue light resistance by bacteria is less likely than that of antibiotic resistance (Ferrer-Espada *et al.*, 2019). Additionally, blue light is considerably less detrimental to mammalian cells in comparison to UV light (Kleinpenning *et al.*, 2010) and unlike photodynamic therapy, is intrinsically antimicrobial without the requirement for exogenous photosensitizers (Dai *et al.*, 2012).

A multitude of studies have investigated the use of blue light therapy in areas such as biofilm inactivation and disinfection of hospital surfaces (Ferrer-Espada *et al.*, 2019, Cabral & Ag, 2019, Bache *et al.*, 2012, Maclean *et al.*, 2010) and blue light has been shown to exhibit a broad spectrum of antimicrobial effect against a wide range of bacterial species including *K. pneumoniae* (Halstead *et al.*, 2016, Halstead *et al.*, 2019, Maclean *et al.*, 2009). However, treatment efficacy is influenced by numerous variables, such as characteristics of incident light, irradiance source, and total light dose as well as the bacterial species being targeted (Cabral & Ag, 2019), indicating that a therapeutic window exists for blue light therapy.

While numerous conclusions can be drawn from this study, wider implications are also apparent. The aforementioned putative blue light therapeutic window evidently warrants further research, considering that blue light therapy could potentially enhance biofilm growth of particular bacteria; in this study's case, Kp52145 harbouring the YcgF

gene. Additionally, the multifactorial nature of the contribution of both capsule and growth media to biofilm formation is an area that warrants clarity, considering the implications particular variables could have on the choice of treatment for biofilm infections.

Appendix

Figure A.1: String test results of Kp52145 strains. Photographic data unavailable due to Covid limitations.

Figure A.2: Qualitative analysis of bioluminescence. Photographic data unavailable due to Covid limitations.

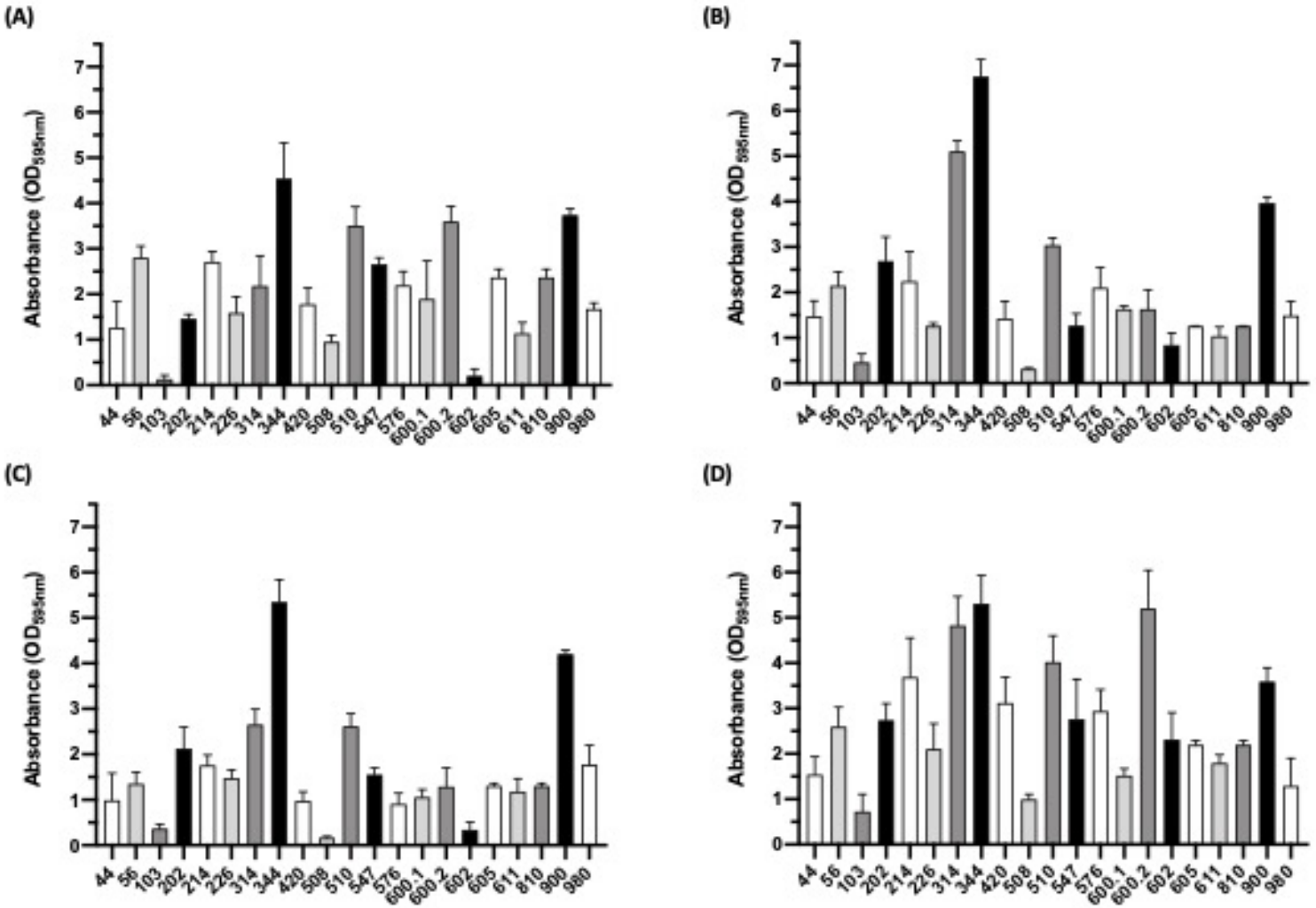

Figure A.3: Biofilm formation of hospital isolates. Bacteria were grown in **(A)** LB; **(B)** LB + glycerol; **(C)** LB + glucose; and **(D)** BHI, for 24 h in 96 well plates. CVAs were carried out and the resulting OD_{595nm} of the CV-stained bacteria was measured. Assays were carried out as described in 2.4.1.1 and 2.4.1.2. Isolates ordered in same manner for each media.

(A)

```
Alignment           of           Sequence_1:[WT_ManCa.seq.xdna]           with
Sequence_2:[Mutant_ManCa.seq.xdna]

Similarity : 1175/1178 (99.75 %)

Seq_1  1     CTATCAGCAGGCGCTGCGTGATGTAGTGGCGTATGCCGTACAGAATGGTATTCCGGTACC  60
             ||||||||||||||||||||||||||||||||||||||||||||||||||#||||||||||
Seq_2  1     CTATCAGCAGGCGCTGCGTGATGTAGTGGCGTATGCCGTACAGAATGGCATTCCGGTACC  60


Seq_1  61    GACTTTCTCTGCTGCAATTGCCTACTACGACAGCTACCGTTCCGCAGTTCTGCCCGCTAA  120
             ||||||||||||||||||||||||||||||||||||||||||||||||||||||||||||
Seq_2  61    GACTTTCTCTGCTGCAATTGCCTACTACGACAGCTACCGTTCCGCAGTTCTGCCCGCTAA  120


Seq_1  121   CCTGATTCAGGCTCAGCGTGATTACTTTGGTGCGCACACCTATAAGCGTACTGATAAAGA  180
             ||||||||||||||||||||||||||||||||||||||||||||||||||||||||||||
Seq_2  121   CCTGATTCAGGCTCAGCGTGATTACTTTGGTGCGCACACCTATAAGCGTACTGATAAAGA  180


Seq_1  181   AGGTGTATTCCATACCGAGTGGTTGGAATAATCTTTATATGCCACAGTCAGGCCATTTGG  240
             ||||||||||||||||||||||||||||||||||||||||||||||||||||||||||||
Seq_2  181   AGGTGTATTCCATACCGAGTGGTTGGAATAATCTTTATATGCCACAGTCAGGCCATTTGG  240


Seq_1  241   CCTGACTGTTATCTATTGTTAGTTATTCTACAATAATCTGATCAAAGTCATCTTATTTGC  300
             ||||||||||||||||||||||||||||||||||||||||||||||||||||||||||||
Seq_2  241   CCTGACTGTTATCTATTGTTAGTTATTCTACAATAATCTGATCAAAGTCATCTTATTTGC  300


Seq_1  301   ACGCCTGCGTTATTTATCCAGCTCTAATAAACCAAATGCTTATCTTTTAAGAATTTGCCA  360
             ||||||||||||||||||||||||||||||||||||||||||||||||||||||||||||
Seq_2  301   ACGCCTGCGTTATTTATCCAGCTCTAATAAACCAAATGCTTATCTTTTAAGAATTTGCCA  360


Seq_1  361   TATTTATACTTTTGTACACTTATAATAAGCTGCTTCTGGCCTCAGAATATATCTGGGTGT  420
             ||||||||||||||||||||||||||||||||||||||||||||||||||||||||||||
Seq_2  361   TATTTATACTTTTGTACACTTATAATAAGCTGCTTCTGGCCTCAGAATATATCTGGGTGT  420
```

```
Seq_1  421   TTAATAACAGGGTTTTAATTAAAGGATATTAATATGTTGCTTCCTGTGATCATGGCTGGT  480
             ||||||||||||||||||||||||||||||||||||||||||||||||||||||||||||
Seq_2  421   TTAATAACAGGGTTTTAATTAAAGGATATTAATATGTTGCTTCCTGTGATCATGGCTGGT  480

Seq_1  481   GGTACCGGCAGTCGTCTCTGGCCGATGTCTCGCGAGCTTTATCCGAAACAGTTCCTCCGG  540
             ||||||||||||||||||||||||||||||||||||||||||||||||||||||||||||
Seq_2  481   GGTACCGGCAGTCGTCTCTGGCCGATGTCTCGCGAGCTTTATCCGAAACAGTTCCTCCGG  540

Seq_1  541   CTGTACGGGCAGAACTCCATGCTGCAGGAAACCATCACCCGCCTCTCGGGCCTTGAAATC  600
             ||||||||||||||||||||||||||||||||||||||||||||||||||||||||||||
Seq_2  541   CTGTACGGGCAGAACTCCATGCTGCAGGAAACCATCACCCGCCTCTCGGGCCTTGAAATC  600

Seq_1  601   CATGAACCGATGGTCATCTGTAACGAAGAGCACCGCTTCCTGGTGGCCGAACAGCTGCGC  660
             ||||||||||||||||||||||||||||||||||||||||||||||||||||||||||||
Seq_2  601   CATGAACCGATGGTCATCTGTAACGAAGAGCACCGCTTCCTGGTGGCCGAACAGCTGCGC  660

Seq_1  661   CAGCTCAACAAGCTGTCCAACAACATTATTCTTGAGCCGGTCGGGCGCAACACCGCCCCG  720
             ||||||||||||||||||||||||||||||||||||||||||||||||||||||||||||
Seq_2  661   CAGCTCAACAAGCTGTCCAACAACATTATTCTTGAGCCGGTCGGGCGCAACACCGCCCCG  720

Seq_1  721   GCCATCGCCCTGGCGTCTCTTCAGGCCACCCGTCACGGCGACGACCCGCTGATGCTGGTC  780
             ||||||||||||||||||||||||||||||||||||||||||||||||||||||||||||
Seq_2  721   GCCATCGCCCTGGCGTCTCTTCAGGCCACCCGTCACGGCGACGACCCGCTGATGCTGGTC  780

Seq_1  781   CTCGCCGCCGACCATATCATCAATAACCAGCCGGTCTTCCACGACGCCATCCGCGTCGCC  840
             ||||||||||||||||||||||||||||||||||||||||||||||||||||||||||||
Seq_2  781   CTCGCCGCCGACCATATCATCAATAACCAGCCGGTCTTCCACGACGCCATCCGCGTCGCC  840

Seq_1  841   GAGCAGTATGCCGATGAAGGCCATCTGGTCACCTTCGGTATCGTGCCGAACGCCCCGGAA  900
             ||||||||||||||||||||||||||||||||||||||||||||||||||||||||||||
Seq_2  841   GAGCAGTATGCCGATGAAGGCCATCTGGTCACCTTCGGTATCGTGCCGAACGCCCCGGAA  900

Seq_1  901   ACCGGCTACGGTTACATCCAGCGCGGCGTGGCCCTCACCGACAGCGCCCACACCCCGTAC  960
             ||||||||||||||||||||||||||||||||||||||||||||||||||||||||||||
Seq_2  901   ACCGGCTACGGTTACATCCAGCGCGGCGTGGCCCTCACCGACAGCGCCCACACCCCGTAC  960
```

```
Seq_1  961   CAGGTGGCCCGCTTCGTGGAGAAGCCGGACCGCGAGCGCGCCGAGGCCTACCTCGCCTCC  1020
             ||||||||||||||||||||:||||||||||||||||||||||||||||||||||||||
Seq_2  961   CAGGTGGCCCGCTTCGTGGANAAGCCGGACCGCGAGCGCGCCGAGGCCTACCTCGCCTCC  1020


Seq_1  1021  GGGGAGTACTACTGGAACAGCGGCATGTTTATGTTCCGCGCCAAAAAATACCTCTCCGAG  1080
             ||||||||||||||||||||||||||||||||||||||||||||||||||||||||||||
Seq_2  1021  GGGGAGTACTACTGGAACAGCGGCATGTTTATGTTCCGCGCCAAAAAATACCTCTCCGAG  1080


Seq_1  1081  CTGGCCAAATTCCGCCCGGATATCCTCGAAGCCTGCCAGGTCGCGGTGAATGCCGCCCAA  1140
             ||||||||||||||||||||||||||||||||||||||||||||||||||||||||||##|
Seq_2  1081  CTGGCCAAATTCCGCCCGGATATCCTCGAAGCCTGCCAGGTCGCGGTGAATGCCGCC--A  1138


Seq_1  1141  CAACGGCAGCGACTTCATCAGCATTCCGCATGACATTT  1178
             ||||||:||||||||||||||||||||||||||||||
Seq_2  1139  CAACGGNAGCGACTTCATCAGCATTCCGCATGACATTT  1176
```

(B)

```
Alignment           of           Sequence_1:[WT_ManCd.seq.xdna]           with
Sequence_2:[Mutant_ManCd.seq.xdna]


Similarity : 1089/1089 (100.00 %)


Seq_1  1     ATCGGGTTGTGGCTGGCCGTCACCTCGATACCGCCATCCACCCCGAGGTGGAAGGTGGCG  60
             ||||||||||||||||||||||||||||||||||||||||||||||||||||||||||||
Seq_2  1     ATCGGGTTGTGGCTGGCCGTCACCTCGATACCGCCATCCACCCCGAGGTGGAAGGTGGCG  60


Seq_1  61    AAGTAAATCTCTTCCGTGCCGCTCAGGCCGATATCCAGCACGTCGGTGCCGGCGTCCATC  120
             ||||||||||||||||||||||||||||||||||||||||||||||||||||||||||||
Seq_2  61    AAGTAAATCTCTTCCGTGCCGCTCAGGCCGATATCCAGCACGTCGGTGCCGGCGTCCATC  120


Seq_1  121   AGCCCGCGGGCCAGCGCCAGCTTCAGCGACTCGCTGGTGAGGCGCACATCGCCCCCCACC  180
             ||||||||||||||||||||||||||||||||||||||||||||||||||||||||||||
Seq_2  121   AGCCCGCGGGCCAGCGCCAGCTTCAGCGACTCGCTGGTGAGGCGCACATCGCCCCCCACC  180
```

```
Seq_1  181   ACTATCTTCCCGGGTTTCAGAAATTCGCCGTAGGCGCGGCCGATACGGTAGGCGATGTCC  240
             ||||||||||||||||||||||||||||||||||||||||||||||||||||||||||||
Seq_2  181   ACTATCTTCCCGGGTTTCAGAAATTCGCCGTAGGCGCGGCCGATACGGTAGGCGATGTCC  240

Seq_1  241   TCGTTCAGCTCCTCGCCCAGTTCACCACGGATGTCATAAGCCTTAAAGCATGTTAACTGT  300
             ||||||||||||||||||||||||||||||||||||||||||||||||||||||||||||
Seq_2  241   TCGTTCAGCTCCTCGCCCAGTTCACCACGGATGTCATAAGCCTTAAAGCATGTTAACTGT  300

Seq_1  301   GTCATTCTGCGTTTTGTCCCGAAAAAATTAGCAACGACCATACTGGTCTTTAATACGAAT  360
             ||||||||||||||||||||||||||||||||||||||||||||||||||||||||||||
Seq_2  301   GTCATTCTGCGTTTTGTCCCGAAAAAATTAGCAACGACCATACTGGTCTTTAATACGAAT  360

Seq_1  361   AATGTCGTCCTCGCCGAGGTACGACCCCGACTGGATCTCCAGCACTTCCAGCGGAATGCG  420
             ||||||||||||||||||||||||||||||||||||||||||||||||||||||||||||
Seq_2  361   AATGTCGTCCTCGCCGAGGTACGACCCCGACTGGATCTCCAGCACTTCCAGCGGAATGCG  420

Seq_1  421   GCCCGGGTTTTCCAGGCTGTGCTCGGCGCCAATCGGAATAAAGGTGGACTGGTTCTCGGT  480
             ||||||||||||||||||||||||||||||||||||||||||||||||||||||||||||
Seq_2  421   GCCCGGGTTTTCCAGGCTGTGCTCGGCGCCAATCGGAATAAAGGTGGACTGGTTCTCGGT  480

Seq_1  481   CAGCAGGAACTGCTTGCCGTTGACCGTCACCTGGCCGGTGCCGGCGAGAATGACCCAGTG  540
             ||||||||||||||||||||||||||||||||||||||||||||||||||||||||||||
Seq_2  481   CAGCAGGAACTGCTTGCCGTTGACCGTCACCTGGCCGGTGCCGGCGAGAATGACCCAGTG  540

Seq_1  541   CTCGGCGCGGTGGTGGTGCATCTGCATCGAGAAGGCGCCGCCCGGTTTCACGGTGATGCG  600
             ||||||||||||||||||||||||||||||||||||||||||||||||||||||||||||
Seq_2  541   CTCGGCGCGGTGGTGGTGCATCTGCATCGAGAAGGCGCCGCCCGGTTTCACGGTGATGCG  600

Seq_1  601   GTTGACGTTGAAGCGCGGGGTCTGGACCACCACGTCGCAGCGGCCCCAGGGACGGTAAAT  660
             ||||||||||||||||||||||||||||||||||||||||||||||||||||||||||||
Seq_2  601   GTTGACGTTGAAGCGCGGGGTCTGGACCACCACGTCGCAGCGGCCCCAGGGACGGTAAAT  660

Seq_1  661   CTCGCGGTGGCGCTTGTACTCGCTGCGCTGGTTCTGCTTGAGGAACTCGACCGCCTTCTT  720
             ||||||||||||||||||||||||||||||||||||||||||||||||||||||||||||
Seq_2  661   CTCGCGGTGGCGCTTGTACTCGCTGCGCTGGTTCTGCTTGAGGAACTCGACCGCCTTCTT  720
```

```
Seq_1  721   CACGTCCTGGGAACGCTCGCGGTTCATCACCAGCACGGCGTCCTTGGTGCTGACAATCAC  780
             ||||||||||||||||||||||||||||||||||||||||||||||||||||||||||||
Seq_2  721   CACGTCCTGGGAACGCTCGCGGTTCATCACCAGCACGGCGTCCTTGGTGCTGACAATCAC  780

Seq_1  781   CAGGTTCTCCACGCCGATGGCCGCCACCAGCTTCTCGTCGCTGTTGATGTAGCAGTTTTC  840
             ||||||||||||||||||||||||||||||||||||||||||||||||||||||||||||
Seq_2  781   CAGGTTCTCCACGCCGATGGCCGCCACCAGCTTCTCGTCGCTGTTGATGTAGCAGTTTTC  840

Seq_1  841   GCTGTTGTGCACCCACGCGTCGCCGCTGAGGACGTTACCCTGCCCGTCTTTCGGGCTGAC  900
             ||||||||||||||||||||||||||||||||||||||||||||||||||||||||||||
Seq_2  841   GCTGTTGTGCACCCACGCGTCGCCGCTGAGGACGTTACCCTGCCCGTCTTTCGGGCTGAC  900

Seq_1  901   CTCCCACAGGGCGGACCAGGAGCCGACGTCGCTCCAGTCGGCATCGAGACCGACCACCAC  960
             ||||||||||||||||||||||||||||||||||||||||||||||||||||||||||||
Seq_2  901   CTCCCACAGGGCGGACCAGGAGCCGACGTCGCTCCAGTCGGCATCGAGACCGACCACCAC  960

Seq_1  961   CGCGTCGGCGGTTTTCTCCATCACCGCGTAGTCCACAGACTCGTCCGGACACTCGCAGAA  1020
             ||||||||||||||||||||||||||||||||||||||||||||||||::|||||||||||
Seq_2  961   CGCGTCGGCGGTTTTCTCCATCACCGCGTAGTCCACAGACTCGTCCGGANNCTCGCAGAA  1020

Seq_1  1021  AATGTCATGCGGAATGCTGATGAAGTCGCTGCCGTTGTCGGCGGCATTCACCGCGACCTG  1080
             ||||||||||||||||||||||||||||||||||||||||||||||||:||||||||||||
Seq_2  1021  AATGTCATGCGGAATGCTGATGAAGTCGCTGCCGTTGTCGGCGGCATTCNCCGCGACCTG  1080

Seq_1  1081  GCAGGCTTC  1089
             |||||||||
Seq_2  1081  GCAGGCTTC  1089
```

Figure A.4: Genomic analysis of the *manC* region of Kp52145 strains. Genomic DNA extracted from WT and mutant Kp52145 was used as template in PCRs to amplify *manC* (described in 4.9.1). Sequences of the purified PCR products were generated by Source BioScience using primers **(A)** manCa and **(B)** manCd. Sequences of WT and mutant Kp52145 were aligned and compared using Serial Cloner. # denotes differences in nucleotides.

References

Ah, Y.M., Kim, A.J., and Lee, J.Y. (2014) Colistin resistance in *Klebsiella pneumoniae*. *Int J Antimicrob Agents* **44**: 8-15.

Ahmed, A., Azim, A., Gurjar, M., and Baronia, A.K. (2014) Current concepts in combination antibiotic therapy for critically ill patients. *Indian J Crit Care Med* **18**: 310-314.

Aidelberg, G., Towbin, B.D., Rothschild, D., Dekel, E., Bren, A., and Alon, U. (2014) Hierarchy of non-glucose sugars in *Escherichia coli*. *BMC systems biology* **8**: 133-133.

Albertí, S., Rodríquez-Quiñones, F., Schirmer, T., Rummel, G., Tomás, J.M., Rosenbusch, J.P., and Benedí, V.J. (1995) A porin from *Klebsiella pneumoniae*: sequence homology, three-dimensional model, and complement binding. *Infect Immun* **63**: 903-910.

Alonso, V.P.P., and Kabuki, D.Y. (2019) Formation and dispersal of biofilms in dairy substrates. *International Journal of Dairy Technology* **72**: 472-478.

Amako, K., Meno, Y., and Takade, A. (1988) Fine structures of the capsules of *Klebsiella pneumoniae* and *Escherichia coli* K1. *J Bacteriol* **170**: 4960-4962.

Arakawa, Y., Wacharotayankun, R., Nagatsuka, T., Ito, H., Kato, N., and Ohta, M. (1995) Genomic organization of the *Klebsiella pneumoniae cps* region responsible for serotype K2 capsular polysaccharide synthesis in the virulent strain Chedid. *J Bacteriol* **177**: 1788-1796.

Athamna, A., Ofek, I., Keisari, Y., Markowitz, S., Dutton, G.G., and Sharon, N. (1991) Lectinophagocytosis of encapsulated *Klebsiella pneumoniae* mediated by surface lectins of guinea pig alveolar macrophages and human monocyte-derived macrophages. *Infect Immun* **59**: 1673-1682.

Bache, S.E., Maclean, M., MacGregor, S.J., Anderson, J.G., Gettinby, G., Coia, J.E., and Taggart, I. (2012) Clinical studies of the High-Intensity Narrow-Spectrum light Environmental Decontamination System (HINS-light EDS), for continuous disinfection in the burn unit inpatient and outpatient settings. *Burns* **38**: 69-76.

Balestrino, D., Ghigo, J.M., Charbonnel, N., Haagensen, J.A., and Forestier, C. (2008) The characterization of functions involved in the establishment and maturation of *Klebsiella pneumoniae* in vitro biofilm reveals dual roles for surface exopolysaccharides. *Environ Microbiol* **10**: 685-701.

Bhaumik, S., and Gambhir, S.S. (2002) Optical imaging of *Renilla luciferase* reporter gene expression in living mice. *Proc Natl Acad Sci U S A* **99**: 377-382.

Boddicker, J.D., Anderson, R.A., Jagnow, J., and Clegg, S. (2006) Signature-tagged mutagenesis of *Klebsiella pneumoniae* to identify genes that influence biofilm formation on extracellular matrix material. *Infect Immun* **74**: 4590-4597.

Bonnet, R. (2004) Growing group of extended-spectrum beta-lactamases: the CTX-M enzymes. *Antimicrob Agents Chemother* **48**: 1-14.

Bowden, G.H., and Li, Y.H. (1997) Nutritional influences on biofilm development. *Adv Dent Res* **11**: 81-99.

Brinkworth, A.J., Hammer, C.H., Olano, L.R., Kobayashi, S.D., Chen, L., Kreiswirth, B.N., and DeLeo, F.R. (2015) Identification of Outer Membrane and Exoproteins of Carbapenem-Resistant Multilocus Sequence Type 258 *Klebsiella pneumoniae*. *PLoS One* **10**: e0123219.

Brisse, S., Passet, V., Haugaard, A.B., Babosan, A., Kassis-Chikhani, N., Struve, C., and Decré, D. (2013) *wzi* Gene sequencing, a rapid method for determination of capsular type for *Klebsiella* strains. *J Clin Microbiol* **51**: 4073-4078.

Bullen, J.J., Rogers, H.J., and Griffiths, E. (1972) Iron binding proteins and infection. *Br J Haematol* **23**: 389-392.

Bush, K., Jacoby, G.A., and Medeiros, A.A. (1995) A functional classification scheme for beta-lactamases and its correlation with molecular structure. *Antimicrobial Agents and Chemotherapy* **39**: 1211-1233.

Cabral, J., and Ag, R. (2019) Blue Light Disinfection in Hospital Infection Control: Advantages, Drawbacks, and Pitfalls. *Antibiotics (Basel, Switzerland)* **8**: 58.

Cannatelli, A., Giani, T., D'Andrea, M.M., Di Pilato, V., Arena, F., Conte, V., Tryfinopoulou, K., Vatopoulos, A., Rossolini, G.M., and Group, C.S. (2014) MgrB inactivation is a common mechanism of colistin resistance in KPC-producing *Klebsiella pneumoniae* of clinical origin. *Antimicrob Agents Chemother* **58**: 5696-5703.

Catalán-Nájera, J.C., Garza-Ramos, U., and Barrios-Camacho, H. (2017) Hypervirulence and hypermucoviscosity: Two different but complementary *Klebsiella* spp. phenotypes? *Virulence* **8**: 1111-1123.

Ceri, H., Olson, M.E., Stremick, C., Read, R.R., Morck, D., and Buret, A. (1999) The Calgary Biofilm Device: new technology for rapid determination of antibiotic susceptibilities of bacterial biofilms. *J Clin Microbiol* **37**: 1771-1776.

Chang, A.C., and Cohen, S.N. (1978) Construction and characterization of amplifiable multicopy DNA cloning vehicles derived from the P15A cryptic miniplasmid. *J Bacteriol* **134**: 1141-1156.

Chen, C., Wei, D., Liu, P., Wang, M., Shi, J., Jiang, B., and Hao, J. (2016) Inhibition of RecBCD in *Klebsiella pneumoniae* by Gam and its effect on the efficiency of gene replacement. *J Basic Microbiol* **56**: 120-126.

Choi, U., and Lee, C.R. (2019) Distinct Roles of Outer Membrane Porins in Antibiotic Resistance and Membrane Integrity in *Escherichia coli*. *Front Microbiol* **10**: 953.

Chung, P.Y. (2016) The emerging problems of *Klebsiella pneumoniae* infections: carbapenem resistance and biofilm formation. *FEMS Microbiol Lett* **363**.

Ciurana, B., and Tomás, J.M. (1987) Role of lipopolysaccharide and complement in susceptibility of *Klebsiella pneumoniae* to nonimmune serum. *Infect Immun* **55**: 2741-2746.

Close, D., Xu, T., Smartt, A., Rogers, A., Crossley, R., Price, S., Ripp, S., and Sayler, G., (2012) The Evolution of the Bacterial Luciferase Gene Cassette (*lux*) as a Real-Time Bioreporter. In: Sensors (Basel). pp. 732-752.

Conway, M., Xu, T., Kirkpatrick, A., Ripp, S., Sayler, G., and Close, D. (2020) Real-time tracking of stem cell viability, proliferation, and differentiation with autonomous bioluminescence imaging. *BMC Biol* **18**: 79.

Cortés, G., Borrell, N., de Astorza, B., Gómez, C., Sauleda, J., and Albertí, S. (2002) Molecular analysis of the contribution of the capsular polysaccharide and the lipopolysaccharide O side chain to the virulence of *Klebsiella pneumoniae* in a murine model of pneumonia. *Infect Immun* **70**: 2583-2590.

Cryz, S.J., Mortimer, P.M., Mansfield, V., and Germanier, R. (1986) Seroepidemiology of *Klebsiella* bacteremic isolates and implications for vaccine development. *J Clin Microbiol* **23**: 687-690.

Cubero, M., Marti, S., Domínguez, M., González-Díaz, A., Berbel, D., and Ardanuy, C. (2019) Hypervirulent *Klebsiella pneumoniae* serotype K1 clinical isolates form robust biofilms at the air-liquid interface. *PLoS One* **14**: e0222628.

Dai, T., Gupta, A., Murray, C.K., Vrahas, M.S., Tegos, G.P., and Hamblin, M.R. (2012) Blue light for infectious diseases: *Propionibacterium acnes, Helicobacter pylori*, and beyond? *Drug resistance updates : reviews and commentaries in antimicrobial and anticancer chemotherapy* **15**: 223-236.

Darfeuille-Michaud, A., Jallat, C., Aubel, D., Sirot, D., Rich, C., Sirot, J., and Joly, B. (1992) R-plasmid-encoded adhesive factor in *Klebsiella pneumoniae* strains responsible for human nosocomial infections. *Infect Immun* **60**: 44-55.

Datsenko, K.A., and Wanner, B.L. (2000) One-step inactivation of chromosomal genes in *Escherichia coli* K-12 using PCR products. *Proc Natl Acad Sci U S A* **97**: 6640-6645.
de Astorza, B., Cortés, G., Crespí, C., Saus, C., Rojo, J.M., and Albertí, S. (2004) C3 promotes clearance of *Klebsiella pneumoniae* by A549 epithelial cells. *Infect Immun* **72**: 1767-1774.
de la Fuente-Núñez, C., Reffuveille, F., Fernández, L., and Hancock, R.E. (2013) Bacterial biofilm development as a multicellular adaptation: antibiotic resistance and new therapeutic strategies. *Curr Opin Microbiol* **16**: 580-589.
Deighan, P., Free, A., and Dorman, C.J. (2000) A role for the *Escherichia coli* H-NS-like protein StpA in OmpF porin expression through modulation of *micF* RNA stability. *Mol Microbiol* **38**: 126-139.
Desjardins, P., and Conklin, D. (2010) NanoDrop microvolume quantitation of nucleic acids. *J Vis Exp* **45**: 2565.
Dewanti, R., and Wong, A.C. (1995) Influence of culture conditions on biofilm formation by *Escherichia coli* O157:H7. *Int J Food Microbiol* **26**: 147-164.
Di Martino, P., Cafferini, N., Joly, B., and Darfeuille-Michaud, A. (2003) *Klebsiella pneumoniae* type 3 pili facilitate adherence and biofilm formation on abiotic surfaces. *Res Microbiol* **154**: 9-16.
Doi, Y., and Chambers, H.F., (2015) Penicillins and β-Lactamase Inhibitors. In: Mandell, Douglas, and Bennett's Principles and Practice of Infectious Diseases (Eighth Edition). J.E. Bennett, R. Dolin & M.J. Blaser (eds). pp. 263-277.
Donlan, R.M. (2001) Biofilms and device-associated infections. *Emerg Infect Dis* **7**: 277-281.
Donlan, R.M. (2002) Biofilms: microbial life on surfaces. *Emerg Infect Dis* **8**: 881-890.
Doorduijn, D.J., Rooijakkers, S.H., van Schaik, W., and Bardoel, B.W. (2016) Complement resistance mechanisms of *Klebsiella pneumoniae*. *Immunobiology* **221**: 1102-1109.
Drawz, S.M., and Bonomo, R.A. (2010) Three decades of beta-lactamase inhibitors. *Clinical microbiology reviews* **23**: 160-201.
Egan, M., Ramirez, J., Xander, C., Upreti, C., and Bhatt, S. (2016) Lambda Red-mediated Recombineering in the Attaching and Effacing Pathogen *Escherichia albertii*. *Biol Proced Online* **18**: 3.
Eswaran, J., Hughes, C., and Koronakis, V. (2003) Locking TolC Entrance Helices to Prevent Protein Translocation by the Bacterial Type I Export Apparatus. *Journal of Molecular Biology* **327**: 309-315.
Fang, C.T., Chuang, Y.P., Shun, C.T., Chang, S.C., and Wang, J.T. (2004) A novel virulence gene in *Klebsiella pneumoniae* strains causing primary liver abscess and septic metastatic complications. *J Exp Med* **199**: 697-705.
Favre-Bonte, S., Joly, B., and Forestier, C. (1999) Consequences of reduction of *Klebsiella pneumoniae* capsule expression on interactions of this bacterium with epithelial cells. *Infect Immun* **67**: 554-561.
Ferrer-Espada, R., Liu, X., Goh, X.S., and Dai, T. (2019) Antimicrobial Blue Light Inactivation of Polymicrobial Biofilms. *Frontiers in Microbiology* **10**.
Flemming, H.-C., and Wingender, J. (2010) The biofilm matrix. *Nature Reviews Microbiology* **8**: 623-633.
Fletcher, M. (1976) The effects of proteins on bacterial attachment to polystyrene. *J Gen Microbiol* **94**: 400-404.
Fournet-Fayard, S., Joly, B., and Forestier, C. (1995) Transformation of wild type *Klebsiella pneumoniae* with plasmid DNA by electroporation. *Journal of Microbiological Methods* **24**: 49-54.
Fuursted, K., Schøler, L., Hansen, F., Dam, K., Bojer, M.S., Hammerum, A.M., Dagnæs-Hansen, F., Olsen, A., Jasemian, Y., and Struve, C. (2012) Virulence of a *Klebsiella pneumoniae*

strain carrying the New Delhi metallo-beta-lactamase-1 (NDM-1). *Microbes Infect* **14**: 155-158.

Fux, C.A., Costerton, J.W., Stewart, P.S., and Stoodley, P. (2005) Survival strategies of infectious biofilms. *Trends Microbiol* **13**: 34-40.

Garcez, A.S., Núñez, S.C., Azambuja, N., Fregnani, E.R., Rodriguez, H.M., Hamblin, M.R., Suzuki, H., and Ribeiro, M.S. (2013) Effects of photodynamic therapy on Gram-positive and Gram-negative bacterial biofilms by bioluminescence imaging and scanning electron microscopic analysis. *Photomed Laser Surg* **31**: 519-525.

Gin, A., Dilay, L., Karlowsky, J.A., Walkty, A., Rubinstein, E., and Zhanel, G.G. (2007) Piperacillin-tazobactam: a β-lactam/β-lactamase inhibitor combination. *Expert Review of Anti-infective Therapy* **5**: 365+.

Gonzalez, R.J., Weening, E.H., Frothingham, R., Sempowski, G.D., and Miller, V.L. (2012) Bioluminescence imaging to track bacterial dissemination of *Yersinia pestis* using different routes of infection in mice. *BMC Microbiol* **12**: 147.

Grant, W.D., Sutherland, I.W., and Wilkinson, J.F. (1969) Exopolysaccharide colanic acid and its occurrence in the *Enterobacteriaceae*. *J Bacteriol* **100**: 1187-1193.

Gregor, C., Gwosch, K.C., Sahl, S.J., and Hell, S.W. (2018) Strongly enhanced bacterial bioluminescence with the *ilux* operon for single-cell imaging. *Proc Natl Acad Sci U S A* **115**: 962-967.

Halstead, F.D., Ahmed, Z., Bishop, J.R.B., and Oppenheim, B.A. (2019) The potential of visible blue light (405 nm) as a novel decontamination strategy for carbapenemase-producing *enterobacteriaceae* (CPE). *Antimicrobial Resistance & Infection Control* **8**: 14.

Halstead, F.D., Thwaite, J.E., Burt, R., Laws, T.R., Raguse, M., Moeller, R., Webber, M.A., and Oppenheim, B.A. (2016) Antibacterial Activity of Blue Light against Nosocomial Wound Pathogens Growing Planktonically and as Mature Biofilms. *Applied and Environmental Microbiology* **82**: 4006.

Harris, P.N.A., Tambyah, P.A., Lye, D.C., Mo, Y., Lee, T.H., Yilmaz, M., Alenazi, T.H., Arabi, Y., Falcone, M., Bassetti, M., Righi, E., Rogers, B.A., Kanj, S., Bhally, H., Iredell, J., Mendelson, M., Boyles, T.H., Looke, D., Miyakis, S., Walls, G., Al Khamis, M., Zikri, A., Crowe, A., Ingram, P., Daneman, N., Griffin, P., Athan, E., Lorenc, P., Baker, P., Roberts, L., Beatson, S.A., Peleg, A.Y., Harris-Brown, T., Paterson, D.L., and Network, M.T.I.a.t.A.S.f.I.D.C.R. (2018) Effect of Piperacillin-Tazobactam vs Meropenem on 30-Day Mortality for Patients With *Escherichia coli* or *Klebsiella pneumoniae* Bloodstream Infection and Ceftriaxone Resistance: A Randomized Clinical Trial. *JAMA* **320**: 984-994.

Helke, D.M., Somers, E.B., and Wong, A.C.L. (1993) Attachment of *Listeria monocytogenes* and *Salmonella typhimurium* to Stainless Steel and Buna-N in the Presence of Milk and Individual Milk Components. *J Food Prot* **56**: 479-484.

Hernández-Allés, S., Conejo, M., Pascual, A., Tomás, J.M., Benedí, V.J., and Martínez-Martínez, L. (2000) Relationship between outer membrane alterations and susceptibility to antimicrobial agents in isogenic strains of *Klebsiella pneumoniae*. *J Antimicrob Chemother* **46**: 273-277.

Hobby, C.R., Herndon, J.L., Morrow, C.A., Peters, R.E., Symes, S.J.K., and Giles, D.K. (2019) Exogenous fatty acids alter phospholipid composition, membrane permeability, capacity for biofilm formation, and antimicrobial peptide susceptibility in *Klebsiella pneumoniae*. *Microbiology Open* **8**: e00635.

Holden, V.I., and Bachman, M.A. (2015) Diverging roles of bacterial siderophores during infection. *Metallomics* **7**: 986-995.

Holden, V.I., Breen, P., Houle, S., Dozois, C.M., and Bachman, M.A. (2016) *Klebsiella pneumoniae* Siderophores Induce Inflammation, Bacterial Dissemination, and HIF-1α Stabilization during Pneumonia. *mBio* **7**: e01397-01316.

Huang, T.W., Lam, I., Chang, H.Y., Tsai, S.F., Palsson, B.O., and Charusanti, P. (2014a) Capsule deletion via a λ-Red knockout system perturbs biofilm formation and fimbriae expression in *Klebsiella pneumoniae* MGH 78578. *BMC Res Notes* **7**: 13.

Huang, Y.K., Chu, C., Wu, C.H., Chen, C.L., and Chiu, C.H. (2014b) Evaluation of Gram-negative bacterial infection by a stable and conjugative bioluminescence plasmid in a mouse model. *J Biomed Sci* **21**: 78.

Ishizuka, H., Hanamura, A., Inada, T., and Aiba, H. (1994) Mechanism of the down-regulation of cAMP receptor protein by glucose in *Escherichia coli*: role of autoregulation of the *crp* gene. *EMBO J* **13**: 3077-3082.

Jacobsen, S.M., Stickler, D.J., Mobley, H.L., and Shirtliff, M.E. (2008) Complicated catheter-associated urinary tract infections due to *Escherichia coli* and *Proteus mirabilis*. *Clin Microbiol Rev* **21**: 26-59.

Jacoby, G.A., and Sutton, L. (1991) Properties of plasmids responsible for production of extended-spectrum beta-lactamases. *Antimicrob Agents Chemother* **35**: 164-169.

Jagnow, J., and Clegg, S. (2003) *Klebsiella pneumoniae* MrkD-mediated biofilm formation on extracellular matrix- and collagen-coated surfaces. *Microbiology* **149**: 2397-2405.

Jerke, K.H., Lee, M.J., and Humphries, R.M. (2016) Polymyxin Susceptibility Testing: a Cold Case Reopened. *Clinical Microbiology Newsletter* **38**: 69-77.

Kadurugamuwa, J.L., Sin, L., Albert, E., Yu, J., Francis, K., DeBoer, M., Rubin, M., Bellinger-Kawahara, C., Parr, T.R., and Contag, P.R. (2003a) Direct continuous method for monitoring biofilm infection in a mouse model. *Infect Immun* **71**: 882-890.

Kadurugamuwa, J.L., Sin, L.V., Yu, J., Francis, K.P., Kimura, R., Purchio, T., and Contag, P.R. (2003b) Rapid direct method for monitoring antibiotics in a mouse model of bacterial biofilm infection. *Antimicrob Agents Chemother* **47**: 3130-3137.

Kalanuria, A.A., Ziai, W., Zai, W., and Mirski, M. (2014) Ventilator-associated pneumonia in the ICU. *Crit Care* **18**: 208.

Kapoor, G., Saigal, S., and Elongavan, A. (2017) Action and resistance mechanisms of antibiotics: A guide for clinicians. *J Anaesthesiol Clin Pharmacol* **33**: 300-305.

Kidd, T.J., Mills, G., Sa-Pessoa, J., Dumigan, A., Frank, C.G., Insua, J.L., Ingram, R., Hobley, L., and Bengoechea, J.A. (2017) A *Klebsiella pneumoniae* antibiotic resistance mechanism that subdues host defences and promotes virulence. *EMBO Mol Med* **9**: 430-447.

Klebba, P.E. (2016) ROSET Model of TonB Action in Gram-Negative Bacterial Iron Acquisition. *J Bacteriol* **198**: 1013-1021.

Kleinpenning, M.M., Smits, T., Frunt, M.H., van Erp, P.E., van de Kerkhof, P.C., and Gerritsen, R.M. (2010) Clinical and histological effects of blue light on normal skin. *Photodermatol Photoimmunol Photomed* **26**: 16-21.

Kline, K.A., Fälker, S., Dahlberg, S., Normark, S., and Henriques-Normark, B. (2009) Bacterial adhesins in host-microbe interactions. *Cell Host Microbe* **5**: 580-592.

Ko, W.C., Paterson, D.L., Sagnimeni, A.J., Hansen, D.S., Von Gottberg, A., Mohapatra, S., Casellas, J.M., Goossens, H., Mulazimoglu, L., Trenholme, G., Klugman, K.P., McCormack, J.G., and Yu, V.L. (2002) Community-acquired *Klebsiella pneumoniae* bacteremia: global differences in clinical patterns. *Emerg Infect Dis* **8**: 160-166.

Kumar, A., Mallik, D., Pal, S., Mallick, S., Sarkar, S., Chanda, A., and Ghosh, A.S. (2015) *Escherichia coli* O8-antigen enhances biofilm formation under agitated conditions. *FEMS Microbiol Lett* **362**: fnv112.

Laemmli, U.K. (1970) Cleavage of structural proteins during the assembly of the head of bacteriophage T4. *Nature* **227**: 680-685.

Langstraat, J., Bohse, M., and Clegg, S. (2001) Type 3 fimbrial shaft (MrkA) of *Klebsiella pneumoniae*, but not the fimbrial adhesin (MrkD), facilitates biofilm formation. *Infect Immun* **69**: 5805-5812.

Lau, C.K., Krewulak, K.D., and Vogel, H.J. (2016) Bacterial ferrous iron transport: the Feo system. *FEMS Microbiol Rev* **40**: 273-298.

Lawlor, M.S., Hsu, J., Rick, P.D., and Miller, V.L. (2005) Identification of *Klebsiella pneumoniae* virulence determinants using an intranasal infection model. *Mol Microbiol* **58**: 1054-1073.

LeChevallier, M.W., Cawthon, C.D., and Lee, R.G. (1988) Factors promoting survival of bacteria in chlorinated water supplies. *Appl Environ Microbiol* **54**: 649-654.

Lee, A.J., Wang, S., Meredith, H.R., Zhuang, B., Dai, Z., and You, L. (2018) Robust, linear correlations between growth rates and β-lactam–mediated lysis rates. *Proceedings of the National Academy of Sciences* **115**: 4069.

Lee, C.H., Chen, I.L., Chuah, S.K., Tai, W.C., Chang, C.C., Chen, F.J., and Chen, J.F. (2016) Impact of glycemic control on capsular polysaccharide biosynthesis and opsonophagocytosis of *Klebsiella pneumoniae*: Implications for invasive syndrome in patients with diabetes mellitus. *Virulence* **7**: 770-778.

Lee, G.C., and Burgess, D.S. (2012) Treatment of *Klebsiella pneumoniae* carbapenemase (KPC) infections: a review of published case series and case reports. *Ann Clin Microbiol Antimicrob* **11**: 32.

Lee, I.R., Sng, E., Lee, K.O., Molton, J.S., Chan, M., Kalimuddin, S., Izharuddin, E., Lye, D.C., Archuleta, S., and Gan, Y.H. (2017) Comparison of Diabetic and Non-diabetic Human Leukocytic Responses to Different Capsule Types of *Klebsiella pneumoniae* Responsible for Causing Pyogenic Liver Abscess. *Front Cell Infect Microbiol* **7**: 401.

Lee, J., Page, R., García-Contreras, R., Palermino, J.M., Zhang, X.S., Doshi, O., Wood, T.K., and Peti, W. (2007) Structure and function of the *Escherichia coli* protein YmgB: a protein critical for biofilm formation and acid-resistance. *J Mol Biol* **373**: 11-26.

Lewis, K. (2010) Persister cells. *Annu Rev Microbiol* **64**: 357-372.

Lin, C.L., Chen, F.H., Huang, L.Y., Chang, J.C., Chen, J.H., Tsai, Y.K., Chang, F.Y., Lin, J.C., and Siu, L.K. (2017) Effect in virulence of switching conserved homologous capsular polysaccharide genes from *Klebsiella pneumoniae* serotype K1 into K20. *Virulence* **8**: 487-493.

Lin, C.T., Chen, Y.C., Jinn, T.R., Wu, C.C., Hong, Y.M., and Wu, W.H. (2013a) Role of the cAMP-dependent carbon catabolite repression in capsular polysaccharide biosynthesis in *Klebsiella pneumoniae*. *PLoS One* **8**: e54430.

Lin, C.T., Lin, T.H., Wu, C.C., Wan, L., Huang, C.F., and Peng, H.L. (2016) CRP-Cyclic AMP Regulates the Expression of Type 3 Fimbriae via Cyclic di-GMP in *Klebsiella pneumoniae*. *PLoS One* **11**: e0162884.

Lin, J., Huang, S., and Zhang, Q. (2002) Outer membrane proteins: key players for bacterial adaptation in host niches. *Microbes Infect* **4**: 325-331.

Lin, T.H., Huang, S.H., Wu, C.C., Liu, H.H., Jinn, T.R., Chen, Y., and Lin, C.T. (2013b) Inhibition of *Klebsiella pneumoniae* Growth and Capsular Polysaccharide Biosynthesis by *Fructus mume*. *Evid Based Complement Alternat Med* **2013**: 621701.

Lin, Y.C., Lu, M.C., Tang, H.L., Liu, H.C., Chen, C.H., Liu, K.S., Lin, C., Chiou, C.S., Chiang, M.K., Chen, C.M., and Lai, Y.C. (2011) Assessment of hypermucoviscosity as a virulence factor for experimental *Klebsiella pneumoniae* infections: comparative virulence analysis with hypermucoviscosity-negative strain. *BMC Microbiol* **11**: 50.

Lin, Y.T., Wang, F.D., Wu, P.F., and Fung, C.P. (2013c) *Klebsiella pneumoniae* liver abscess in diabetic patients: association of glycemic control with the clinical characteristics. *BMC Infect Dis* **13**: 56.

Link, A.J., Phillips, D., and Church, G.M. (1997) Methods for generating precise deletions and insertions in the genome of wild-type *Escherichia coli*: application to open reading frame characterization. *J Bacteriol* **179**: 6228-6237.

Liu, Y.F., Yan, J.J., Lei, H.Y., Teng, C.H., Wang, M.C., Tseng, C.C., and Wu, J.J. (2012) Loss of outer membrane protein C in *Escherichia coli* contributes to both antibiotic resistance and escaping antibody-dependent bactericidal activity. *Infect Immun* **80**: 1815-1822.
Llobet, E., March, C., Giménez, P., and Bengoechea, J.A. (2009) *Klebsiella pneumoniae* OmpA confers resistance to antimicrobial peptides. *Antimicrob Agents Chemother* **53**: 298-302.
Llobet, E., Tomás, J.M., and Bengoechea, J.A. (2008) Capsule polysaccharide is a bacterial decoy for antimicrobial peptides. *Microbiology* **154**: 3877-3886.
Maclean, M., MacGregor, S.J., Anderson, J.G., and Woolsey, G. (2009) Inactivation of bacterial pathogens following exposure to light from a 405-nanometer light-emitting diode array. *Appl Environ Microbiol* **75**: 1932-1937.
Maclean, M., MacGregor, S.J., Anderson, J.G., Woolsey, G.A., Coia, J.E., Hamilton, K., Taggart, I., Watson, S.B., Thakker, B., and Gettinby, G. (2010) Environmental decontamination of a hospital isolation room using high-intensity narrow-spectrum light. *Journal of Hospital Infection* **76**: 247-251.
Magill, S.S., Edwards, J.R., Bamberg, W., Beldavs, Z.G., Dumyati, G., Kainer, M.A., Lynfield, R., Maloney, M., McAllister-Hollod, L., Nadle, J., Ray, S.M., Thompson, D.L., Wilson, L.E., Fridkin, S.K., and Team, E.I.P.H.-A.I.a.A.U.P.S. (2014) Multistate point-prevalence survey of health care-associated infections. *N Engl J Med* **370**: 1198-1208.
Malachowa, N., and DeLeo, F.R., (2011) *Staphylococcus aureus* survival in human blood. In: Virulence. pp. 567-569.
March, C., Cano, V., Moranta, D., Llobet, E., Pérez-Gutiérrez, C., Tomás, J.M., Suárez, T., Garmendia, J., and Bengoechea, J.A. (2013) Role of bacterial surface structures on the interaction of *Klebsiella pneumoniae* with phagocytes. *PLoS One* **8**: e56847.
March, C., Moranta, D., Regueiro, V., Llobet, E., Tomás, A., Garmendia, J., and Bengoechea, J.A. (2011) *Klebsiella pneumoniae* outer membrane protein A is required to prevent the activation of airway epithelial cells. *J Biol Chem* **286**: 9956-9967.
Martin, R.M., and Bachman, M.A. (2018) Colonization, Infection, and the Accessory Genome of *Klebsiella pneumoniae*. *Front Cell Infect Microbiol* **8**: 4.
May, K.L., and Grabowicz, M. (2018) The bacterial outer membrane is an evolving antibiotic barrier. *Proc Natl Acad Sci U S A* **115**: 8852-8854.
Medeiros, A.A. (1984) Beta-lactamases. *Br Med Bull* **40**: 18-27.
Meighen, E.A. (1994) Genetics of bacterial bioluminescence. *Annu Rev Genet* **28**: 117-139.
Merino, S., Camprubí, S., Albertí, S., Benedí, V.J., and Tomás, J.M. (1992) Mechanisms of *Klebsiella pneumoniae* resistance to complement-mediated killing. *Infect Immun* **60**: 2529-2535.
Miethke, M., and Marahiel, M.A. (2007) Siderophore-based iron acquisition and pathogen control. *Microbiol Mol Biol Rev* **71**: 413-451.
Mizuta, K., Ohta, M., Mori, M., Hasegawa, T., Nakashima, I., and Kato, N. (1983) Virulence for mice of *Klebsiella* strains belonging to the O1 group: relationship to their capsular (K) types. *Infect Immun* **40**: 56-61.
Mobley, H.L., Green, D.M., Trifillis, A.L., Johnson, D.E., Chippendale, G.R., Lockatell, C.V., Jones, B.D., and Warren, J.W. (1990) Pyelonephritogenic *Escherichia coli* and killing of cultured human renal proximal tubular epithelial cells: role of hemolysin in some strains. *Infect Immun* **58**: 1281-1289.
Moradigaravand, D., Martin, V., Peacock, S.J., and Parkhill, J. (2017) Evolution and Epidemiology of Multidrug-Resistant *Klebsiella pneumoniae* in the United Kingdom and Ireland. *MBio* **8**: e01976-01916.
Moura, Q., Esposito, F., Fernandes, M.R., Espinoza-Muñoz, M., Souza, T.A., Santos, S.R., Cerdeira, L., Cassettari, V., and Lincopan, N. (2017) Genome sequence analysis of a

hypermucoviscous/hypervirulent and MDR CTX-M-15/K19/ST29 *Klebsiella pneumoniae* isolated from human infection. *Pathog Dis* **75**. 9.
Moynihan, S., (2018) The Role of the *wzy* Gene in Serum Resistance. Unpublished: Trinity College Dublin.
Murphy, C.N., Mortensen, M.S., Krogfelt, K.A., and Clegg, S. (2013) Role of *Klebsiella pneumoniae* type 1 and type 3 fimbriae in colonizing silicone tubes implanted into the bladders of mice as a model of catheter-associated urinary tract infections. *Infect Immun* **81**: 3009-3017.
Murphy, K.C. (2016) λ Recombination and Recombineering. *EcoSal Plus* **7**.
Murphy, K.C., and Campellone, K.G. (2003) Lambda Red-mediated recombinogenic engineering of enterohemorrhagic and enteropathogenic *E. coli*. *BMC Mol Biol* **4**: 11.
Nassif, X., Fournier, J.M., Arondel, J., and Sansonetti, P.J. (1989) Mucoid phenotype of *Klebsiella pneumoniae* is a plasmid-encoded virulence factor. *Infect Immun* **57**: 546-552.
Nassif, X., and Sansonetti, P.J. (1986) Correlation of the virulence of *Klebsiella pneumoniae* K1 and K2 with the presence of a plasmid encoding aerobactin. *Infect Immun* **54**: 603-608.
Naves, P., del Prado, G., Huelves, L., Gracia, M., Ruiz, V., Blanco, J., Rodríguez-Cerrato, V., Ponte, M.C., and Soriano, F. (2008) Measurement of biofilm formation by clinical isolates of *Escherichia coli* is method-dependent. *J Appl Microbiol* **105**: 585-590.
Nikaido, H. (2003) Molecular basis of bacterial outer membrane permeability revisited. *Microbiol Mol Biol Rev* **67**: 593-656.
Nordmann, P. (2014) Carbapenemase-producing *Enterobacteriaceae*: overview of a major public health challenge. *Med Mal Infect* **44**: 51-56.
O'Kelly, F., Kavanagh, S., Manecksha, R., Thornhill, J., and Fennell, J.P. (2016) Characteristics of Gram-negative urinary tract infections caused by extended spectrum beta lactamases: pivmecillinam as a treatment option within South Dublin, Ireland. *BMC Infect Dis* **16**: 620.
O'Toole, G.A. (2011) Microtiter dish biofilm formation assay. *J Vis Exp* **47**: 2437.
Olsen, I. (2015) Biofilm-specific antibiotic tolerance and resistance. *Eur J Clin Microbiol Infect Dis* **34**: 877-886.
Paczosa, M.K., and Mecsas, J. (2016) *Klebsiella pneumoniae*: Going on the Offense with a Strong Defense. *Microbiol Mol Biol Rev* **80**: 629-661.
Paczosa, M.K., Silver, R.J., McCabe, A.L., Tai, A.K., McLeish, C.H., Lazinski, D.W., and Mecsas, J. (2020) Transposon Mutagenesis Screen of *Klebsiella pneumoniae* Identifies Multiple Genes Important for Resisting Antimicrobial Activities of Neutrophils in Mice. *Infect Immun* **8**: e0034-0020.
Padayatti, P.S., Helfand, M.S., Totir, M.A., Carey, M.P., Carey, P.R., Bonomo, R.A., and van den Akker, F. (2005) High resolution crystal structures of the trans-enamine intermediates formed by sulbactam and clavulanic acid and E166A SHV-1 {beta}-lactamase. *J Biol Chem* **280**: 34900-34907.
Padilla, E., Llobet, E., Doménech-Sánchez, A., Martínez-Martínez, L., Bengoechea, J.A., and Albertí, S. (2010) *Klebsiella pneumoniae* AcrAB efflux pump contributes to antimicrobial resistance and virulence. *Antimicrob Agents Chemother* **54**: 177-183.
Paley, M.A., and Prescher, J.A. (2014) Bioluminescence: a versatile technique for imaging cellular and molecular features. *Medchemcomm* **5**: 255-267.
Pan, Y.J., Fang, H.C., Yang, H.C., Lin, T.L., Hsieh, P.F., Tsai, F.C., Keynan, Y., and Wang, J.T. (2008) Capsular polysaccharide synthesis regions in *Klebsiella pneumoniae* serotype K57 and a new capsular serotype. *J Clin Microbiol* **46**: 2231-2240.
Pan, Y.J., Lin, T.L., Chen, C.T., Chen, Y.Y., Hsieh, P.F., Hsu, C.R., Wu, M.C., and Wang, J.T. (2015) Genetic analysis of capsular polysaccharide synthesis gene clusters in 79 capsular types of *Klebsiella* spp. *Sci Rep* **5**: 15573.

Pan, Y.J., Lin, T.L., Chen, Y.H., Hsu, C.R., Hsieh, P.F., Wu, M.C., and Wang, J.T. (2013) Capsular types of *Klebsiella pneumoniae* revisited by *wzc* sequencing. *PLoS One* **8**: e80670.

Papp-Wallace, K.M., Bethel, C.R., Distler, A.M., Kasuboski, C., Taracila, M., and Bonomo, R.A. (2010) Inhibitor resistance in the KPC-2 beta-lactamase, a preeminent property of this class A beta-lactamase. *Antimicrob Agents Chemother* **54**: 890-897.

Papp-Wallace, K.M., Endimiani, A., Taracila, M.A., and Bonomo, R.A. (2011) Carbapenems: past, present, and future. *Antimicrob Agents Chemother* **55**: 4943-4960.

Patro, L.P.P., and Rathinavelan, T. (2019) Targeting the Sugary Armor of *Klebsiella* species. *Front Cell Infect Microbiol* **9**: 367.

Perry, C.M., and Markham, A. (1999) Piperacillin/tazobactam: an updated review of its use in the treatment of bacterial infections. *Drugs* **57**: 805-843.

Piperaki, E.T., Syrogiannopoulos, G.A., Tzouvelekis, L.S., and Daikos, G.L. (2017) *Klebsiella pneumoniae*: Virulence, Biofilm and Antimicrobial Resistance. *Pediatr Infect Dis J* **36**: 1002-1005.

Podschun, R., Sievers, D., Fischer, A., and Ullmann, U. (1993) Serotypes, hemagglutinins, siderophore synthesis, and serum resistance of *Klebsiella* isolates causing human urinary tract infections. *J Infect Dis* **168**: 1415-1421.

Podschun, R., and Ullmann, U. (1998) *Klebsiella* spp. as nosocomial pathogens: epidemiology, taxonomy, typing methods, and pathogenicity factors. *Clin Microbiol Rev* **11**: 589-603.

Pos, K.M. (2009) Drug transport mechanism of the AcrB efflux pump. *Biochim Biophys Acta* **1794**: 782-793.

Poudyal, A., Howden, B.P., Bell, J.M., Gao, W., Owen, R.J., Turnidge, J.D., Nation, R.L., and Li, J. (2008) *In vitro* pharmacodynamics of colistin against multidrug-resistant *Klebsiella pneumoniae*. *J Antimicrob Chemother* **62**: 1311-1318.

Pratt, L.A., and Kolter, R. (1998) Genetic analysis of *Escherichia coli* biofilm formation: roles of flagella, motility, chemotaxis and type I pili. *Mol Microbiol* **30**: 285-293.

Qureshi, Z.A., Paterson, D.L., Potoski, B.A., Kilayko, M.C., Sandovsky, G., Sordillo, E., Polsky, B., Adams-Haduch, J.M., and Doi, Y. (2012) Treatment outcome of bacteremia due to KPC-producing *Klebsiella pneumoniae*: superiority of combination antimicrobial regimens. *Antimicrob Agents Chemother* **56**: 2108-2113.

Rahn, A., Drummelsmith, J., and Whitfield, C. (1999) Conserved organization in the *cps* gene clusters for expression of *Escherichia coli* group 1 K antigens: relationship to the colanic acid biosynthesis locus and the *cps* genes from *Klebsiella pneumoniae*. *J Bacteriol* **181**: 2307-2313.

Ramirez, P., Bassi, G.L., and Torres, A. (2012) Measures to prevent nosocomial infections during mechanical ventilation. *Curr Opin Crit Care* **18**: 86-92.

Rawat, D., and Nair, D. (2010) Extended-spectrum β-lactamases in Gram Negative Bacteria. *J Glob Infect Dis* **2**: 263-274.

Regué, M., Izquierdo, L., Fresno, S., Jimenez, N., Piqué, N., Corsaro, M.M., Parrilli, M., Naldi, T., Merino, S., and Tomás, J.M. (2005) The incorporation of glucosamine into enterobacterial core lipopolysaccharide: two enzymatic steps are required. *J Biol Chem* **280**: 36648-36656.

Reisner, A., Krogfelt, K.A., Klein, B.M., Zechner, E.L., and Molin, S. (2006) *In vitro* biofilm formation of commensal and pathogenic *Escherichia coli* strains: impact of environmental and genetic factors. *J Bacteriol* **188**: 3572-3581.

Riss, T.L., Moravec, R.A., and Niles, A.L. (2011) Cytotoxicity testing: measuring viable cells, dead cells, and detecting mechanism of cell death. *Methods Mol Biol* **740**: 103-114.

Roberts, A.E., Kragh, K.N., Bjarnsholt, T., and Diggle, S.P. (2015) The Limitations of *In Vitro* Experimentation in Understanding Biofilms and Chronic Infection. *J Mol Biol* **427**: 3646-3661.

Rodriguez, C.A., Agudelo, M., Aguilar, Y.A., Zuluaga, A.F., and Vesga, O. (2016) Impact on Bacterial Resistance of Therapeutically Nonequivalent Generics: The Case of Piperacillin-Tazobactam. *PLoS One* **11**: e0155806.

Rodríguez-Baño, J., López-Cerero, L., Navarro, M.D., Díaz de Alba, P., and Pascual, A. (2008) Faecal carriage of extended-spectrum beta-lactamase-producing *Escherichia coli*: prevalence, risk factors and molecular epidemiology. *J Antimicrob Chemother* **62**: 1142-1149.

Russo, T.A., Olson, R., MacDonald, U., Beanan, J., and Davidson, B.A. (2015) Aerobactin, but not yersiniabactin, salmochelin, or enterobactin, enables the growth/survival of hypervirulent (hypermucoviscous) *Klebsiella pneumoniae ex vivo* and *in vivo*. *Infect Immun* **83**: 3325-3333.

Russo, T.A., Shon, A.S., Beanan, J.M., Olson, R., MacDonald, U., Pomakov, A.O., and Visitacion, M.P. (2011) Hypervirulent *K. pneumoniae* secretes more and more active iron-acquisition molecules than "classical" *K. pneumoniae* thereby enhancing its virulence. *PLoS One* **6**: e26734.

Rättö, M., Verhoef, R., Suihko, M.L., Blanco, A., Schols, H.A., Voragen, A.G., Wilting, R., Siika-Aho, M., and Buchert, J. (2006) Colanic acid is an exopolysaccharide common to many *enterobacteria* isolated from paper-machine slimes. *J Ind Microbiol Biotechnol* **33**: 359-367.

Römling, U., and Balsalobre, C. (2012) Biofilm infections, their resilience to therapy and innovative treatment strategies. *J Intern Med* **272**: 541-561.

Sahly, H., Podschun, R., Oelschlaeger, T.A., Greiwe, M., Parolis, H., Hasty, D., Kekow, J., Ullmann, U., Ofek, I., and Sela, S. (2000) Capsule impedes adhesion to and invasion of epithelial cells by *Klebsiella pneumoniae*. *Infect Immun* **68**: 6744-6749.

Scheld, W.M. (1991) Developments in the pathogenesis, diagnosis and treatment of nosocomial pneumonia. *Surg Gynecol Obstet* **172 Suppl**: 42-53.

Schembri, M.A., Blom, J., Krogfelt, K.A., and Klemm, P. (2005) Capsule and fimbria interaction in *Klebsiella pneumoniae*. *Infect Immun* **73**: 4626-4633.

Schembri, M.A., Dalsgaard, D., and Klemm, P. (2004) Capsule shields the function of short bacterial adhesins. *J Bacteriol* **186**: 1249-1257.

Schuetz, A.N., Reyes, S., and Tamma, P.D. (2018) Point-Counterpoint: Piperacillin-Tazobactam Should Be Used To Treat Infections with Extended-Spectrum-Beta-Lactamase-Positive Organisms. *J Clin Microbiol* **56**: e01917-01917.

Sebghati, T.A., Korhonen, T.K., Hornick, D.B., and Clegg, S. (1998) Characterization of the type 3 fimbrial adhesins of *Klebsiella* strains. *Infect Immun* **66**: 2887-2894.

Seifi, K., Kazemian, H., Heidari, H., Rezagholizadeh, F., Saee, Y., Shirvani, F., and Houri, H. (2016) Evaluation of Biofilm Formation Among *Klebsiella pneumoniae* Isolates and Molecular Characterization by ERIC-PCR. *Jundishapur J Microbiol* **9**: e30682.

Serra, D.O., Richter, A.M., Klauck, G., Mika, F., and Hengge, R. (2013) Microanatomy at cellular resolution and spatial order of physiological differentiation in a bacterial biofilm. *mBio* **4**: e00103-00113.

Sharp, R.R., Stoodley, P., Adgie, M., Gerlach, R., and Cunningham, A. (2005) Visualization and characterization of dynamic patterns of flow, growth and activity of biofilms growing in porous media. *Water Science and Technology* **52**: 85-90.

Shetty, N., Hill, G., and Ridgway, G.L. (1998) The Vitek analyser for routine bacterial identification and susceptibility testing: protocols, problems, and pitfalls. *J Clin Pathol* **51**: 316-323.

Shigeta, M., Tanaka, G., Komatsuzawa, H., Sugai, M., Suginaka, H., and Usui, T. (1997) Permeation of antimicrobial agents through *Pseudomonas aeruginosa* biofilms: a simple method. *Chemotherapy* **43**: 340-345.

Shon, A.S., Bajwa, R.P., and Russo, T.A. (2013) Hypervirulent (hypermucoviscous) *Klebsiella pneumoniae*: a new and dangerous breed. *Virulence* **4**: 107-118.

Shu, H.Y., Fung, C.P., Liu, Y.M., Wu, K.M., Chen, Y.T., Li, L.H., Liu, T.T., Kirby, R., and Tsai, S.F. (2009) Genetic diversity of capsular polysaccharide biosynthesis in *Klebsiella pneumoniae* clinical isolates. *Microbiology* **155**: 4170-4183.

Singh, A.K., Prakash, P., Achra, A., Singh, G.P., Das, A., and Singh, R.K. (2017) Standardization and Classification of *In vitro* Biofilm Formation by Clinical Isolates of *Staphylococcus aureus*. *J Glob Infect Dis* **9**: 93-101.

Singh, A.K., Yadav, S., Chauhan, B.S., Nandy, N., Singh, R., Neogi, K., Roy, J.K., Srikrishna, S., Singh, R.K., and Prakash, P. (2019) Classification of Clinical Isolates of *in vitro* Biofilm Forming Capabilities and Elucidation of the Biofilm Matrix Chemistry With Special Reference to the Protein Content. *Front Microbiol* **10**: 669.

Skyberg, J.A., Siek, K.E., Doetkott, C., and Nolan, L.K. (2007) Biofilm formation by avian E*scherichia coli* in relation to media, source and phylogeny. *J Appl Microbiol* **102**: 548-554.

Smani, Y., Fàbrega, A., Roca, I., Sánchez-Encinales, V., Vila, J., and Pachón, J. (2014) Role of OmpA in the multidrug resistance phenotype of *Acinetobacter baumannii*. *Antimicrob Agents Chemother* **58**: 1806-1808.

Smith, S.G., Mahon, V., Lambert, M.A., and Fagan, R.P. (2007) A molecular Swiss army knife: OmpA structure, function and expression. *FEMS Microbiol Lett* **273**: 1-11.

Soto, E., Dennis, M.M., Beierschmitt, A., Francis, S., Sithole, F., Halliday-Simmons, I., and Palmour, R. (2017) Biofilm formation of hypermucoviscous and non-hypermucoviscous *Klebsiella pneumoniae* recovered from clinically affected African green monkey (Chlorocebus aethiops sabaeus). *Microb Pathog* **107**: 198-201.

Stahlhut, S.G., Tchesnokova, V., Struve, C., Weissman, S.J., Chattopadhyay, S., Yakovenko, O., Aprikian, P., Sokurenko, E.V., and Krogfelt, K.A. (2009) Comparative structure-function analysis of mannose-specific FimH adhesins from *Klebsiella pneumoniae* and *Escherichia coli*. *J Bacteriol* **191**: 6592-6601.

Stewart, P.S. (1996) Theoretical aspects of antibiotic diffusion into microbial biofilms. *Antimicrob Agents Chemother* **40**: 2517-2522.

Struve, C., Bojer, M., and Krogfelt, K.A. (2009) Identification of a conserved chromosomal region encoding *Klebsiella pneumoniae* type 1 and type 3 fimbriae and assessment of the role of fimbriae in pathogenicity. *Infect Immun* **77**: 5016-5024.

Struve, C., and Krogfelt, K.A. (2003) Role of capsule in *Klebsiella pneumoniae* virulence: lack of correlation between *in vitro* and *in vivo* studies. *FEMS Microbiol Lett* **218**: 149-154.

Struve, C., Roe, C.C., Stegger, M., Stahlhut, S.G., Hansen, D.S., Engelthaler, D.M., Andersen, P.S., Driebe, E.M., Keim, P., and Krogfelt, K.A. (2015) Mapping the Evolution of Hypervirulent *Klebsiella pneumoniae*. *mBio* **6**: e00630.

Subramaniam, S., Erler, A., Fu, J., Kranz, A., Tang, J., Gopalswamy, M., Ramakrishnan, S., Keller, A., Grundmeier, G., Müller, D., Sattler, M., and Stewart, A.F. (2016) DNA annealing by Redβ is insufficient for homologous recombination and the additional requirements involve intra- and inter-molecular interactions. *Scientific Reports* **6**: 34525.

Sugawara, E., Kojima, S., and Nikaido, H. (2016) *Klebsiella pneumoniae* Major Porins OmpK35 and OmpK36 Allow More Efficient Diffusion of β-Lactams than Their *Escherichia coli* Homologs OmpF and OmpC. *Journal of bacteriology* **198**: 3200-3208.

Sun, W., Khosravi, F., Albrechtsen, H., Brovko, L.Y., and Griffiths, M.W. (2002) Comparison of ATP and *in vivo* bioluminescence for assessing the efficiency of immunomagnetic sorbents for live *Escherichia coli* O157:H7 cells. *J Appl Microbiol* **92**: 1021-1027.

Sánchez, M.C., Llama-Palacios, A., Marín, M.J., Figuero, E., León, R., Blanc, V., Herrera, D., and Sanz, M. (2013) Validation of ATP bioluminescence as a tool to assess antimicrobial

effects of mouthrinses in an *in vitro* subgingival-biofilm model. *Med Oral Patol Oral Cir Bucal* **18**: e86-92.
Tamma, P.D., Cosgrove, S.E., and Maragakis, L.L. (2012) Combination therapy for treatment of infections with gram-negative bacteria. *Clin Microbiol Rev* **25**: 450-470.
Tamma, P.D., and Rodriguez-Bano, J. (2017) The Use of Noncarbapenem β-Lactams for the Treatment of Extended-Spectrum β-Lactamase Infections. *Clinical infectious diseases : an official publication of the Infectious Diseases Society of America* **64**: 972-980.
Tomassini, J., Roychoudhury, R., Wu, R., and Roberts, R.J. (1978) Recognition sequence of restriction endonuclease KpnI from *Klebsiella pneumoniae*. *Nucleic acids research* **5**: 4055-4064.
Tomás, A., Lery, L., Regueiro, V., Pérez-Gutiérrez, C., Martínez, V., Moranta, D., Llobet, E., González-Nicolau, M., Insua, J.L., Tomas, J.M., Sansonetti, P.J., Tournebize, R., and Bengoechea, J.A. (2015) Functional Genomic Screen Identifies *Klebsiella pneumoniae* Factors Implicated in Blocking Nuclear Factor κB (NF-κB) Signaling. *J Biol Chem* **290**: 16678-16697.
Tsai, S.S., Huang, J.C., Chen, S.T., Sun, J.H., Wang, C.C., Lin, S.F., Hsu, B.R., Lin, J.D., Huang, S.Y., and Huang, Y.Y. (2010) Characteristics of *Klebsiella pneumoniae* bacteremia in community-acquired and nosocomial infections in diabetic patients. *Chang Gung Med J* **33**: 532-539.
Tsai, Y.K., Fung, C.P., Lin, J.C., Chen, J.H., Chang, F.Y., Chen, T.L., and Siu, L.K. (2011) *Klebsiella pneumoniae* outer membrane porins OmpK35 and OmpK36 play roles in both antimicrobial resistance and virulence. *Antimicrob Agents Chemother* **55**: 1485-1493.
Tschowri, N., Busse, S., and Hengge, R. (2009) The BLUF-EAL protein YcgF acts as a direct anti-repressor in a blue-light response of *Escherichia coli*. *Genes Dev* **23**: 522-534.
Tschowri, N., Lindenberg, S., and Hengge, R. (2012) Molecular function and potential evolution of the biofilm-modulating blue light-signalling pathway of *Escherichia coli*. *Mol Microbiol* **85**: 893-906.
Tuomanen, E., Cozens, R., Tosch, W., Zak, O., and Tomasz, A. (1986) The rate of killing of *Escherichia coli* by beta-lactam antibiotics is strictly proportional to the rate of bacterial growth. *J Gen Microbiol* **132**: 1297-1304.
Vasudevan, R.T. (2014) Biofilms: Microbial Cities of Scientific Significance. *Journal of microbiology & experimentation* **1**.
Viale, P., Giannella, M., Lewis, R., Trecarichi, E.M., Petrosillo, N., and Tumbarello, M. (2013) Predictors of mortality in multidrug-resistant *Klebsiella pneumoniae* bloodstream infections. *Expert Rev Anti Infect Ther* **11**: 1053-1063.
Vuotto, C., Longo, F., Balice, M.P., Donelli, G., and Varaldo, P.E. (2014) Antibiotic Resistance Related to Biofilm Formation in *Klebsiella pneumoniae*. *Pathogens* **3**: 743-758.
Walker, K.A., and Miller, V.L. (2020) The intersection of capsule gene expression, hypermucoviscosity and hypervirulence in *Klebsiella pneumoniae*. *Curr Opin Microbiol* **54**: 95-102.
Walker, K.A., Miner, T.A., Palacios, M., Trzilova, D., Frederick, D.R., Broberg, C.A., Sepúlveda, V.E., Quinn, J.D., and Miller, V.L. (2019) A *Klebsiella pneumoniae* Regulatory Mutant Has Reduced Capsule Expression but Retains Hypermucoviscosity. *mBio* **10**: e00089-00019.
Walker, R.C., and Wright, A.J. (1991) The fluoroquinolones. *Mayo Clin Proc* **66**: 1249-1259.
Wang, X., Xie, Y., Li, G., Liu, J., Li, X., Tian, L., Sun, J., Ou, H.Y., and Qu, H. (2018a) Whole-Genome-Sequencing characterization of bloodstream infection-causing hypervirulent *Klebsiella pneumoniae* of capsular serotype K2 and ST374. *Virulence* **9**: 510-521.
Wang, Y., Wang, S., Chen, W., Song, L., Zhang, Y., Shen, Z., Yu, F., Li, M., and Ji, Q. (2018b) CRISPR-Cas9 and CRISPR-Assisted Cytidine Deaminase Enable Precise and Efficient Genome Editing in *Klebsiella pneumoniae*. *Appl Environ Microbiol* **84**: e01834-01818.

Wei, D., Wang, M., Shi, J., and Hao, J. (2012) Red recombinase assisted gene replacement in *Klebsiella pneumoniae*. *J Ind Microbiol Biotechnol* **39**: 1219-1226.
Weiss, D., Gawlik, D., Hotzel, H., Engelmann, I., Mueller, E., Slickers, P., Braun, S.D., Monecke, S., and Ehricht, R. (2019) Fast, economic and simultaneous identification of clinically relevant Gram-negative species with multiplex real-time PCR. *Future Microbiol* **14**: 23-32.
Whitfield, C. (2006) Biosynthesis and assembly of capsular polysaccharides in *Escherichia coli*. *Annu Rev Biochem* **75**: 39-68.
Whitfield, C., and Roberts, I.S. (1999) Structure, assembly and regulation of expression of capsules in *Escherichia coli*. *Mol Microbiol* **31**: 1307-1319.
Widder, E., and Falls, B. (2014) Review of Bioluminescence for Engineers and Scientists in Biophotonics. *Selected Topics in Quantum Electronics, IEEE Journal of* **20**: 1-10.
Wijesinghe, G., Dilhari, A., Gayani, B., Kottegoda, N., Samaranayake, L., and Weerasekera, M. (2019) Influence of Laboratory Culture Media on *in vitro* Growth, Adhesion, and Biofilm Formation of *Pseudomonas aeruginosa* and *Staphylococcus aureus*. *Med Princ Pract* **28**: 28-35.
Wilson, B.R., Bogdan, A.R., Miyazawa, M., Hashimoto, K., and Tsuji, Y. (2016) Siderophores in Iron Metabolism: From Mechanism to Therapy Potential. *Trends Mol Med* **22**: 1077-1090.
Wilson, C., Lukowicz, R., Merchant, S., Valquier-Flynn, H., Caballero, J., Sandoval, J., Okuom, M., Huber, C., Brooks, T.D., Wilson, E., Clement, B., Wentworth, C.D., and Holmes, A.E. (2017) Quantitative and Qualitative Assessment Methods for Biofilm Growth: A Mini-review. *Res Rev J Eng Technol* **6**. 4.
Wilson, T., and Hastings, J.W. (1998) Bioluminescence. *Annu Rev Cell Dev Biol* **14**: 197-230.
Wu, M.C., Lin, T.L., Hsieh, P.F., Yang, H.C., and Wang, J.T. (2011) Isolation of genes involved in biofilm formation of a *Klebsiella pneumoniae* strain causing pyogenic liver abscess. *PLoS One* **6**: e23500.
Wu, Y.-H., Chen, P.-L., Hung, Y.-P., and Ko, W.-C. (2014) Risk factors and clinical impact of levofloxacin or cefazolin nonsusceptibility or ESBL production among uropathogens in adults with community-onset urinary tract infections. *Journal of Microbiology, Immunology and Infection* **47**: 197-203.
Ye, Y., Xu, L., Han, Y., Chen, Z., Liu, C., and Ming, L. (2018) Mechanism for carbapenem resistance of clinical *Enterobacteriaceae* isolates. *Exp Ther Med* **15**: 1143-1149.
Yoshida, K., Matsumoto, T., Tateda, K., Uchida, K., Tsujimoto, S., and Yamaguchi, K. (2000) Role of bacterial capsule in local and systemic inflammatory responses of mice during pulmonary infection with *Klebsiella pneumoniae*. *J Med Microbiol* **49**: 1003-1010.
Yu, Z., Qin, W., Lin, J., Fang, S., and Qiu, J. (2015) Antibacterial mechanisms of polymyxin and bacterial resistance. *Biomed Res Int* **2015**: 679109.
Zhang, W., Sun, J., Ding, W., Lin, J., Tian, R., Lu, L., Liu, X., Shen, X., and Qian, P.Y. (2015) Extracellular matrix-associated proteins form an integral and dynamic system during *Pseudomonas aeruginosa* biofilm development. *Front Cell Infect Microbiol* **5**: 40.
Zhang, X.S., García-Contreras, R., and Wood, T.K. (2008) *Escherichia coli* transcription factor YncC (McbR) regulates colanic acid and biofilm formation by repressing expression of periplasmic protein YbiM (McbA). *ISME J* **2**: 615-631.
Zheng, J.X., Lin, Z.W., Chen, C., Chen, Z., Lin, F.J., Wu, Y., Yang, S.Y., Sun, X., Yao, W.M., Li, D.Y., Yu, Z.J., Jin, J.L., Qu, D., and Deng, Q.W. (2018) Biofilm Formation in *Klebsiella pneumoniae* Bacteremia Strains Was Found to be Associated with CC23 and the Presence of *wcaG*. *Front Cell Infect Microbiol* **8**: 21.
Ørskov, I., and Ørskov, F., (1984) 4 Serotyping of *Klebsiella*. In: Methods in Microbiology. T. Bergan (ed). Academic Press, pp. 143-164.